From The DEPARTMENT OF LABORATORY MEDICINE,
Karolinska Institutet, Stockholm, Sweden

Pathophysiological Role and Therapeutic Potential of Extracellular Vesicles in Cancer

Doste Mamand

Stockholm 2024

Published by Karolinska Institutet.
Printed by Universitetsservice US-AB, 2024

ISBN 978-91-8017-257-8

Pathophysiological Role and Therapeutic Potential of Extracellular Vesicles in Cancer

THESIS FOR DOCTORAL DEGREE (Ph.D.)

By

Doste Mamand

The thesis will be defended in public at Månen, Karolinska Institutet ANA Futura, Alfred Nobels allé 8, 141 52 Huddinge, January 26th, 2024, 09:00 am

Principal Supervisor:
Dr. Oscar Wiklander
Karolinska Institutet
Department of Laboratory Medicine
Division of Biomolecular and Cellular Medicine

Co-supervisor (s):
Professor Samir EL Andaloussi
Karolinska Institutet
Department of Laboratory Medicine
Division of Biomolecular and Cellular Medicine

Dr. Dara Mohammad
Karolinska Institutet
Department of Medicine, Huddinge
Division of Haematology

Dr. Andre Görgens
Karolinska Institutet
Department of Laboratory Medicine
Division of Biomolecular and Cellular Medicine

Opponent:
Associate Professor Dirk Michiel Pegtel
University of Amesterdam,
Medical Centre

Examination Board:
Associate Professor Rainer Heuchel
Karolinska Institutet
Department of Clinical Science, Intervention and Technology

Associate Professor Per Hydbring
Karolinska Institutet
Department of Oncology-Pathology

Associate Professor Linda Bojmar
University of Lindköping
Department of Biomedical and Clinical Sciences
Division of Surgery, Orthopedics and Oncology

To my family, relatives, friends, and Pirzin folks

ABSTRACT

Extracellular vesicles (EVs) are nanosized lipid bilayer vesicles that are endogenously generated through various biogenesis pathways within most cellular entities. Subsequently, they are released into the extracellular milieu to facilitate intercellular communication. They are composed of diverse bioactive molecules with important roles in physiological and pathological states. Over the past few decades, the therapeutic potential of EVs has garnered significant interest in the drug delivery field. However, deepened understanding of EV biology and further technological advances are needed to bridge the gap between research and clinical translation. In this thesis, we address these challenges and investigate EVs as novel biomedical agents.

EVs are crucial components of physiological processes and disease development. Sensitive visualisation techniques are needed to better understand their function as therapeutic agents. In paper I, a bioluminescent labelling system was developed to track EVs *in vitro* and *in vivo*. The system uses genetic modifications to enable the encapsulation of sensitive luciferase-variants in EVs. The system was used *in vivo* to enable highly sensitive detection of EV distribution pattern. Exogenously administered EVs were found to rapidly distribute within different organs, with a preference for the spleen, lung, and liver.

In addition to endogenously engineered EVs for *in vivo* tracking, exogenously engineered EVs can be utilised as promising drug delivery platforms. However, cargo loading is often insufficient, requiring improved EV loading approaches. In paper II, we developed an optimised cargo loading method using electroporation. An optimised protocol was designed to load EVs with doxorubicin, which increased cargo loading, EV recovery, and drug potency by 190-fold over free doxorubicin.

Owing to their potential to cross biological barriers, transport bioactive cargo, and targetability, EVs can be exploited as delivery vehicles for targeting of therapeutics. EVs were used as delivery vectors in paper III by coating their surfaces with an Fc domain-specific antibody-binding moiety. These Fc-EVs were then decorated with various IgG antibodies and targeted to cells of interest. *In vitro* and *in vivo* antibody targeting studies showed the broad potential of this technology for cancer therapy. The platform efficiently targeted EVs to cancer cells, including HER2 and PD-L1 positive cells. As proof of concept, Fc-EVs with PD-L1 antibody accumulate in tumour tissue and, when loaded with doxorubicin, reduce tumour burden, and increase survival in melanoma-bearing mice.

Despite significant EV engineering advances, we have a limited understanding of the biology of tumour-derived extracellular vesicles (tEVs). In paper IV, we investigated the role of *in vitro*-generated melanoma-derived EVs as indirect communicators in tumour-induced haematopoiesis dysregulation. The tEVs, which contain high levels of angiogenic factors like VEGF, osteopontin, and tissue factor, were found to cause splenomegaly, extramedullary haematopoiesis, expansion of splenic immature erythroid progenitors, reduced bone marrow cellularity, medullary expansion of granulocytic myeloid suppressor cells, and anaemia in syngeneic mice. These findings suggest that tEVs dysregulate haematopoiesis during the immune escape phase of cancer immunoediting, making them potential targets for overcoming immune evasion and restoring normal haematopoiesis.

To summarise, the tools generated in this thesis, including the ability to detect EVs *in vivo*, effective cargo loading, display antibody binding moieties on EV surfaces for targeting, and understanding the pathophysiological role of tEVs, contribute to the advancement of EVs for biomedical purposes, and clinical translation down the line.

LIST OF SCIENTIFIC PUBLICATIONS

1. Gupta, Dhanu[&], Xiuming Liang[&], Svetlana Pavlova, Oscar P. B. Wiklander, Giulia Corso, Ying Zhao, Osama Saher, Jeremy Bost, Antje M. Zickler, Andras Piffko, Cecile L. Maire, Franz L. Ricklefs, Oskar Gustafsson, Virginia Castilla Llorente, Manuela O. Gustafsson, R. Beklem Bostancioglu, **Doste R. Mamand**, Daniel W. Hagey, André Görgens, Joel Z. Nordin, and Samir EL Andaloussi. 2020. "Quantification of Extracellular Vesicles in Vitro and in Vivo Using Sensitive Bioluminescence Imaging." *Journal of Extracellular Vesicles* 9(1).

2. Lennaárd, Angus J.[&], **Doste R. Mamand**[&], Rim Jawad Wiklander, Samir E. L. Andaloussi, and Oscar P. B. Wiklander. 2022. "Optimised Electroporation for Loading of Extracellular Vesicles with Doxorubicin." *Pharmaceutics* 14(1).

3. Oscar P. B. Wiklander[&], **Doste R. Mamand**[&], Dara K. Mohammad Wenyi Zheng, Rim Jawad Wiklander, Taras Sych, Antje M. Zickler, Dhanu Gupta, Xiuming Liang, Heena Sharma4, Andrea Lavado4, Jeremy Bost1, Giulia Corso1, Angus J. Lennaárd, Manuchehr Abedi-Valugerdi, Imre Mäger, Erdinc Sezgin, Joel Z. Nordin, André Görgens, Samir EL Andaloussi "Targeted Therapy by Antibody Displaying Extracellular Vesicles". Manuscript under 2nd revision in *Nature Biomedical Engineering.*

4. **Doste R. Mamand**, Safa Bazaz, Dara K. Mohammad, Xiuming Liang, Carsten Mim, Susanne Gabrielsson, Oscar Wiklander, Manuchehr Abedi-Valugerdi, Samir El-Andaloussi. "Extracellular vesicles originating from melanoma cells promote dysregulation in haematopoiesis as a component of cancer immunoediting. Running title: Induction of haematopoiesis dysregulation by melanoma cell derived EVs". Revised manuscript in preparation for resubmission in *Journal of Extracellular Vesicles.*

& These authors contributed equally

LIST OF ADDITIONAL PUBLICATIONS

1. Sara Cavallaro, Federico Pevere, Fredrik Stridfeldt, André Görgens, Carolina Paba, Siddharth S. Sahu, **Doste R. Mamand**, Dhanu Gupta, Samir El Andaloussi, Jan Linnros, and Apurba Dev "Multiparametric profiling of single nanoscale extracellular vesicles by combined atomic force and fluorescence microscopy: correlation and heterogeneity in their molecular and biophysical features." *Small* 17.14 (2021): 2008155.

2. Dhanu Gupta, Oscar P. B. Wiklander, André Görgens, Mariana Conceição , Giulia Corso, Xiuming Liang, Yiqi Seow, Sriram Balusu, Ulrika Feldin1 , Beklem Bostancioglu, Rim Jawad, **Doste R. Mamand**, Yi Xin Fiona Lee, Justin Hean, Imre Mäger, Thomas C. Roberts , Manuela Gustafsson, Dara K. Mohammad, Helena Sork, Alexandra Backlund, Per Lundin, Antonin de Fougerolles, C. I. Edvard Smith, Matthew J. A. Wood, Roosmarijn E. Vandenbroucke, Joel Z. Nordin and Samir El-Andaloussi "Amelioration of systemic inflammation via the display of two different decoy protein receptors on extracellular vesicles." *Nature Biomedical Engineering* 5.9 (2021): 1084-1098.

3. Jeremy P. Bost, Osama Saher, Daniel Hagey, **Doste R. Mamand**, Xiuming Liang, Wenyi Zheng, Giulia Corso, Oskar Gustafsson, André Görgens, CI Edvard Smith, Rula Zain, Samir El Andaloussi, and Dhanu Gupta "Growth media conditions influence the secretion route and release levels of engineered extracellular vesicles." *Advanced Healthcare Materials* 11.5 (2022): 2101658.

4. Safa Bazaz, Tõnis Lehto, Rahel Tops, Olof Gissberg, Dhanu Gupta, Burcu Bestas, Jeremy Bost, Oscar P. B. Wiklander, Helena Sork, Eman M. Zaghloul, **Doste R. Mamand**, Mattias Hällbrink, Rannar Sillard, Osama Saher, Kariem Ezzat, C. I. Edvard Smith‡, Samir EL Andaloussi and Taavi Lehto, "Novel Orthogonally Hydrocarbon-Modified Cell-Penetrating Peptide Nanoparticles Mediate Efficient Delivery of Splice-Switching Antisense Oligonucleotides In Vitro and In Vivo." *Biomedicines* 9.8 (2021): 1046.

5. André Görgens, Giulia Corso, Daniel W. Hagey, Rim Jawad Wiklander, Manuela O. Gustafsson, Ulrika Felldin, Yi Lee, R. Beklem Bostancioglu, Helena Sork, Xiuming Liang, Wenyi Zheng, Dara K. Mohammad, Simonides I. van de Wakker, Pieter Vader, Antje M. Zickler, **Doste R. Mamand**, Li Ma, Margaret N. Holme, Molly M. Stevens, Oscar P. B. Wiklander, Samir EL Andaloussi, "Identification of storage conditions stabilizing extracellular vesicles preparations." *Journal of extracellular vesicles* 11.6 (2022): e12238.

6. Xiuming Liang, Zheyu Niu, Valentina Galli, Nathalie Howe, Ying Zhao, Oscar P B Wiklander, Wenyi Zheng, Rim Jawad Wiklander, Giulia Corso, Christopher Davies, Justin Hean, Eleni Kyriakopoulou, **Doste R. Mamand**, Risul Amin, Joel Z Nordin, Dhanu Gupta, Samir El Andaloussi "Extracellular vesicles engineered to bind albumin demonstrate extended circulation time and lymph node accumulation in mouse models." *Journal of Extracellular Vesicles* 11, no. 7 (2022): e12248.

7. Juul, Nikolai, Oliver Willacy, **Doste R. Mamand**, Samir El Andaloussi, Jesper Eisfeldt, Clara Ibel Chamorro, and Magdalena Fossum. "Insights into cellular behavior and micromolecular communications in urothelial micrografts." *Scientific Reports* 13 (2023) :13589.

8. Wenyi Zheng, Julia Rädler, Helena Sork, Zheyu Niu, Samantha Roudi, Jeremy P. Bost, André Görgens, Ying Zhao, **Doste R. Mamand**, Xiuming Liang, Oscar P. B. Wiklander, Taavi Lehto, Dhanu Gupta, Joel Z. Nordin & Samir EL Andaloussi. Identification of scaffold proteins for improved endogenous engineering of extracellular vesicles. *Nature Communications* 14 (2023): 4734.

TABLE OF CONTENTS

LIST OF ABBREVIATIONS

3'UTR	3' untranslated regions
ADAM-10	metalloprotease ADAM-10
AFM	Atomic force microscopies
ARF6	ADP-ribosylation factor-6
ARRDC1	Arrestin 1 domain-containing protein 1
BASP1	Brain acid soluble protein 1
BBB	Blood-brain barrier
BE-SEC	Bind-elute size exclusion chromatography
CCR5	C-C Motif Chemokine Receptor 5
CM	Cell-conditioned media
CML	Chronic myeloid leukaemia
CXCR-4	Chemokine receptor specific for stromal-derived-factor-1
DAF	Decay-accelerating factor
DCs	Dendritic cells
DiR	1,1′-dioctadecyl-3,3,3′,3′-tetramethylindotricarbocyanine iodide
DLS	Dynamic Light Scatter
DMEM	Dulbecco's Modified Eagle's Medium
Dox	Doxorubicin
DPBS	Dulbecco's Phosphate Buffer Saline
EE	Early endosome
EGFR	Epidermal growth factor receptor
EM	Electron Microscopy
EMH	Extramedullary haematopoiesis
EPCs	Endothelial progenitor cells
ERK	Extracellular signal-regulated kinase
ESCRT	Endosomal sorting complexes required for transport
EVs	Extracellular vesicles
FBS	Foetal bovine serum
Fc-EVs	Fc-engineered extracellular vesicles
FCM	Flow cytometry
FFFF	Flow field-flow fractionation
FYVE	Zinc finger domain
G-MDSCs	Granulocytic myeloid-derived suppressor cells
GPCRs	G protein-coupled receptors
GPI	Glycosylphosphatidylinositol
GRP78	Glucose-regulated protein 78
HCT-116	Colorectal adenocarcinoma
HDLs	High-density lipoproteins
HEK293	Human embryonic kidney
HIF	Hypoxia-inducible factor
hIgG1	Human IgG1
HIV	Human immunodeficiency virus
hnRNPA2B1	Heterogeneous nuclear ribonucleoproteins A2/B1
hnRNPU	Heterogeneous nuclear ribonucleoprotein U
HSC60	Heat shock cognate 60
HSC70	Heat shock cognate 71
HSP90B	Heat shock protein HSP 90-beta

HSPGs	Heparan sulphate proteoglycans
ICAM-1	Intercellular adhesion molecule 1
IFN	Interferon-gamma
IgSF-8	Immuno-globulin superfamily-8
IL-6R	Interleukin-6 receptor
IL-6ST	Interleukin-6 signal transducer
ILVs	Intraluminal vesicles
ISEV	International Society on Extracellular Vesicles
kDa	Kilodaltons
LAMP2	Lysosome-associated membrane protein 2
LE	Late endosome
Lipodox	Liposomal formulation of Doxorubicin
MDA-MB-231	Breast carcinoma
MHC-I	Major histocompatibility complexes I
MHC-II	Major histocompatibility complexes II
MiRNAs	MicroRNAs
MLCK	Myosin light chain kinase
mNG	mNeongreen
mRNA	Messenger RNA
MS	Mass spectrometry
MSCs	Mesenchymal stromal cells
MT1-MMP	Membrane type-1 matrix metalloproteinase 1
mtDNA	mitochondrial DNA
MVB	Multivesicular body
MVs	Microvesicles
MWCO	Molecular weight cut-off
NK cells	Natural Killer Cells
nLuc	Nano-Luciferase
NP	Nanoparticle
NSCLC	Non–small cell lung cancer
NTA	Nano sight Tracking Analysis
PBMC	peripheral blood mononuclear cell
PDGF	Platelet-Derived Growth Factor
PD-L1	Programmed death-ligand 1
PEG	Polyethene glycol
PIGF	Placental Growth Factor
PLD	Phospholipase D
PROSPR	Protein organic solvent precipitation
PTM	post-translational modification
PtNPs	lutein-infused platinum nanoparticles
PTX	Paclitaxel
PVDF	Polyvinylidene difluoride
RAB22A	Ras-related protein Rab-22A
rRNAs	ribosomal RNAs
RS	Raman spectroscopy
RVG	Rabies virus glycoprotein
SEC	Size exclusion chromatography
SKBR-3	HER2-positive breast cancer cells
snoRNAs	small nucleolar RNAs
Socs1	suppressor of cytokine signalling 1

SPP	single-particle profiler
SR-B1	Type B-1 scavenger receptor
SRM	Super-resolution microscopy
STOSE	ovarian cancer
SYNCRIP	Synaptotagmin-binding, cytoplasmic RNA-interacting protein
TEM	Tumour-derived EVs
TFF	Tangential flow filtration
TGFβ-1	transforming growth factor β-1
TIMP-1	Metalloproteinase-1
TME	Tumour microenvironment
TNF	Tumour necrosis factor
TNFR1	Tumour necrosis factor receptor 1
tRNAs	transfer RNAs
TRPS	Tunable Resistive Pulse Sensing
TSEM	Transmission Scanning Electron Microscopy
TSG101	Tumour susceptibility gene 101 protein
TSP-2	Thrombospondin-2
U-87 MG	Neuronal glioblastoma
UC	Ultracentrifugation
UF	Ultrafiltration
V	Voltage
VAMP3	Vesicle-associated membrane protein 3
VEGF	Vascular Endothelial Growth Factor
VPS4	Vacuolar protein sorting-associated protein 4A
WB	Western Blotting
μF	Capacitances

1. INTRODUCTION

1.1 A BRIEF HISTORY OF EXTRACELLULAR VESICLES

Extracellular vesicles (EVs) and their physiological roles were first described in the middle of the 20th century through functional studies, electron microscopy, and ultracentrifugation[1]. In 1946, Erwin Chargaff and Randolph West asserted that the ultra-centrifugal blood plasma pellets had procoagulant characteristics[2]. In 1967, Peter Wolf further discovered microparticles while conducting research on blood coagulation. He found that these microparticles were produced by platelets, referred to as "platelet dust"[3]. Simultaneously, the calcification properties of EVs within the bone matrix were independently elucidated by Ermanno Bonucci and Clarke Anderson[4], [5]. During the 1970s, several organisations acknowledged EVs' vesicular and extracellular properties and in 1971 they were officially designated as "extracellular vesicles"[4]. Subsequently, it was observed that EVs originating from cells in the follicular thyroid of bats were produced in response to arousal, suggesting they may have involvement in endocrine mechanisms[6]. The presence of EVs in samples obtained from intestinal villi and human cancer have been mentioned in previous literature, with similar data reported, despite the absence of definitive conclusions about the release of EVs [7]–[9]. EVs from cells and from bovine serum were further detected in cell-conditioned media[10]. Here, in 1974, the differentiation between multivesicular body vesicles (MVB) and microvesicles was established and the resemblances between enveloped viruses and EVs were observed[10].

In the early to mid-1980s, Johnstone and Stahl's labs made enormous strides in terms of identifying EVs from cancer cells and identified that they are released from reticulocytes[11]–[13]. Their studies revealed that EVs could be discharged from the cell surface or plasma membrane and through fusion with the plasma membrane facilitated by MVBs[11], [13], [14]. Additionally, EVs were described based on their organ of origin, as exemplified by "prostasomes," which have been discovered to boost sperm motility in seminal fluid[15]. During the 1990s, EV involvement in immune responses became increasingly apparent, as demonstrated by the findings of Graça Raposo *et al*.[16]. Studies have shown that EVs facilitate the translocation of transmembrane proteins across immune system cells. For instance, CXCR4 and CCR5, co-receptors of the human immunodeficiency virus (HIV), can be transferred to a non-resistant cell through microparticles originating from an HIV-susceptible cell, thereby rendering the recipient cell vulnerable to infection [17], [18]. Moreover, EVs possess significant potential as a promising and versatile class of therapeutics, positioning them as a potential breakthrough tool in the medical field. The exponential rise in publications over the past few decades mirror the growth in the EV field which has contributed to a greater comprehension of EV composition, biological function, and biogenesis (Figure 1).

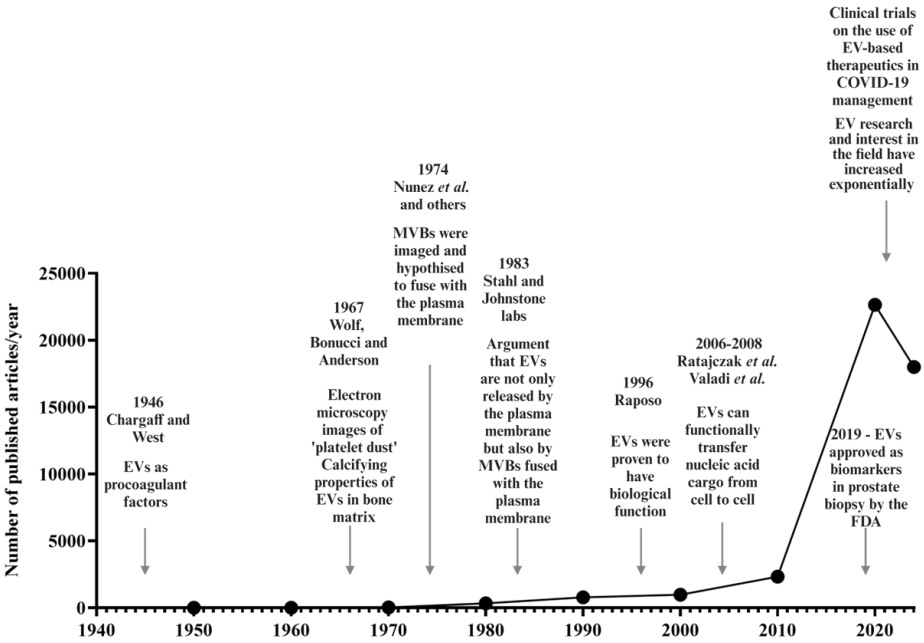

Figure 1. Noteworthy discoveries of EVs and their associated publications recognised on PubMed from the 1940s onwards that included the terms “extracellular vesicles”, “microvesicles”, or “exosomes”.

1.2 NOMENCLATURE OF EXTRACELLULAR VESICLES

EVs are a broad term that includes membrane vesicles, dexosomes, argosomes, ectosomes, membrane particles, exovesicles, microvesicles, those that shed from cells, and those that are blebbing out. These vesicles are released by single-celled and multicellular organisms. Exosomes and microvesicles are the most widely recognised subtypes of EVs; nonetheless, numerous subtypes have been categorised using varying criteria. The introduction of this term was motivated by a need for clarity and to facilitate effective communication among researchers and society. The word EV refers to a wide variety of criteria developed from many types of *in vitro* investigations and outdated separation and detection techniques.

The acquisition of novel data through enhanced detection and isolation methods has expeditiously resulted in widespread agreement about numerous cellular pathways involved in the formation and release of diverse EV types. However, this has also revealed that diverse EVs exhibit more similarities than initially anticipated. Nevertheless, "exosomes" continues to be used to describe small EVs, ranging from 40 nm to 120 nm, that are generated by all cell types. They are equipped with multifunctional membranes that are derived from endosomal fusion with the plasma membrane. Exosomes also consist of a collection of proteins referred to as tetraspanins, including CD63 and CD81[19].

At the 2015 meeting of the International Society on Extracellular Vesicles (ISEV) in the US, the following claims were made: (i) EVs that cannot be distinguished from exosomes were demonstrated to be discharged from the plasma membrane; (ii) exosomes were defined as having diameters of up to 250 nm; and (iii) proteins like tetraspanins were not found to be

unique to exosomes[19]. In 2018, the ISEV endorsed using "extracellular vesicle" (EV) as the accepted terminology for describing spontaneously released cell particles encased by a lipid bilayer and lacking a functional nucleus for replication[20]. Currently, EVs are categorised into three classes depending on their biogenesis: exosomes, microvesicles, and apoptotic bodies [21].

1.3 BIOGENESIS OF EXTRACELLULAR VESICLES

1.3.1 Biogenesis of Exosomes

Exosomes are a subtype of EVs, typically ranging between 40 to 120 nm in diameter[22]. In 1981 Tram *et al.,* first observed that these membrane vesicles were released by neoplastic cells and possessed 5'-nucleotidase activity [23]. The exosome biogenesis is regulated by different receptors present on the cellular surface [24], [25]. Based on the proteins involved in exosome biogenesis there are two distinct pathways , the endosomal sorting complexes required for transport (ESCRT)-dependent pathway [26] and ESCRT-independent mechanism[27].

The synthesis of exosomes typically involves four primary stages: initiation, endocytosis, production of MVBs, and sorting[28], [29]. Following initiation, the endocytosis of the plasma membrane takes place, leading to the internalisation and ubiquitination of the cell membrane and surface proteins, respectively[30]. The ubiquitinated surface proteins bind to the zinc finger domain (FYVE) on ESCRT and sort into early endosomes. This protein complex is essential for the functioning of ESCRT-0 [31]. Subsequently, the formation of MVBs occurs by the process of inward budding, wherein ESCRT-I and ESCRT-II are incorporated into the endosomal membranes, early endosome (EE) followed by late endosome (LE) (Figure 2). This process gives rise to MVBs, which consist of intraluminal vesicles (ILVs)[31]. During the last phase of the process, ESCRT-III facilitates either the degradation of the MVB through fusion with lysosomes or the release of exosomes by merging the MVB with the cell membrane, thereby enabling the secretion of ILVs into the extracellular milieu[22].

In addition to the ESCRT-dependent route, previous research has demonstrated the formation of exosomes in the absence of ESCRT. The process of exosome formation in oligodendroglial cell lines does not depend on ESCRT but on the generation of ceramide by the sphingomyelinase enzyme[32]. The aforementioned observations align with the existence of elevated levels of ceramide and its derivatives within exosomes[32]–[34]. Moreover, tetraspanins are known to impact the ESCRT-independent pathway significantly. A study found that dendritic cells lacking the CD9 gene released fewer exosomes than cells expressing CD9[35]. Similarly, HEK293 cells lacking CD63 released fewer smaller particles than those with CD63. Despite this, there is insufficient data on which tetraspanins demonstrate potential functionality in EV biogenesis [36].

The existing body of literature has established a comprehensive understanding that both of the aforementioned pathways play a crucial role in exosome biogenesis[37]. However, it is essential to note that the two routes discussed are not mutually exclusive[38]. Distinct exosome subpopulations may arise from diverse biogenesis mechanisms, and these pathways may operate in a coordinated manner. In addition, cellular homeostasis and cell type may influence the machinery responsible for regulating exosome secretion[39]. During biogenesis, exosomes are known to include a diverse range of cargo[40]. Hence, understanding the biogenesis process and exploring methods to manipulate it can contribute to advancing innovative EV therapies.

1.3.2 Biogenesis of Microvesicles

Microvesicles (MVs) are small membrane-bound vesicles, 100 nm to 1 μm in diameter, that bud directly from the cell membrane [41]. Their biogenesis is less well-defined than that of exosomes [42]. Findings from cellular model systems used to study MV biogenesis and release/ shedding from the plasma membrane [42] suggest their primary biogenesis mechanism involves plasma membrane outward budding and fission [37] (Figure 2). MV production is thought to result from several processes, including the transport of the active ingredient phosphatidylserine to the leaflet margins and creation of the actin-myosin machinery contract[43]. Once the enzyme phospholipase D (PLD) is turned on, it starts a chain reaction that results in ARF6 production, which is essential for MV release [44]. Following this, extracellular signal-regulated kinase (ERK) recruits the serine/threonine-specific protein kinase (MLCK) to the plasma membrane[45]. The MVs are released when MLCK phosphorylates and triggers the myosin light chain. These MVs are often enriched in ADP-ribosylation factor-6 (ARF6), vesicle-associated membrane protein 3 (VAMP3), MHC-I, β1 integrins, and membrane type-1 matrix metalloproteinase 1 (MT1-MMP) [43], [44].

Interestingly, evidence has demonstrated that tumour susceptibility gene 101 protein (TSG101), an ESCRT-I subunit, which binds to Arrestin 1 domain-containing protein 1 (ARRDC1) tetrapeptide protein, resulting in the formation of MVs [42]. In addition, the interaction of E3 ligase WWP2 and VPS4 ATPase ubiquitinates ARRDC1 and plays a part in MV development[46]. External stimuli may also trigger MV release. For instance, phospholipids rearrangement due to calcium influx enhances the release of MVs [47]. Furthermore, studies show the induction of hypoxia can stimulate the release of MVs by upregulating the expression of Ras-related protein Rab-22A (RAB22A) through the hypoxia-inducible factor (HIF) pathway[48]. The content of the MVs can be used to discriminate between the various processes of MV release[49].

1.3.3 Biogenesis of Apoptotic Bodies

Apoptotic bodies, a less extensively studied subset of EVs, are produced by blebbing in dying cells (Figure 2). These structures can potentially encapsulate diverse components derived from the interior organelles of cells[50], [51]. Apoptotic bodies tend to be larger in size, reaching sizes of up to 2μm in diameter[41]. However, it is worth noting that they can also be as small as 0.5 μm [41]. Furthermore, the interaction between actin and myosin may play a significant role in the process of membrane blebbing[52].

As previously stated, there are multiple distinct mechanisms involved in the synthesis of EVs. Nevertheless, there remain several unanswered questions. Our limited understanding of their biogenesis results in difficulties in accurately distinguishing these EVs.

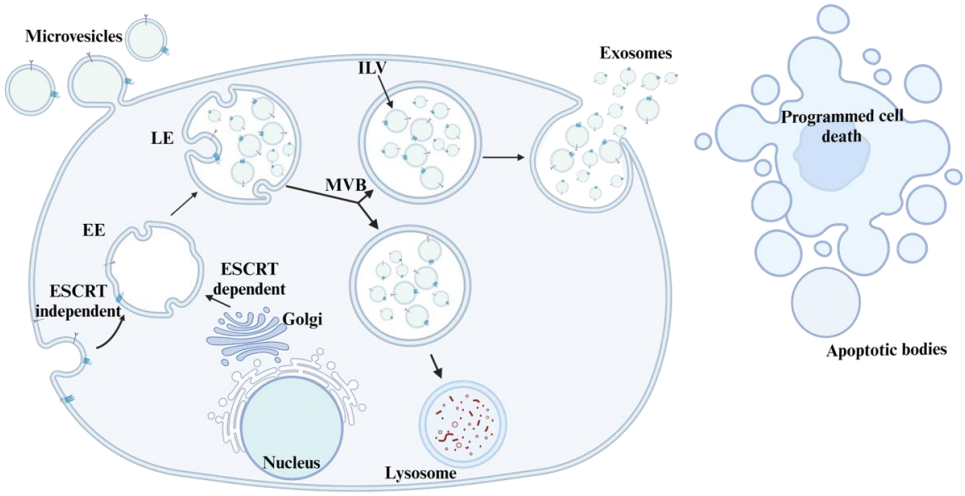

Figure 2. An illustration of EV biogenesis. Exosome formation by endosomal pathways: Early endosome (EE), late endosome (LE), multivesicular body (MVB), intraluminal vesicle (ILV). Microvesicles formation by cellular budding. Apoptotic bodies formation by programmed cell death.

1.4 COMPOSITION OF EVs

1.4.1 Protein Composition

EVs transport diverse membrane and luminal proteins (Figure 3). Several proteomic studies have been conducted on EVs derived from different cells and tissues. For example, in a proteomic study conducted on EVs from 60 different tumour cell lines, over 6000 proteins were identified, with over 200 proteins being unique to each cell type[53]. Similarly, another study found 3000 proteins in EVs isolated from cell-conditioned media from 14 distinct cell types, where they found over 600 unique proteins across different cell types [54]. These studies showed that a significant portion of the EV proteomes is widely distributed, contains more proteins implicated in their formation, and is associated with partner interaction.

EVs are significantly enriched with diverse tetraspanins, including CD9, CD63, and CD81[55], [56]. Tetraspanin family proteins do not own enzymatic or catalytic receptor properties. However, they have the potential to facilitate the organisation and arrangement of protein cargos, particularly those that interact with tetraspanins, including MHC class II proteins[55], [57], intercellular adhesion molecule 1 (ICAM-1)[58], Integrins[59], syntenin-1[60] and immuno-globulin superfamily-8 (IgSF-8)[61]. Thus, sorting cargo through tetraspanin-mediated mechanisms could be associated with a distinct pathway for MVB biogenesis. There has also been speculation that CD63 only appears on vesicles that are MVB-derived. In contrast, CD81 and CD9, predominantly localised on the surface of the cell, is preferably sorted into vesicles produced from the plasma membrane by outward budding[62], [63]. In combination with tetraspanins, various scaffolding transmembrane proteins, including the Flotillin family[64], are linked to EVs and several receptors, including chimeric antigen receptor[65], IL-6R[66], T cell receptor[67], EGFR[68], and Notch receptors[69], present on the EV surface. Moreover, the surface of EVs contains a substantial number of proteases and ligands, including

metalloprotease ADAM10 (ADAM)[70], transforming growth factor β-1 (TGFβ-1)[71], and programmed cell death ligand 1(PDL1)[72], as well as an abundance of membrane-interacting proteins including proteins that possess glycosylphosphatidylinositol (GPI) anchors, such as complement-inhibiting proteins MAC-IP and decay-accelerating factor (DAF) [73], glycoprotein 2, and Glypican-1[74] .

Furthermore, the inner structure of the EV membrane contains a variety of proteins, including GTPases, that play a crucial role in biogenesis and are anchored to the inner leaflet through prenylation, a post-translational modification (PTM) process[75]. Myristoylated proteins, such as Src signalling kinases[76]and BASP-1, MARCKSL1, and MARCKS [77], also exhibit interactions with the inner membrane and undergo sorting into EVs. The Gag protein from HIV employs myristoylation of N-terminal glycine to incorporate into EVs, viral-like particles or viruses[78]. Additional PTMs that have been demonstrated to facilitate payload sorting into EVs include phosphorylation, SUMOylation, and ubiquitination. Other proteins have been observed to interact with or form constituents of ESCRT machinery, including TSG101, ALIX, and syntenins[79]. In addition to proteins associated with biogenesis, EVs also contain molecular chaperones, including Hsp20, Hsp60, Hsp70, and Hsp90[80]–[83]. Cytosolic proteins, including tubulin and actin, are also sorted into EVs, particularly during MV shedding from the plasma membrane[84].

1.4.2 Nucleic acid composition

The extracellular milieu contains various nucleic acids, including double-stranded DNA (dsDNA), and different RNA species[42] (Figure 3). One of the primary focuses of EV research has been to understand the composition and significance of associated nucleic acid cargos in the context of disease pathophysiology[85]–[87]. EVs contain a diverse range of nucleic acids, including small nuclear RNAs (snRNAs), non-coding RNA, microRNAs (miRNAs), and full length and fragmented mRNA and DNA[88]–[90]. However, the presence of dsDNA within EVs has been a topic of contention. DNA has long been considered a contaminant that co-purifies with EVs. Further, its release may be facilitated by autophagy, although this process is not necessarily limited to vesicular particles[63]. Moreover, upon subjecting EVs to DNase treatment, a significant reduction in DNA content is observed, suggesting that most of the DNA is not within the EVs but associated to their membrane[91]. However, other studies have shown that cells undergoing pyroptosis -a form of cell death- release mitochondrial DNA (mtDNA) packaged within EVs[92]. Similarly, other studies have found that during early pancreatic cancer progression, mutant KRAS DNA levels are highest in both small and large EVs. However, small EVs had the highest tumour-derived DNA concentration throughout disease development based on size exclusion chromatography (SEC) analyses [93].

The exact composition of small RNAs in EVs remains unknown, as multiple studies have reported varying findings[94]. This is likely because the employed purification technique can significantly affect the detection of RNA within EVs[95]. The differentiation between small RNAs derived from human sources and those from foetal bovine serum (FBS) poses a significant challenge[96] as FBS contamination may account for the observed abundance of specific highly enriched miRNAs in EVs[97], [98]. Similarly, it has been shown that serum-free media were also enriched with miRNAs 122-5p and 415a that co-isolated with EVs[99]. However, the diversity of RNAs in EVs is still significant, following contaminant removal.

We are only recently beginning to understand the molecular pathways involved in sorting RNA into EVs and have identified two distinct mechanisms: the passive and active loading mechanisms [100]. The cellular concentration of specific RNAs significantly influences passive

uptake into EVs. The degree of enrichment is entirely contingent upon the cell type and is considered a critical factor in diagnosis[101], [102]. The presence of specific patterns in the nucleic acid cargo indicates the presence of active loading mechanisms in addition to the passive loading of RNA cargo. For example, miRNA with 5' oligopyrimidine sequences and mRNA fragments with 3' untranslated regions (3'UTR) are enriched into EVs[103], [104]. Certain types of RNA molecules are selectively organised based on their specific sequence through interactions with RNA-binding proteins, such as hnRNPU and hnRNPA2B1[105], [106]. The protein SYNCRIP facilitates the process of sorting different miRNAs into EVs by forming a binding interaction with the hEXO motif[107], [108]. Nevertheless, our understanding of the RNA biology of EVs is limited, highlighting the importance of standard purification methods to accurately determine the RNA composition of EVs.

1.4.3 Lipid composition

EV lipid composition depends on the type of producer cell and the stage of physiological development, which have a pivotal role in the fate and function of the EV membrane. Recently, there has been a notable focus on investigating EV nucleic acids and proteins in various studies to elucidate their involvement in biological processes for therapeutic applications. Lipids are a less explored category of abundant bioactive molecules found within EVs[109]. They contribute to the structural integrity of EVs and play a pivotal role in regulating various functions within recipient cells. Lipids, which are necessary components of all cell types, are the main components of the EV membrane. Cholesterol, sphingolipids, and phospholipids are the major lipids in EV composition[110]–[114] (Figure 3). Several studies have extensively examined the lipid composition of EVs derived from various sources and have shown that some lipid classes are more prevalent in the producer cells[115]. For example, EV derived from B lymphocytes are up to three times more enriched in cholesterol than those from the cell membrane[33]; this may be due to the sorting mechanism[116]. Furthermore, lipidomic studies on human plasma have found 244 lipids and 191 lipids identified in EVs and plasma, respectively. The samples were categorised into 10 distinct lipid classes; the major modifications were found in the content of lysophosphatidylcholines, diacylglycerols, phosphatidylcholines, and triacylglycerols, whereas sulfatides, phosphatidylinositols, and sphingomyelins demonstrated similar profiles in EVs and plasma [110]. Owing to its highly ordered structure and glycosphingolipid enrichment, EVs are very stable in extracellular environments[111]. Phosphatidylserines are typically found in the inner layer of the membrane, whereas, sphingomyelin and phosphatidylcholine are generally located in the outer leaflet of the asymmetrically distributed EV lipid membrane[117].

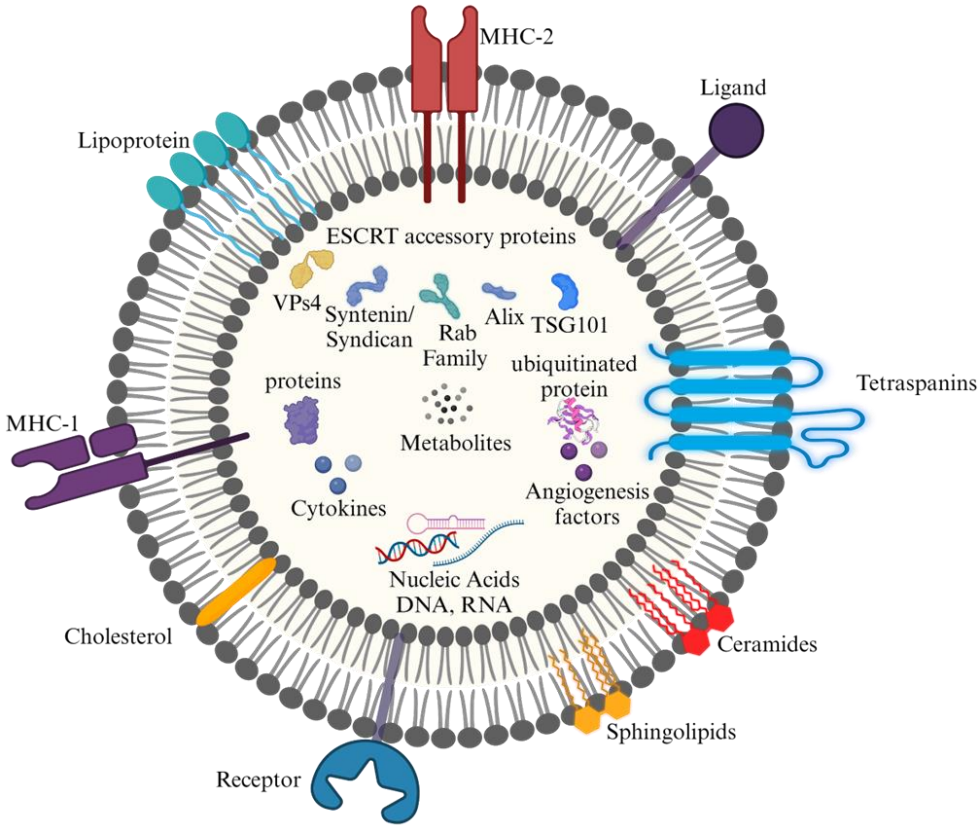

Figure 3. Protein, nucleic acid, and lipid composition on/in EVs.

1.5 ISOLATION METHODS OF EVs

Interest in EV research has grown dramatically owing to its prospective benefits in therapy. However, lack of defined procedures for EV separation and isolation limits their clinical application[118]. EVs have traditionally been isolated by ultracentrifugation (UC) procedures, which was widely regarded as the standard method in the field. However, this technique comes with several challenges resulting in the development of alternative approaches (figure 4), such as size exclusion chromatography-based techniques, precipitation, and immunoaffinity capture [119], [120]. However, these approaches do not strictly isolate EVs only, as other impurities from the extracellular environment can be co-isolated[1], [41]. This is primarily due to the complex composition of biological fluids from which EVs are isolated, the similarities in the biochemical and physiochemical properties of EV subtypes, and the EVs intrinsic heterogeneity[120], [121]. Therefore, there remains a need to develop effective techniques enabling the accurate isolation of EVs and EV subpopulations. Such techniques should be time saving, efficient, replicable, and suitable for implementation in clinical environments[37]. Currently, as an alternative to subpar isolation methods several techniques are utilised

consecutively to augment the purity of isolated EVs. However, this is costly, time-consuming and requires advanced technical proficiency, reducing its usefulness in clinical settings[122].

1.5.1 Differential ultracentrifugation (UC)

UC continues to be widely recognised as the gold standard technique for EV isolation,resulting in fairly pure EV preparations[123]. In this method, EVs are isolated using a sedimentation procedure that exploits the density of particles and aims to segregate them from other constituents, such as cells and detritus. However, the efficacy of this approach is limited when applied to very viscous biological fluids, such as serum or plasma[124]. Moreover, we are faced with several challenges when using UC as it is time-consuming, not scalable, operator dependent and may result in EV aggregation and membrane damage due to the high g forces required [125][126].

1.5.2 Density gradient centrifugation

The methodology involves the utilisation of UC in combination with a density gradient, typically composed of iodixanol or sucrose. One notable benefit of employing this approach is its ability to augment the isolation of low-density EVs from a more comprehensive array of impurities or particles while simultaneously maintaining the structural integrity of EV membranes[127]. However, it is time-consuming, and the duration of centrifugation plays a crucial role in determining the end products. Furthermore, loading and unloading the density gradient requires considerable precision, a task that may be challenging to do in real-world scenarios and significantly lowers throughput[128] .

1.5.3 Filtration

Filtration represents an additional method for purifying EVs based on their size. Primarily, ultrafiltration (UF) is conducted using membranes with molecular weight cut-off (MWCO) values ranging from 10 to 100 kilodaltons (kDa). It is a user-friendly method that isolates EVs at a much faster rate than the UC[129]. Nevertheless, protein contamination, membrane degradation, and distortion of EVs are significant issues associated with UF techniques. Thus, Thus, the hollow fibre tangential flow filtration (TFF), also known as crossflow filtration, is often employed as an alternate method for the separation of EVs. In TFF, the transportation of fluids containing EVs occurs in a divergent manner via a hollow fibre membrane. The larger EVs undergo recirculation and concentration through this process, whereas smaller molecules are eliminated. The TFF method is superior to other filtration methods since it mitigates common issues like cake formation as observed in other filtration methods[130]. Furthermore, by utilising TFF, EVs can be effectively separated from diluted materials on a large scale.

1.5.4 Size exclusion chromatography (SEC)

The SEC technique uses hydrodynamic volume or molecular size to separate macromolecules [131]. Furthermore, the bind-elute size exclusion chromatography (BE-SEC) columns have been demonstrated to possess scalability and reproducibility for the purification of EVs[125], [128]. SEC can be used to separate EVs from both bacterial and eukaryotic samples and is frequently used to separate distinct EV populations. However, this remains challenging due to

the existing limitations in resolution[132], therefore two-dimensional SEC can be alternatively employed. In a past study, this technique was employed to distinguish between three subgroups of urine EVs, namely larger (102 nm), medium (60 nm), and small (36 nm) EVs. The pre-isolated EVs were subjected to purification using a column with a smaller pore size (0.05 µm) and subsequently fractionated into three distinct sizes using a column with a larger pore size (0.2 µm)[133]. In the context of EV separation, SEC is considered superior to both UC and chemical precipitation methods as the shear stress exerted during centrifugation and the use of chemical reagents compromise EV membrane integrity[126]. Moreover, co-isolation of high-density lipoproteins (HDLs) and EVs exhibiting a comparable range of densities is often observed following density gradient ultracentrifugation[134]. However, this phenomenon was not seen when employing SEC due to the larger size of EVs compared to HDLs. However, it should be noted that SEC dilutes the isolated EVs, and VLDL can be co-isolated with EVs because of similar size[135].

1.5.5 Affinity-based techniques

Affinity-based methodologies rely on the precise and specific interactions between antibodies and ligands on the membrane proteins or receptors present on EVs[136]. Magnetic beads and polymers, such as monolithic and column agarose beads, can immobilise or conjugate ligands, such as antibodies for affinity-based isolation. Two distinct forms of affinity-based separation techniques exist: affinity chromatography and immunoaffinity capture. The predominant method for isolating EVs is affinity-based techniques, namely by utilising antibodies that target proteins present on the surface of EVs. Typically, the antibodies are covalently linked to magnetic beads through biotinylation[136]. The tetraspanins CD81, CD63, and CD9 are commonly employed as specific targets for EVs[56], [137]. However, these approaches are limited by high costs, rendering them less feasible for large-scale EV production. Additionally, some of these procedures, such as carboxylic beads, require a specific pH and non-physiological salt to effectively separate EVs from the beads, which may affect the EVs' biological activity. Nevertheless, these techniques can be employed for specific EV isolation from small sample volumes and yield high-purity fractions suitable for diagnostic purposes[138].

1.5.6 Other isolation methods

Lectins[139], protein organic solvent precipitation (PROSPR)[140], Total Exosome Isolation Reagent (ThermoFisher Scientific), and hydrophilic polymers, such as, polyethylene glycol (PEG)[141], have been observed to decrease the solubility of EVs by reducing their hydration, leading to them being precipitated out of the sample. These methods can efficiently concentrate EVs at reduced centrifugal speeds, leading to higher yields than those produced by UC. However, the introduction of precipitation reagents leads to a decrease in protein solubility, thereby introducing protein impurities in the isolate, which may be detrimental to downstream analyses. Nevertheless, such methods are beneficial across diverse applications. Firstly, EV structural integrity is maintained, ensuring the fidelity of their representation during analysis[142]. Secondly, the use of precipitation reagents obviates the need for a complex apparatus, thereby enhancing accessibility and cost-effectiveness. Finally, using these reagents allows manipulation of pH levels that closely mimic the physiological range, thereby augmenting the accuracy of experimental results[143]. Thus, precipitation reagents facilitate isolation from large samples, enhancing operational effectiveness and sample processing capacity. However, several limitations need to be considered regarding impurity levels, reproducibility and polymer retention[138].

1.5.7 Charge-based isolation techniques

Ion-exchange procedures use positively charged cations to interact with anionic elements of EV membranes, as defined by their zeta potential[144] . Owing to their charge, electrophoresis can be used to differentiate EVs by electrophoretic mobility and separate them into pure fractions[145]. Di-electrophoresis is a label-free isolation technique that does not require the presence of specific biomarkers on EVs for isolation. By making an uneven alternating current electric field inside a microfluidic chamber, di-electrophoresis uses an electrode microarray to separate particles from a liquid medium[146]. Previous studies have shown that using hydrophilic polymer precipitation to isolate EVs is preferable to UC [132]. However, the separation of EVs from blood and plasma is challenging with this method because of the abundance of charged substances. Thus, techniques to eliminate viral contamination and other proteins from EV isolates are required to enhance purity [136].

1.6 CHARACTERISATION METHODS OF EVs

The characterisation of isolated EVs has primarily relied on analysing their protein concentration[147]. However, it is crucial to acknowledge that the protein concentration of isolated EVs is often inaccurately represented due to impurity. Furthermore, this assessment does not consider the unique protein profiles that may vary among EV subpopulations[147]. As a result, due to the growing prevalence and heightened interest in EVs, researchers have progressively utilised sophisticated approaches to examine their EV isolates. Currently, isolated vesicles undergo two main types of analyses: physical and chemical/biochemical/compositional analyses. Physical characteristics, such as the concentration and size of particles, are determined using several methodologies, such as nano sight tracking analysis (NTA), electron microscopy (EM), and flow cytometry (FCM), described further below. Staining, immunoblotting, and proteomic analysis techniques are frequently employed for chemical, biological, and compositional analyses. One of the main challenges faced is the development of methodologies that can effectively distinguish between different EV subtypes, adaptable for standardisation, and that enable efficient multiplexing. This is especially necessary following the observation that proteomic profiles of EVs are modified based on EV isolation techniques, even when the same cell line is used[148].

1.6.1 Nanoparticle Tracking Analysis (NTA)

Nanoparticle Tracking Analysis (NTA) can be applied to detect particle concentration and size. The scattered light is captured by a camera attached to a microscope positioned inside the chamber where the laser light is in contact with the particles, the size is determined by Brownian movement[149]. The NTA software analyses video information captured by a light sensitive camera to estimate particle concentration and size [149]. Sample concentration, measurement parameters, data collection and analysis settings must be optimised[150]. In addition, the quantification of the particles is affected by the camera level and detection threshold. One limitation with NTA is the inability to distinguish between EVs and other particles in the same size range. However, the advantage of NTA is that it is fast and easy to handle.

1.6.2 Dynamic Light Scatter (DLS)

Like NTA, dynamic light scattering (DLS), also known as photon correlation spectroscopy, is used to measure particle size and concentration by measuring light scattering from moving particles. DLS utilises fluctuations in the amount of scattered light to assess the size of the particles[151]. Due to the smaller sample volumes needed, fewer parameters to tune and thus, a shorter optimisation time required, DLS is more efficient than NTA [150], [151]. However, when both tiny and large particles are mixed, it is difficult to discriminate between them.

1.6.3 Tunable Resistive Pulse Sensing (TRPS)

Tunable Resistive Pulse Sensing (TRPS) uses electrical zone sensing to identify and measure particle size[152]. This approach may use larger number of samples than optical sensing and require improved micro/nano-fluidic sensitivity[153]. Complex nano-structure manufacturing, limited sampling efficiency, and calibration are drawbacks.

1.6.4 Electron Microscopy (EM)

Electron Microscopy (EM) is used for the detection of EV morphology. Transmission Scanning Electron Microscopy (TSEM) has been utilised to identify and analyse particles with an image resolution of 1 nm[154]. The capacity of Transmission Electron Microscopy (TEM) to identify and describe a single EV is highly considered in EV research[155]. EV surface proteins can also be labelled and assessed in TEM to reveal the biochemical characteristics of surface proteins[144]. Additionally, the utilisation of immune-EM with gold nanoparticle labelling provides an opportunity to gather biochemical data. Owing to the fact that TEM is carried out in a vacuum and EV samples must be fixed and dehydrated, their size and shape may be affected. However, there are no ultrastructural alterations or rearrangement of atoms, and the sample does not need to be dehydrated or fixed when Cryo-TEM is employed[156]. EVs that have been fixed via chemicals and compared with methylcellulose with or without uranyl acetate before TEM have been shown to have a cup form, whereas cryo-TEM characterized EVs have a rounded shape[157]. One of the main issues using EM is that it can only measure a few samples at a time[158].

1.6.5 Atomic force microscopy (AFM)

Atomic force microscopies (AFM) records surface structure using a laser probe[159]. AFM can detect particles as small as 10-20 nm in diameter[160]. Even if these particles are not EVs[161], the findings show the method's capacity to characterise EVs in their nano-size range (30-40 nm) and study EV isolation purity[162]. It is used to obtain 3D surface structure images. However, several experimental factors can affect the accuracy of AFM analysis[162]. These factors include temperature variations, the condition of the AFM tip, the force applied between the probe and EV samples, and fluctuations in scanning velocity which are the drawbacks of the technique.

1.6.6 Super-resolution microscopy (SRM)

Super-resolution microscopy (SRM) accurately identifies EVs and quickly detects EVs[163]. *In vivo* imaging and tracking of EVs using lipophilic dyes and direct stochastic optical reconstruction microscopy (dSTORM)-a type of SRM- can be used to identify and measure intraluminal proteins and the membrane composition of EVs[164]. SRM can create image features of 50-nm particles. Detecting fluorescence signals forms the basis for the most commonly employed techniques in single molecule detection[165]. However, it is essential to note that these methodologies have certain limitations, including potential photobleaching and phototoxicity.

1.6.7 Protein analysis

One of the most common techniques for analysing proteins is Western Blotting (WB)[166]. Protease inhibitors and denaturants can be added to the lysis buffer used to lyse vesicles. Then, the desaturated proteins are separated by SDS–PAGE and transferred to a membrane made by polyvinylidene difluoride (PVDF) for immunoblotting of a particular protein[167]. Commonly investigated EV proteins include TSG101, Alix, Flotillin-1, HSP70, HSP71, and tetraspanins. Similar methods, such as dot plots, have been used for EV proteins[167]. In addition, a well-developed method, mass spectrometry (MS), is used to identify and characterise the protein composition of EVs[168].

1.6.8 Flow cytometry (FCM)

One of the most powerful methods for analysing single large particles is FCM. Classical FCM cannot differentiate particles under 0.5 μm[169]. However, there are two general strategies available to analyse EVs by FCM, bead-based EV FCM (BB-FCM) and high-resolution single EV FCM. In BB-FCM, vesicles are captured on micrometre-sized latex beads in large quantities, and fluorescent detection antibodies are used to stain captured EVs, thereby enabling the detection of their protein markers[169], [170]. However, this approach may not detect various signatures because it cannot fully differentiate vesicle subpopulations. Thus, Stoner and colleagues developed a sensitive single EV FCM approach for quantifying and molecularly describing single EVs as small as 0.1 μm[171]. Furthermore, Görgens and colleagues used imaging FCM (IFCM) which facilitates the analysis of single EVs and EV subpopulations, making it possible to examine CD9, CD63, and CD81 expression on single EVs from a human MSC-conditioned medium and other EV sources[172]. Flow cytometry is highly appropriate for analysing clinical samples, particularly in combination with electron microscopy, NTA, and WB[171].

1.6.9 Raman spectroscopy (RS)

Raman spectroscopy (RS) is an analytical and optical protective examination method based on vibrations that can potentially characterise groups of EVs derived from diverse cell types[173]. RS rapidly provides a comprehensive biochemical image of an EV preparation quickly, making it a valuable tool for evaluating EV composition and purity. However, it has a significant downside in the form of an exceedingly weak signal and is therefore more rarely used [174].

Of note, there are no standardised protocols for reliable and quick EV isolation of sufficient purity and yield. Before clinical application, it is necessary to overcome problems relating to the scalability of EV production, isolation processes, and storage recommendations. Owing to their variety and small size, there are hurdles in analysing EVs that prevent the smooth investigation of their molecular information and interactions. The literature shows that researchers increasingly combine approaches (Figure 4) due to the strengths and limitations that exist with each approach. For example, filtration-based processes with SEC generate the finest EVs for specific applications. Understanding EV subpopulations' roles and traits is crucial as the EV industry accelerates. Some affinity-based methods, like immunoaffinity, can selectively separate EVs from many biological sources, while others are more reliable for obtaining EVs with specific properties. Such combined approaches will enable better research into EV biogenesis, EV subpopulations, cargo sorting, the routes for internalisation, and trafficking in recipient cells that will enable our ability to optimise using EVs as drug carriers.

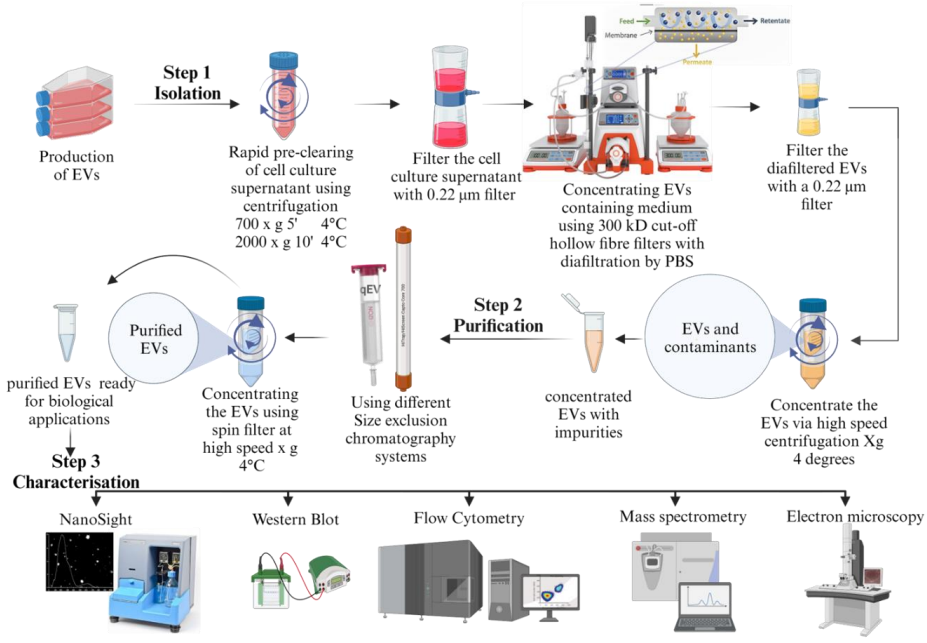

Figure 4. Some strategies employed to isolate, purify, and characterise EVs used in this thesis.

1.7 CELLULAR UPTAKE OF EVs

Cells may internalise EVs in one of two ways: by endocytosis (the engulfment and internalisation of molecules, such as proteins, into a cell) or fusion (merging with the cell membrane)[175]. Phagocytosis, clathrin-mediated, macropinocytosis, caveolin, and lipid-raft are all endocytosis processes (figure 5). In addition to the cell type and physiologic situation, the mechanism by which an EV is taken up may be governed by whether or not the ligands expressed on EVs bind to cell surface receptors or vice versa[175]. Different cell types have been found to employ various internalisation mechanisms. For instance, microglia predominantly use micropinocytosis[176], dendritic cells engage in phagocytosis or receptor-mediated endocytosis[177], neurons use clathrin-dependent endocytosis or phagocytosis[178], caveolin-mediated endocytosis in epithelial cells [179], whereas tumour cells have been shown to rely on cholesterol for endocytosis[180]. In the plasma membrane of the receiving cells, heparan sulphate proteoglycans (HSPGs) are essential factors for EV absorption, as inhibiting these with heparin prevents the internalisation of EVs *in vitro*[181], [182]. EV absorption is further reduced when mixed with an artificial HDL, simulating HDL-based nanoparticle (NP). This lipid NP inhibits the type B-1 scavenger receptor (SR-B1), which reduces EV uptake[183]. EVs can also be internalised under low pH conditions. Tagging pH-sensitive fusogenic peptides to EVs promote EV and endosome fusion, which releases EV cargo into the cytoplasm and increases both internalisation and release of EV contents[184], [185].

Various mechanisms mediate the delivery of EV payloads to surface receptors and within cells. However, the precise roles of these mechanisms are yet to be fully elucidated. Non-specific pharmacological inhibitors are commonly used to determine endocytic routes; however, their efficiency needs to be revised for conclusive and reproducible findings. As a complementary method, knock-out or knock-in methods are now being used to elucidate how EVs release their cargo and enter cells[186].

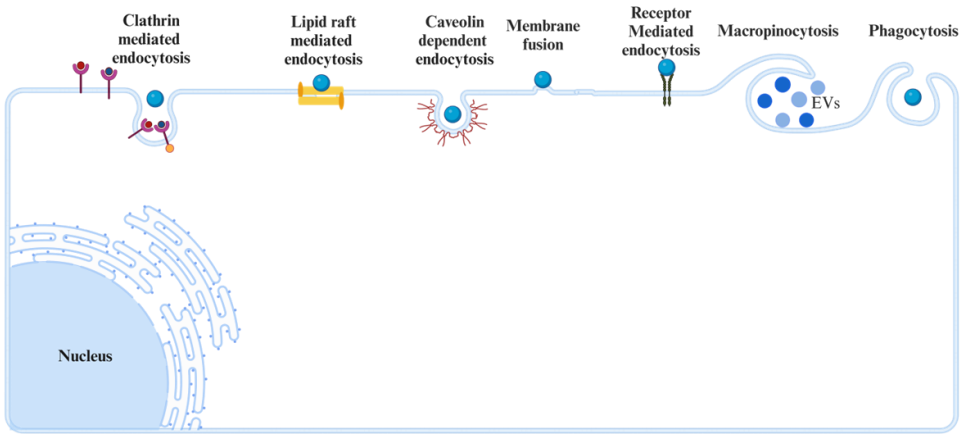

Figure 5. Simplified illustration of various uptake mechanisms of EVs by recipient cells.

1.8 BIODISTRIBUTION OF EVs

"Biodistribution" refers to the monitoring of the distribution of EVs of interest throughout the body. For effective use as therapeutic agents and drug delivery vehicles, tracking EV location in the body without disrupting their function is crucial. The biodistribution and pharmacokinetics of injected EVs have been investigated for more than ten years. However, the methods used to investigate distribution vary between the studies and are associated with different challenges. The first study utilising luciferase labelled EVs to trace EV distribution *in vivo* was performed by Lai et al [187]. They tracked the destination of intravenously injected EVs using bioluminescence and found that they spread throughout the mouse's body, mainly concentrating in the lungs, liver, kidney, spleen, and brain a few minutes after injection. Heart, muscle, and fat cells also displayed signals, whereas the blood signal half-life was 30 minutes and was eliminated after 6 hours[187]. They hypothesized that EVs were excreted by the kidneys and liver and was measurable in urine after 60 minutes. Most significantly, intravenously injected EVs were distributed to tumour cells, presumably due to the tumour cells' higher permeability and retention effect, as well as the vascular leakiness of the tumour[187].

A year later, Wiklander et al. investigated EV distribution by comparing a fluorescent fusion protein and XenoLight DiR, a lipophilic dye that labels the membrane of EVs. The DiR labelled vesicles were detected in the spleen, lung, liver, kidney, intestines, brain, and tumour tissues[188]. However, imaging data from dyes showed a longer EV detection (24 hours), than imaging data with bioluminescent tracking (6 h)[187]. This might be due to the membrane-labelling dyes residing in the recipient cells longer and degrading slower than the reporter proteins inside or on the vesicles. Alternatively, it could be because the free dye was being tracked. They also found that various injection techniques determine EVs' in vivo distribution patterns and that the biodistribution patterns of different EV sources varied.

The studies above employed bioluminescence, fluorescent proteins, or dyes to track EVs in vivo. Another study compared five distinct nuclear tracers and optical imaging systems for in vivo biodistribution of EVs using the same EV sources and doses. It was shown that the radioactivity approach provided the most precise measurement of vesicle biodistribution compared to bioluminescent and fluorescent approaches[189]. As elaborated below, EVs have demonstrated promise as possible treatments for various disorders. However, their quick clearance after injection may need to be improved. To address this issue, a recent study has shown increased circulation time of EVs by displaying albumin-binding domains on the surface of the EVs[190].

EV biodistribution is now being studied using a variety of techniques. Unfortunately, EV doses, sources, delivery routes, time points, examined organs, types of animals, tracking techniques (radiolabel, bioluminescence, fluorescent proteins, or dyes), and EV separation processes differ between the studies. This diversity reflects the complexity of EVs, making it difficult to compare studies and fully understand the biodistribution of EVs.

1.9 PATHOLOGICAL ROLE OF TUMOUR-DERIVED EVs (tEVs)

Neoplastic cells secrete EVs that are associated with tumours and cancer patients exhibit a higher abundance of EVs than healthy individuals. Different cancer cells exhibit unique contents and receptors, and tEVs differ from normal cells due to the presence of distinct luminal oncogenic nucleic acids and surface oncogenic proteins [191]. The cancer-associated proteins are involved in the advancement of tumours, and there is significant variation in the relative

abundance of proteins and nucleic acids in EVs derived from malignant cells compared to healthy cells[153].

The potential impact of tEVs on the pre-metastatic niche formation and remodelling of the tumour microenvironment (TME), indicates potential as a promising target for therapeutic interventions in cancer therapy. For instance, the process of angiogenesis, the proliferation of cancer cells to distant sites (metastasis), and the detrimental intercellular communication among tumour cells can be impeded through the inhibition of EV release, effectively halting tumorigenic cell invasion to neighbouring healthy cells[192].

Numerous publications have shown drug resistance exhibited by tumour cells facilitated by tEVs. The transition of tumour cells from being sensitive to drugs to becoming resistant to drugs has various implications for the effectiveness of chemotherapy[193], [194]. In this context, eliminating tEVs could enhance chemotherapy's efficacy in targeting tumour cells. Additionally, there have been reports indicating that Her-2 positive MVs have the potential to significantly diminish the inhibitory effect of the Her-2 antibody trastuzumab on various breast cancer cell lines. Hence, the efficacy of trastuzumab in inhibiting cell proliferation can be augmented by eliminating Her-2 positive MVs from the TME[195]. Furthermore, significant research has been conducted on the involvement of miRNAs in developing drug resistance in cancer patients undergoing chemotherapy. MicroRNAs found in tEVs can influence cellular response to drugs, reducing treatment efficacy[194]. To further understand this, studies have examined specific miRNA species, such as miR-100 and miR-222, in tEVs derived from breast cancer patients who showed drug resistance[192]. The transfer of miR-221/222 from cells resistant to tamoxifen to tumour cells that are sensitive to tamoxifen, facilitated by exosomes, led to drug resistance in the recipient cell. The downregulation in expression of the estrogen receptor (ER-Alpha) and the targeted p27 gene has been associated with drug-resistant responses and the deregulation of the cell cycle[192].

EV miRNAs also play a significant role in facilitating communication among cancer cells and their TME, thereby influencing tumour growth and the cellular response to specific therapeutic agents[193]. More recently, tEVs are known to have a significant impact on the process of cancer-induced hepatic reprogramming, leading to the development of a fatty liver[196]. The secretion of tEVs, specifically in the presence of palmitic acid, induces the release of tumour necrosis factor (TNF), thereby fostering a pro-inflammatory milieu that hinders fatty acid metabolism and oxidative phosphorylation. Therefore, TNF blockade results in a reduction in the development of fatty liver caused by tEVs. The liver's metabolic reprogramming, which is dependent on tEVs and inhibition of TNF, could potentially restrict the tolerance of chemotherapy in individuals with cancer[196]. Furthermore, tEVs have been shown to exert a downregulatory effect on transient receptor potential cation channel subfamily v member 4 (TRPV4) expression at the post-translational level, causing abnormal angiogenesis through the activation of Rho/Rho kinase/YAP/VEGFR2 signalling pathways. This suggests that tEVs and TRPV4 could be potential targets for therapeutic interventions aiming to normalize vascular function and kill tumour cells[197].

The process by which tEVs integrate with the recipient cell via endocytosis and subsequently release their payloads into the cytoplasm of the recipient cell makes these vesicles highly effective as carriers for the precise delivery of anti-cancer therapies and agents for cancer treatment[198]. As an example, EVs isolated from prostate cancer cell lines were altered to facilitate the transportation of paclitaxel (PTX) to the recipient cell through the endocytic pathway[194]. The cytotoxic effects *in vitro* were significantly enhanced using modified EVs. In addition, the growth of recipient neuronal glioblastoma (U-87 MG) cells decreased when exposed to EVs derived from U-87 MG and loaded with PTX or Doxorubicin (DOX)[198]. Similarly, the efficacy of DOX loaded into EVs derived from colorectal adenocarcinoma (HCT-

116) and breast carcinoma (MDA-MB-231) remains intact *in vivo* and *in vitro* experiments. Simultaneously, in the case of immunodeficient mice, the administration of EV loaded-DOX did not result in any adverse effects on the heart, unlike the mice treated with EV -free DOX[199]. Additionally, the study showed a decrease in the accumulation of DOX in the cardiac tissue[199]. Comparable findings have been documented in animal models of MDA-MB-231 and STOSE (ovarian cancer)[200]. Thus, tEVs play crucial roles in facilitating the growth of tumours, evading the immune system, and promoting resistance to medications. Therefore, the positive therapeutic potential of tEV can be utilised to augment the effectiveness of antitumor drugs in clinical contexts.

1.10 EXTRACELLULAR VESICLES AS THERAPEUTICS

EVs contain diverse biologically active compositions, which play significant roles in mediating interorgan and intercellular communication. Thus, they present a compelling avenue for advancing nanotherapeutics to treat specific diseases due to their inherent capacity to modulate stability, selectively target tissues, and effectively transport therapeutic payloads. However, the current limitations in manufacturing therapeutic-grade EVs on a significant scale, along with the knowledge gaps regarding heterogeneity and biogenesis of EV, pose substantial challenges to their application as clinical therapies for targeted conditions[201]. Here, I discuss the innate therapeutic ability of EVs and the engineering of EVs for therapeutic delivery.

1.10.1 Intrinsic effects of EVs for therapeutic applications

Mesenchymal stromal cells (MSCs) have been used to treat many disorders and have been wildly successful at tissue regeneration[202]. However, the idea that MSCs, via cellular differentiation, might restore injured tissue was initially rejected as unfeasible[203], [204]. Studies have shown that MSC CM that contain the secretome of the cells may accomplish therapeutic effect comparable to MSC treatment in a wide range of clinical and pre-clinical scenarios[205], [206]. As EVs are part of the secretome of MSC, the therapeutic effect of MSC-CM therapies has been suggested to be derived from EVs in the CM[207]. MSC-EVs have indeed been shown in pre-clinical studies to have various beneficial properties including the treatment of a wide range of conditions, such as inflammatory diseases of the lung, kidney, liver, central nervous system, cartilage, and bone, as well as regenerative medicine for heart and lung diseases[208], [209], [218]–[220], [210]–[217].

Nevertheless, the therapeutic efficacy of MSC-EVs is still up for debate due to the complexities of MSCs in terms of cell culture condition and differences owing to different MSC cell sources. Moreover, the purification and isolation of EVs with other components in the MSC secretome may lead to inaccurate conclusions about EV composition and function, due to the possible co-isolation of nucleic acids and proteins.

Interestingly, MSC-EVs and the activation of cell-to-cell signalling pathways can enhance angiogenesis, wound healing, inflammatory responses, and apoptosis[221]. In addition, the content that MSC-EVs carry can also regulate or induce these processes. These combined effects can alleviate the negative consequences of disease vascularisation and promote healing [208], [209], [218]–[220], [210]–[217]. MSC-derived EVs have so far dominated the field of EV-based therapeutics, however only one of several inherent cell types that produce EVs, which could potentially be utilised for therapeutic purposes. EVs isolated from different cell types, such as endothelial progenitor cells, amniotic epithelial cells, dendritic cells (DCs), embryonic, and induced pluripotent stem cells have also been shown to have therapeutic

potential in animal models of arterial repair, wound healing, myocardial infarction, and pulmonary fibrosis[217], [222]–[228].

In contrast to MSC-EVs' immune-suppressing properties, immune cell-derived EVs have immune-stimulating properties that have been used in pre-clinical studies to suppress cancer[229], [230]. In 2005, two clinical studies were completed using autologous immature DC-EVs pulsed with tumour antigenic peptides to treat SCLC and melanoma[228], [230]. Both studies showed that weekly EV delivery over four weeks was feasible and safe, although the treatment had little to no therapeutic effects. The immune system responds differently to EVs produced by mature DCs and immature DCs. Later studies showed that EVs isolated from immature DCs tend to be immunosuppressive, while EVs released from mature DCs are immunostimulatory[231]. Thus, interferon-gamma (IFN-γ) was employed in a later phase 2 trial of NSCLC to mature DCs and render EVs that would boost the immune response [83]. Studies also showed that IFN-γ-DC-EVs loaded with MHC class-restricted tumour antigens could be used as maintenance immunotherapy following neoadjuvant chemotherapy in individuals with untreatable NSCLC. Moreover, by boosting the NK cells against tumours, DC-EVs could improve treatment response of individuals with advanced cancer [232]. Both DC-EVs and tumour-derived EVs have been shown to have PD-L1 expression and PD-L1 display may act as a means for tumours to evade the body's natural defence mechanisms[233]. PD-L1 positive EVs have been shown to reduce the effect of anti-PD1 therapy in cancer.

EVs derived from pathogens or infected cells can be used as a vaccination and studies have demonstrated promising effects against pathogens [234]–[238]. However, pathogen-derived EVs may carry risks. Despite this fact, evidence from clinical and pre-clinical studies suggests that EV-based vaccines are safe and well-tolerated against cancer and other diseases[239].

1.10.2 Extracellular Vesicles as a Delivery Vector

EVs have the potential to act as vehicles for efficient and safe delivery of therapeutics to specific tissues [240]. EV therapies have shown encouraging results in various xerographic model. The clinical translation of EVs has already begun, in the treatment of cancer and in organ transplantation where their safety has been proven. Although EV therapies have demonstrated encouraging outcomes in different diseases, the clinical application of EVs is still in its early stages, and several challenges still need to be overcome before they can be appropriately used in therapies. Cargo loading into EVs often requires EV or parental cell modifications. As discussed below, there are two main ways to get therapeutics into or onto EVs: exogenous loading, also called "non-cell-based loading," and endogenous loading, involving the manipulation EV cell source (figure 6).

1.10.2.1 Exogenous loading

This approach involves the loading of isolated and purified EVs with various micro- and macromolecular cargoes. As outlined below, several chemical and physical methods have been explored for exogenous drug loading.

1.10.2.1.1 Electroporation

Electroporation is a type of mechanical transfection approach where one applies an electric field to the membrane to form micropores, which leads to increased membrane permeability and enables the entry of foreign molecules to enter. The membrane reseals once the electric field ceases[241]. Electroporation became widespread after using a custom-built electroporation chamber to transfer DNA into mouse cells in the 1980s [242]. In recent years, the approach has been significantly applied in EV research. When therapeutic molecules such as RNAs and hydrophilic chemicals are electroporated into EV membranes, they can enter them more efficiently [243].

A study employed gene pulser cell electroporation and found that siRNA was electroporated into exosomes and could inhibit a target protease in Alzheimer's disease [244]. However, loading was inefficient due to the aggregation of siRNA by electroporation pulses, which is one disadvantage of electroporation.

Additionally, the pulses may impact EVs' stability and zeta potential, increasing their aggregation [245]. Electroporation was used to load Dox into iRGD-EVs derived from DC cells specific to integrins. To separate DOX -loaded exosomes from free Dox, ultracentrifugation was employed, and DOX loading was determined by fluorescence spectroscopy. IRGD exosomes containing Dox were more effective at killing cancer cells than control exosomes containing DOX. DOX -loaded iRGD exosomes were intravenously delivered to mice harbouring MDA-MB-231 tumours, reducing tumour progression without apparent side effects [246]. Electroporation has also been used to load additional chemotherapeutic agents, such as PTX, into exosomes generated from macrophages [247]. The loading efficiency by electroporation is often higher than that of other loading approaches listed below. However, achieving both sufficient loading and avoiding cargo aggregation remains challenging.

1.10.2.1.2 Sonication

Sonication compromises EV membrane integrity, allowing drug loading by mechanical shear force. Kim *et al.*[248] loaded exosomes with PTX via sonication. In their hands, sonication was more efficient than electroporation and incubation in loading PTX into EVs. EVs loaded with chemotherapy successfully treated multidrug-resistant cancer cells [248], [249]. However, though sonication can load a fair amount, the damage it cases to the membrane is an issue for large-scale applications. It also affects the stability of EVs and the way their payloads are aggregated[245].

1.10.2.1.3 Simple incubation

Incubation is a simple approach based on concentration gradients, allowing cargo entry into EVs via diffusion without compromising EV membrane integrity [250]. This approach is convenient and adaptable for passively loading a variety of lipophilic compounds into exosomes, such as curcumin [250], DOX [251], [252], and PTX [249]. However, the ability to load these drugs is insufficient, and only hydrophobic molecules can be loaded. Hydrophobic molecules are more likely to be incorporated into the EVs' lipid bilayer than hydrophilic compounds, which cannot integrate with the EVs' membrane to enter the aqueous phase [247].

1.10.2.1.4 Extrusion

Extrusion is a physical method that stimulates membrane recombination by compressing a mixture of EVs and cargo in an extruder [253]. Haney and colleague loaded EVs with catalase and found that catalase loading increased following room-temperature (RT) incubation, freezing-thawing cycles, sonication, and extrusion. It has been shown that extruded and sonicated EVs are more neuroprotective than RT and freeze-thaw approaches. Due to its larger cargo loading capacity, extrusion has the benefit of delivering a homogeneous combination of exosomes and payloads. However, enlargement and deformation of exosomes were observed when EVs were extruded compared to when they were incubated at RT[254]. This is important because it can affect EV functionality[255].

1.10.2.1.5 Freeze-thaw cycle

A freeze-thaw process involved mixing molecules with EVs, which are then chilled at minus 80 °C and thawed at 25°C, destabilising and restructuring the membrane, thereby allowing an influx of the molecules[256]. The advantage of the freeze-thaw method is an increased loading efficiency compared to simple incubation at RT, even though the loading level of protein catalase was low [254]. However, many EV proteins can be degraded, EVs shape and size may change, and EV aggregation may be promoted by freezing and thawing [255]. In addition, it has lower drug loading efficiency than extrusion and sonication techniques.

1.10.2.1.6 Saponification

Saponin improves cargo loading by permeating the membranes [249]. Drugs and other substances may enter EVs via surface-active agents that form pores in the lipid membrane of EVs. It has been found that the loading capacity of different kinds of compounds in EVs is greatly enhanced by saponin compared to the basic incubation approach[249]. For example, compared to passive loading, the saponin approach achieves 11 times greater loading of hydrophilic compounds [247]. However, saponin may inactivate or degrade loaded cargo, thereby affecting their therapeutic benefits[254]. Another disadvantage is that saponin concentrations for loading drugs must be rigorously regulated. Saponin is a haemolytic agent *in vivo* and must thus be removed through further purification steps[257].

1.10.2.1.7 Transfection

Apart from the transfection of EV donor cells, one alternative method for obtaining EVs with therapeutic molecules is through direct transfection of EVs[258]. Abreu *et al*. used Exo-Fect, a commercially available transfection agent to transfect EVs. Their findings indicated that Exo-Fect-based miRNA transfection demonstrated the highest level of loading efficiency than other techniques. Exo-Fect has been shown to disrupt EV membrane while protecting miRNAs against enzymatic degradation. The above process facilitates the cargo's intracellular transit and delivery[259]. The technology described above demonstrates a significant loading efficiency and molecular stability level, eliminating the requirement for specialised experimental equipment. However, several commonly used transfection reagents display cytotoxicity and may give rise to safety considerations[260]. Furthermore, recent studies have indicated that transfection reagents can introduce impurities into EVs during the transfection procedure[255]. Similarly, it has been determined that existing differential centrifugation techniques cannot

efficiently separate transfection complexes from EVs. This can obscure the delivery capabilities of EVs and may alter the delivery of payloads within EVs to specific cells[261], [262].

1.10.2.2 Endogenous loading

Endogenous loading involves engineering cells to release pre-loaded EVs with the molecules of interest. To accomplish this, the parental cells are directly incubated with the molecules of interest, or an engineering technique (transfection or transduction of cells) is used.

1.10.2.2.1 Co-incubation

A method of pre-loading pharmaceuticals into EVs is to co-culture EV-producing cells with exogenous chemicals [263]. The advantage of the method is that it is simple, and the membrane integrity of EVs is not compromised. A study shown that MSCs exosomes could be loaded with drug by treating parental cells with the chemotherapeutic drug PTX [264]. Additionally, co-incubation of parental cells with other anticancer drugs, including etoposide, doxorubicin, irinotecan, epirubicin, carboplatin, and mitoxantrone, have successfully demonstrated drug loading in EVs [264]–[267]. However, this method generates poor yields and loading efficiency as drug loading cannot be controlled and may induce cytotoxicity in the producer/parental cells.

1.10.2.2.2 Genetic modification of parental cells

In this approach, cells are engineered to generate EVs with modified properties, also described as bioengineered EVs. This is commonly done by transfecting or transducing cells for ectopic expression of peptides, nucleic acids, or proteins of interest, which are then incorporated in EVs[255]. For instance, the therapeutic effect of miR-122-enriched EVs in treating hepatocellular carcinoma was shown using a Lipofectamine-based procedure to transfect MSC cells with a plasmid expressing miR-122[218], to produce miR-122 positive EVs. Other studies used HEK293 cells transfected with BCR-ABL siRNA and isolated EVs from the conditioned media[268].

Similarly, cells have been transduced with fusion constructs to express RNA-binding protein fused to the EV sorting domain CD9 to produce EVs loaded with miR-155[269]. These EVs were successfully transported into recipient cells, where they suppress expression of suppressor of cytokine signalling 1(Socs1), an endogenous target. EVs high in miR-155 were injected intravenously into mice and were found to reduce the expression of Socs1 in the kidneys, spleen, liver, and lungs [269]. In addition, others have produced EVs capable of delivering exogenously loaded siRNA to specific brain areas. The DC cells were transfected with a plasmid DNA encoding Lamp2b, an EV sorting domain, tagged to a rabies virus glycoprotein (RVG) peptide to enhance the EVs' brain targeting capabilities[244]. MSC and HEK293T cells were recently transduced with signalling incompetent IL-6ST or tumour necrosis factor receptor 1 (TNFR1) tagged to an EV-sorting protein, to express decoy receptors displayed on the EVs surface to capture pro-inflammatory cytokines. The decoy EVs successfully ameliorated intestinal inflammation, systemic inflammation, and neuroinflammation in animal models [270]. Methods that enhance cargo sorting by transfection are typical for loading EVs with macromolecules. However, the poor loading efficiency of these systems that sort cargo inside cells remains an obstacle [269].

EVs have tremendous potential as novel nanomedicine vehicles, specifically for delivering their native cargoes, which can be encapsulated into EVs by the cellular endogenous EV packing

machinery. Modification approaches could expand EVs' therapeutic abilities further than their initial purpose. Horizontal gene transfer (HGT), for example, is an innate feature of EVs. However, through direct loading or genetic modification, non-native oligonucleotides can be added to target cells to change their gene expression[271]. Several approaches for packaging EVs and coupling them with specific moieties have been established by engineering the cells that generate EVs. Understanding the system's complexity is critical while selecting a modification strategy. Modified EVs have the potential to disrupt several vesicle-cell interactions. If their capability is impaired to integrate with target cells, the result of whatever cargo they transport will be severely changed[272]. Modifications can also cause changes in membrane stiffness. This is important for therapeutic uses and shows how crucial it is to define how EVs work and what features they have.

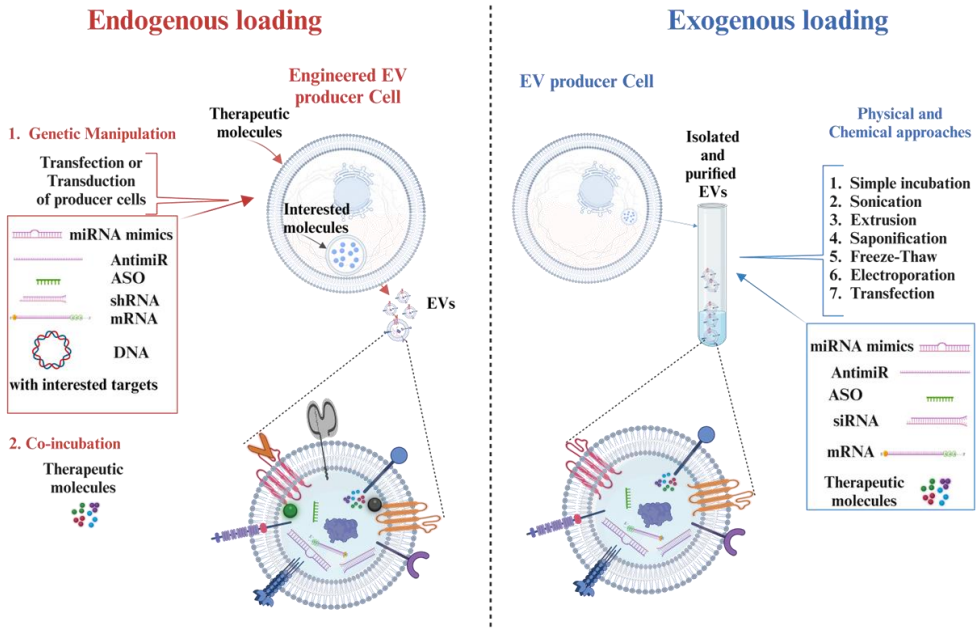

Figure 6. Strategies are employed to augment the advancement of therapeutic EVs in engineering. Changing both the membrane and the payload of EVs using either endogenous or exogenous engineering methods to reach therapeutic goals is possible. Endogenous EV engineering involves changing the parental cells for EV release by causing stress-related conditions or transfecting exogenous macromolecules such as lipids, proteins, small molecules, and nucleic acids into the parental cells. EV engineering exogenously involves making changes to EVs that are isolated. The alterations can be accomplished by utilising the hydrophobic properties of EV membranes, which enable the transport of specific cargo on the surface of the EV, or the permeability of membranes in EVs can be assessed by several approaches, including electroporation, chemical transfection, surfactant treatment, sonication, or freeze-thaw processes. These strategies facilitate the effective encapsulation of the intended payload inside the EVs.

2. AIMS

Recent evidence has shown that EVs are essential in different physiological and pathological processes. They have gained attention as promising nanotherapeutics for clinical applications, owing to their ability to transport bioactive molecules. Inspired by this, the primary aim of this thesis is to develop a highly sensitive tool for *in vivo* quantification of EVs. A secondary aim is to develop a novel loading tool for chemotherapies into EVs. The third, aim is to develop engineering EVs as a novel drug delivery and targeting tool and, finally, the fourth aim is to explore the pathophysiological role of tEV in haematopoiesis dysregulation. The individual objectives and aims of the research projects are as follows:

2.1 Paper I

- To develop an efficient and relatively high-throughput strategy for accurate labelling of EVs using bioluminescence to enable their quantification both *in vivo* and *in vitro*.
- To assess the *in vivo* pharmacokinetics of labelled EVs and investigate the impact of various routes of administration on the biodistribution of EVs.

2.2 Paper II

- To develop a novel electroporation approach to load EVs with the chemotherapeutic compound doxorubicin.
- To investigate the therapeutic efficacy of Doxorubicin-loaded EVs *in vitro*.

2.3 Paper III

- To develop a bioengineered EV platform with the ability to bind and display antibodies for targeted delivery of EVs.
- To assess if the system could be used for targeted delivery of therapeutics *in vitro* and *in vivo*.

2.4 Paper IV

- To explore the pathophysiological role of EVs derived from malignant melanoma with focus on haematopoiesis
- To investigate the function of the EVs on haematopoietic cells.

3. MATERIALS AND METHODS

The methods described in this thesis are generally consistent across various published works and manuscripts, with additional methods presented in the original papers.

3.1 Chemicals and reagents

Dulbecco's Modified Eagle's Medium (DMEM) (Gibco Life Technology), FreeStyle medium (FreeStyle 293; Gibco Life Technology), RPMI 1640 Medium (Gibco Life Technology) ,Opti-MEM (Gibco Life Technology), Dulbecco's Phosphate Buffer Saline (DPBS) (Gibco Life Technology), foetal bovine serum, sodium pyruvate, L-glutamine, 2-mercaptoethanol, trypsin/EDTA, and 100X Antibiotic Antimycotic were all obtained from (Gibco Life Technology).

3.2 Cell culture

FreeStyle 293F cells were cultured in FreeStyle medium (FreeStyle 293; Gibco Life Technology) supplemented with 1% Antibiotic Antimycotic (Gibco Life Technology) and 4.5 g/L pyruvate (Invitrogen). HEK293T, Huh7 (hepatocellular carcinoma), Cord blood MSCs, SKBR3, and B16F10 cells were cultured in DMEM high glucose medium (DMEM; Gibco Life Technology), supplemented with 1% Antibiotic Antimycotic (Invitrogen) and 10% FBS (Gibco, USA), Bone marrow cells were cultured in RPMI supplemented with 1% Antibiotic Antimycotic (Invitrogen) and 20% FBS (Gibco, USA). Mycoplasma testing was routinely performed, and all cell lines were kept at 37°C with 5% CO2 in a humidified atmosphere.

3.3 Production of engineered EVs

Plasmid constructs and cloning: For the different Fc-binding constructs, the amino acid sequence for all nine EV sorting domains, nine Fc-binders listed in, mNeongreen (mNG), and nano-luciferase (nLuc) were confirmed by Uniprot. They were subsequently synthesized (Integrated DNA Technologies) as gene blocks and cloned into a lentiviral p2CL9IPwo5 backbone downstream of the SFFV promoter using NotI and EcoRI and upstream of an internal ribosomal entry site-puromycin resistance cDNA cassette. To create the plasmid expressing mNG fused to the C or N-terminus of the EV sorting domains, mNG was subcloned into the p2CL9IPw5-EV (plasmid was kindly given from Professor Helmut Hanenberg, University Hospital Essen, Germany) sorting domain construct using NotI and SphI or AgeI and EcoRI, respectively. The nLuc was subcloned into the p2CL9IPw5-EV sorting domain construct using NotI and SphI. The Fc-binders were then cloned into the p2CL9IPw5-EV sorting domains using Kpn2I and Bsp119I. Prior to use the constructs, all plasmid constructs were confirmed by Sanger sequencing (Eurofins Genomics, Germany).

3.4 Virus production and transduction

Lentiviral supernatants were produced using HEK-293T. In brief, HEK-293T cells were co-transfected with the p2CL9IPw5 construct, including CD63-Fc fused either to mNG or nLuc proteins, the human foamy virus envelope construct pcoPE, and the helper construct pCD/NL-BH using the transfection reagent JetPEI (Polyplus, Illkrich Cedex). 18 hours post transfection, gene expression from the human CMV immediate-early gene enhancer/promoter was induced

with 10 mM sodium butyrate (Sigma-Aldrich) for 6 to 7 hours before fresh media was added to the cells, and the supernatant was collected after 22 hours. Viral particles were then pelleted at 25,000 × g for 90 min at 4°C. The pellet was resuspended in 1 ml of Iscove's Modified Dulbecco's Media supplemented with 20% FBS and 1% antibiotic antimycotic after the supernatant had been removed. Until use, the viruses were kept at 80°C. The FreeStyle 293F cells were then transduced overnight with the virus and passaged at a minimum of five times under puromycin selection to make stable cell lines.

3.5 EV isolation

FreeStyle 293F cells (250K/ml) were cultured in FreeStyle medium supplemented with 1% Antibiotic Antimycotic and 4.5 g/L pyruvate. Once a concentration of $2 \times 10^6 \pm 2 \times 10^5$ FreeStyle 293F cells/ml was obtained, the condition media (CM) was collected and centrifuged at 700 RCF for five minutes to remove cells. The pellet was discarded, and the CM was centrifuged for an additional 10 minutes at 2000 x *g* to remove cell debris and additional larger contaminants. Next purification by 0.22 µm filtration was performed (Nalgene Rapid-Flow; Thermo Fisher Scientific) and the EVs were concentrated by tangential flow filtration (KrosFlo Research 2i TFF system; Spectrum labs) at a flow rate of 100 ml/min and a transmembrane pressure around 3 psi using a 300 kDa polyether sulfone hollow fibre filter (MidiKros, 370 cm2 surface area, SpectrumLabs). The sample was diafiltered with twice the original CM volume using 0.22 µm filtered (Nalgene Rapid-Flow; Thermo Fisher Scientific) 0.1 M PBS and collected at a final volume of 20-35 ml. The concentrate was purified by 0.22 µm suction filtration (Nalgene Rapid-Flow; Thermo Fisher Scientific) and the filtrate was further concentrated by ultrafiltration at 4000 RCF in 10 kDa spin columns (Amicon Ultra-15; Millipore) to a final volume of 400-600 µl. The EVs were stored in PBS-HAT (Human Albumin +Trehalose) buffer at -80 °C until further use.

B16F10 or HEK-293T cells at the concentration of 10 million cells in 20 ml per Petri dish, 150 x 20 mm (SARSTEDT AG & Co. KG, Germany) were grown in DMEM as described above. After 24 hours, the culture medium was changed to Opti-MEM (serum free medium). Forty-eight hours later, the conditioned media (CM) were collected for further purification and isolation of EVs as described above.

3.6 Size Exclusion Chromatography (SEC)

To confirm the binding affinity of FC-EVs with antibodies, 1×10^{11} mNG-FC-EV or control mNG-EV was incubated for 2 hours at 37 °C in 400 µl of 0.22-µm filtered PBS with 2.5µg REA(S)-APC human IgG isotype control antibodies (Miltenyi Biotec). Following this, the samples were fractionated using 70 nm, 500 µl qEV columns (qEV original; IZON Science LTD), yielding 25 fractions of 1 ml per fraction. The fractions were analysed by fluorometer (SpectraMax® i3x; Molecular Devices LLC).

3.7 Characterization of EVs

3.7.1 Nanoparticle Tracking Analysis (NTA)

The size distribution and concentration of EVs purified from the cell culture were determined employing the NS500 nanoparticle analyzer (NanoSight, Malvern, Worcestershire, UK). In brief, diluted samples (100x-10,000x) were loaded into the NTA device, and five 30-second videos were recorded for each sample with a 7-second delay between recordings and a camera

level of 14-15. The analysis was performed with the screen gate set at 10 and the detection threshold at 7, with all remaining settings set to automatic.

3.7.2 Flow Cytometry

The validation of purified EVs was conducted through the use of flow cytometry, employing two distinct methodologies.

3.7.2.1 Multiplex bead-based flow cytometry analysis

Multiplex bead-based flow cytometry analysis (MACSPlex Exosome Kit, human, Miltenyi Biotec) was implemented to characterize the general surface protein composition of Fc-EVs and to assess the binding of specific antibodies to the Fc-receptor expressed on the EVs. In brief, EVs were used at an input dose of 1×10^9 NTA-based particles per assay, diluted with MACSPlex buffer to a total volume of 120 µl and incubated with 15 µl of MACSPlex exosome capture beads overnight in wells of a pre-wet and drained MACSPlex 96-well 0.22 µm filter plate at 450g at room temperature. The beads were washed with 200 µl MACSPlex buffer and the liquid was removed by applying a vacuum (Sigma-Aldrich, Supelco PlatePrep; −100 mBar). For counterstaining of captured EVs, either a mixture of APC-conjugated anti-CD9, anti-CD63 and anti-CD81 detection antibodies (supplied in the MACSPlex kit, 5 µl each) or AlexaFluor-647-conjugated human IgG Fc fragments (The Jackson Laboratory, cat 009-600-008, 100 ng) were added to each well in a total volume of 135 µl and the plate was incubated at 450 x g for 1 h at room temperature. Next, the samples were washed twice, resuspended in MACSPlex buffer and analysed by flow cytometry with a MACSQuant Analyzer 10 flow cytometer (Miltenyi Biotec). FlowJo (v.10.6.2, FlowJo) was used to analyse flow cytometry data.

3.7.2.2 Single Vesicle Imaging flow cytometry

Single Vesicle Imaging was performed by using either an Amnis ImageStream X Mk II or an Amnis Cellstream instrument (Amnis/Luminex). In brief, 2.5×10^8 EVs (NTA-based particles) were stained (unless indicated otherwise) in a total volume of 25 µl with 8 nM of fluorescent antibodies against the tetraspanins CD9, CD63, and CD81 or REA(S)-APC human IgG isotype control antibodies (Miltenyi Biotec). EVs were incubated overnight at room temperature in the dark with a subsequent dilution to a concentration of 1×10^7 EVs/ml in a final volume of 100 µl before data acquisition. Unstained samples and non-EV containing samples incubated with antibodies were included as controls, respectively. PBS-HAT buffer was used as diluent for all steps. The results were analysed with FlowJo software (v. 10.7.2; FlowJo LLC).

3.7.3 Transmission Electron Microscopy

Purified Fc-EVs or control-EVs were incubated with a 1 µl volume of 1% BSA solution diluted in PBS for 5 minutes. The experimental procedure involved adding and incubating 10nm gold nanoparticle-conjugated rabbit anti-goat antibodies (obtained from BBI Solutions) for a duration of 45 minutes. Subsequently, a volume of 5 µl labelled EVs was introduced onto glow-discharged formvar-carbon-type-B-coated electron microscopy grids (Ted Pella) and incubated for 3 minutes. The grid was dried using filter paper, rinsed twice with distilled water, and then gently dried by blotting with filter paper. After washing, the grid was stained using a solution containing 2% uranyl acetate in double-distilled water (obtained from Sigma-Aldrich). The staining procedure lasted 10 seconds, after which the filter paper was used to dry the grid. The

grid was subjected to air drying and subsequently examined using a transmission electron microscope (Tencai 10).

3.7.4 Cryo transmission electron microscopy

For sample preparation, a 2/2 mesh 300, Cu sample grid (Quantifoil, Germany) was glow discharged (20mA, 60sec). Then 3µl of the sample was applied. The grids were blotted for 8 sec, at 100% humidity at 16°C with a Vitrobot (ThermoFisher, Netherlands) and vitrified into liquid ethane. The grids were imaged with a Talos Arctica at 200kV (ThermoFisher, Netherlands). The images were collected on a Falcon III (ThermoFisher, Netherlands) camera in integrating mode and the images were summed without motion correction at a dose of 50 electrons/Å2 and a defocus of -3 µm at a nominal magnification of XX (The images were visualized with ImageJ.).

3.7.5 Nanoimager microscope

For the antibody to Fc-EVs conjugation, 5 µg of antibody was mixed with $1x10^{11}$ Fc-EVs in PBS 0.2% Human albumin serum in a final volume of 100 µl, overnight on a thermoblock plate at 25°C with a 300-rpm rotation and protected from light. For sample purification, a qEV column was initially equilibrated with 2 ml volume of PBS. Following reaction completion, the samples were purified by adding the full 100 µl of the reaction mixture onto a qEV column (Izon qEV Single-use Columns, Cat. No. 15928090, fisher scientific). Fraction collection was performed by adding 3 ml of PBS to the column and eluting by counting eight drops per fraction, on a total of 21 fractions. For imaging, each well of a µ-Slide 18 Well Glass Bottom slide (Cat.No:81817, IbiDi) was washed with distilled water twice followed by a wash with potassium hydroxide 1M and a final wash with distilled water for surface cleaning. For surface coating, 100 µl of Poly-L-lysine solution (Cat. No. 25988-63-0, Sigma) was added and incubated at 37°C for 2 hours. Upon incubation period completion Poly-L-lysine solution was carefully removed with a pipette and the sample of Antibody-FC EVs was added (50 µl), the plate was left overnight at 4°C. Prior imaging, the plate was allowed to reach room temperature. The high-resolution experiment was performed using a Nanoimager S Mark II microscope from ONI (Oxford Nanoimaging, Oxford, UK) equipped with a 100×, 1.4 NA oil immersion objective, an XYZ closed-loop piezo 736 stage and triple emission channels split at 488, 555 and 640 nm. For the evaluation of Antibody-Fc-EV conjugation the manufacturer's protocol was used.

3.7.6 Western Blotting

The Western blot technique was employed to determine the presence of tetraspanins CD9, CD81, and CD63, which are associated with EVs. Additionally, the intravesical proteins Alix and Tsg101 were also assessed. In all published and manuscript work, a total of $5x10^9$ or $2x10^{10}$ EVs and $2x10^6$ HEK-293T, B16F10, or FreeStyle 293F cells were subjected to lysis using 100 µL of radioimmunoprecipitation buffer (RIPA; BioRad, Hercules, CA, USA). The specimens were incubated at a low temperature (0°C) for 30 minutes, followed by brief vortexing (10 seconds) at regular intervals of 5 minutes. A total of twenty-four µL of EV and cell lysates were combined with eight µL of loading buffer containing 10% glycerol, 88% sodium dodecyl sulfate, 0.5 M dithiothreitol, and 0.4 M sodium carbonate. The mixture was then incubated at 70 °C for 5 minutes. Subsequently, the mixture was loaded onto the NuPAGE+ (Invitrogen, Novex 412% Bis-Tris gel) and electrophoresed at a voltage of 120 V for 1.5 hours. The proteins

were transferred to an iBlot membrane (iBlot 2 Transfer Stacks; Invitrogen) using the iBlot system (iBlot 2 Dry Blotting System; Invitrogen) for 7 minutes. The membrane underwent incubation with a blocking buffer (Odyssey Blocking Buffer; LI-COR Biosciences, Lincoln, NE, USA) at room temperature for one hour. Subsequently, it was incubated overnight at 4 °C with newly prepared primary antibodies. The primary antibodies used were anti-Tsg101 (ab30871, Abcam) at a dilution of 1:1000, anti-Alix (ab117600, Abcam) at a dilution of 1:1000, anti-NanoLuc (Promega) at a dilution of 1:2000, anti-CD9 (ab92726, Abcam) at a dilution of 1:2000, anti-CD81 (A1816) at a dilution of 1:1000, anti-Alix (K1115) at a dilution of 1:1000, anti-CD9 (10626D, Invitrogen) at a dilution of 1:200, anti-CD63 (10628D, Invitrogen) at a dilution of 1:200, and anti-Alix (sc-53540, Santa Cruz) at a dilution of 1:400. The membranes underwent four washes using TBS-T 0.1% for 5 minutes each, while being agitated on a shaker. Following this, the membranes were incubated for 60 minutes with a secondary antibody (goat anti-mouse, C00322) that had been diluted to a ratio of 1:10,000. The membrane was subjected to three washes using phosphate-buffered saline (PBS), and the outcomes were observed using an infrared imaging system known as LI-COR Odyssey CLx.

3.8 Proteomic profiling of angiogenesis factors and Cytokines

The relative expression levels of 31 proteins associated with mouse angiogenesis and 40 cytokines and chemokine in the cell culture supernatants and/or 2 x 10^{11} tEVs derived from B16F10 cells were visualized using a proteome profiler mouse angiogenesis array kit (R&D Systems, Minneapolis, MN, USA). The assay was performed in accordance with the manufacturer's instruction, except for the last step in which Tetramethylbenzidine (TMB) liquid substrate system (Sigma-Merck, Darmstadt, Germany) was used for the colour development. Pixel colour densities on the membranes were analysed using the image analysis software, ImageJ.

3.9 Stability of antibody display of Fc-EVs

To assess the stability of antibody-functionalised EVs, we initially coated Fc-EVs (containing intravesicular mNG reporter) with a specific human IgG1-APC antibody (obtained from Miltenyi; Catalogue Number 130-11-434). This experiment used a total volume of 0.2 mL to mix 1 x 1011 Fc-EVs with 25 µg of antibody. The mixture was then subjected to an incubation period of 2 hours at 37℃. Following the addition of 0.2 mL of DPBS, the EVs were subjected to purification using qEV columns (Izon; SP1) as per the instructions provided by the manufacturer. In order to assess the stability of engineered EVs in plasma, a total of 1 x 108 EVs labelled with APC (in a volume of 20 µL) were subjected to incubation with 10 µL of plasma obtained from either healthy human individuals or mice. This incubation process took place in 96-well V-bottom plates at a temperature of 37℃. Following a time interval of either 1 or 10 minutes, the samples underwent a dilution process with DPBS at a ratio of 1500:1. Subsequently, the diluted samples were subjected to analysis utilising the CellStream flow cytometer, employing the methodology outlined below. The stability of APC-labeled EVs in the presence of other antibodies was assessed by incubating 1x108 EVs with 25 ng of PE-conjugated antibody. The calculation was performed to determine the proportion of APC+mNG+ (DP+; double positive) EVs among the total population of mNG+ EVs. The experiment incorporated the following PE-conjugated antibodies: hIgG1-PE (Miltenyi; Cat. No. 130-113-438), hIgG4-PE (BioLegend; Cat. No. 403704), mIgG1-PE (Miltenyi; Cat. No. 130-113-200), and mIgG2-PE (Miltenyi; Cat. No. 130-092 215).

3.10 Binding affinity of Fc-EVs with antibody

To assess the characterization binding capacity between Fc-EVs and antibodies, a total of $1x10^8$ EVs containing the intravesicular mNG reporter, suspended in 20 µL, were subjected to incubation with varying concentrations of PE-conjugated antibodies (ranging from 0.0125 to 10 µg/mL) in 10 µL volumes. This incubation process was carried out in 96-well V-bottom plates at 37℃. After being incubated for two hours, the samples were diluted 1500 times with DPBS and then analyzed using the CellStream instrument, following the steps below. The proportion of APC+mNG+ (DP+; double positive) EVs out of the total mNG+ EVs was determined and analyzed by fitting it to the one-site total binding model from GraphPad concerning the concentration of antibodies. If applicable, the anticipated equilibrium dissociation constant (Kd) was provided for each antibody type. The study incorporated the following PE-conjugated antibodies: hIgG1-PE (Miltenyi; Cat. No. 130-113-438), hIgG4-PE (BioLegend; Cat. No. 403704), mIgG1-PE (Miltenyi; Cat. No. 130-113-200), and mIgG2-PE (Miltenyi; Cat. No. 130-092-215).

3.11 Antibody quantification per EVs

To determine the quantity of antibodies that bind to Fc-EVs. The Fc-EVs, which contained the intravesicular mNG reporter, were initially coated with the human IgG1-APC antibody (Miltenyi; Catalogue Number 130-11-434) or the Mouse IgG2b (Miltenyi Biotec 130-092-215). Similarly, the Ctrl-EVs, also containing the intravesicular mNG reporter, were coated with the human IgG1-APC antibody (Miltenyi; Catalogue Number 130-11-434) or the Mouse IgG2b (Miltenyi Biotec 130-092-215). This experiment used a total volume of 200µl to mix 1 x 10^{11} Fc-EVs or Ctrl-EVs with 25 µg of antibody. The mixture was then incubated at 37℃ for 2 hours. Following dilution with 200 µl of DPBS, the Fc-EVs were subjected to purification using qEV columns (Izon; SP1) according to the guidelines provided by the manufacturer. The quantification of antibodies per EVs was conducted using the single-particle profiler (SPP) method, performed 25 times. This experiment measured the fluorescence intensity fluctuations to investigate the free diffusion of fluorescently labelled EVs within the observation volume. The histogram representing the fluorescent brightness of antibodies per EV was transformed into a histogram that quantifies the number of antibodies per particle. This transformation was achieved by utilising the fluorescence brightness of unbound antibodies, which was measured through fluorescence correlation spectroscopy. The curves were subjected to three-dimensional diffusion fitting, and molecular brightness was quantified.

The variable N represents the quantity of molecules present within the observed volume, while molecular brightness is measured in counts per second per particle. The SPP experiment was conducted utilising the fluorescence correlation spectroscopy setup installed on a Zeiss LSM 780 microscope. The mNeonGreen fluorophore was excited using a 488-nm argon ion laser, while APC detection was performed using a 633 nm He−Ne laser. The light was focused using a water immersion objective with a NA of 1.2 and a magnification of 40x. The laser power was adjusted to a range of 0.1-0.5% of the total laser power, equivalent to 2-10 µW. The emission detection ranges for mNeonGreen and APC were configured to be 490–560 and 650–700, respectively.

3.12 Cell uptake experiment

For Huh-7 cells uptake of human IgG Fc fragment bound to Fc-EVs, 100,000 Huh-7 cells were seeded overnight in 24 well plate before Fc-EV treatment. $1x10^{11}$ mNG+ control- or Fc-EVs were incubated with 2ug of Human IgG Fc Fragment (AF647-conjugated) overnight at 4°C

with rotation. The next day, Huh-7 cells were treated with the Fc-Fragment, with or without control- or Fc-EVs and incubated at 37°C with 5% CO2 for 2 hours. The Huh-7 cells were then analysed in a motorized Olympus IX-81 inverted fluorescence microscope equipped with an XM10-monochrome-camera and narrow band-filter cube for UV (DAPI), green (GFP) and red (APC) excitation.

For B16F10, stimulated with or without 40 ng/ml of interferon gamma (IFNg, PMC4031, Gibco Life technology) and SKBR-3 cell lines, the cells were seeded in a 96-well plate format at $1x10^4$ and $2.5x10^4$ cells per well, respectively. The cells were incubated and maintained at 37 °C with 5% CO2 in a humidified atmosphere for 24 hours prior to treatment. After that, the cells were treated for 2 hours with either mNG-Fc-EVs + 2.5µg anti-PD-L1 (Atezolizumab) or 2.5µg anti-HER2 (Trastuzumab) antibodies or control mNG-EVs + anti-PD-L1 (Atezolizumab) or anti-HER2 (Trastuzumab) antibodies. The cells were then washed with PBS, trypsinized, and resuspended in fresh DMEM medium for flow cytometry using a MACSQuant Analyzer 10 flow cytometer (Miltenyi Biotec). FlowJo (v. 10.6.2, FlowJo) was used to analyse flow cytometry data.

To assess the effect on EV uptake by pretreatment of HER2-antibody, 25 x 103 SKBR-3 cells were seeded in a 96-well plate format per well for 24 hours in DMEM high glucose medium (DMEM; Gibco Life Technology), supplemented with 1% antibiotic antimycotic (Invitrogen) and 10% FBS (Gibco, USA). The plate was maintained at 37°C with 5% CO2 in a humidified atmosphere. The cells were then treated with 2.5µg of anti-HER2 (Trastuzumab) or left untreated for 2 hours. mNG-Fc-EVs + 2.5 µg of anti-HER2 (Trastuzumab) or Fc-EVs alone or mNG-Fc-EVs + 2.5 µg of human IgG isotype control antibody (Catalogue #12000C, Thermo Fisher) were subsequently added to the cells for another 2 hours. The cells were subsequently washed with PBS, trypsinized, and resuspended in fresh DMEM medium for flow cytometry using a MACSQuant Analyzer 10 flow cytometer (Miltenyi Biotec). FlowJo (v. 10.6.2, FlowJo) was used to analyse flow cytometry data.

3.13 Fluorescence microscopy

B16F10 cells were seeded at 20 000 cells per well in 8-well glass-bottom Nunc Lab-Tek II Chamber Slide (Thermo Scientific, USA). Cells were allowed to adhere for 24 h and then stimulated with or without 40 ng/ml of interferon gamma (IFNg, PMC4031, Gibco Lifetechnology). Cells were treated for 2 hours with labelled antibody (anti-PD-L1-APC, Sinobiological, Cat: 50010-R485-A), or mNG+ Fc-EVs alone, or mNG+ Fc-EVs with PD-L1-antibody (Atezolizumab or anti-PD-L1-APC) as described above. After the treatment period, cells were washed 1x with PBS, and then fixed with 4% PFA (Fisher Scientific, USA) for 10 min at RT. Both PBS and fixation solutions were warmed up to 37 °C and the pipetting was conducted swiftly to avoid sample drying. Following fixation, nuclei were stained with DAPI (Fisher Scientific, USA) for 15 minutes. Stained cells were then washed 3x with PBS. Images were acquired using a confocal microscope (A1R confocal, Nikon, Japan) and analysed by the NIS-Elements software (Nikon, Japan).

3.14 Live cell imaging assays

Live cell imaging was performed using IncuCyte instrument. The IncuCyte machine was placed in a humidified incubator at 37°C and 5% CO2. 75 x 105 bone marrow cells were seeded per well in a 24-well plate format as described above. While cells were seeded, the tEVs were added to the wells as follows: 5×10^9 non-heated tEVs, 5×10^9 56 ºC heated tEVs, and 5×10^9 100 ºC

heated tEVs. The confluency of the cells was monitored (phase contrast, 9 images per well) every day for 5 days using an IncuCyte® S3 Live Cell Analysis System (Sartorius).

3.15 Loading EVs with Doxorubicin

The experimental conditions were varied in terms of the number of EVs, the concentration of DOX (Sigma Aldrich; Merck, Germany), the composition of the electroporation buffer, and the characteristics of the electric pulse. These variations are extensively described in the results section of paper II. However, only the commonly employed practices will be further elucidated here. DOX was diluted to a concentration of 10 mM using ultrapure water to prevent aggregation during subsequent stages. The doxorubicin was combined with diluted EVs using 0.22 µm filtered (Nalgene Rapid-Flow; Thermo Fisher Scientific) 0.1 M PBS. The mixture was then incubated at 4°C for 30 minutes. The EVs were subjected to electroporation using a prepared buffer of 400 mM sucrose in PBS at a 1:1 ratio. A total volume of 400 µl of the EV sample was electroporated using an electroporation system (GenePulser Xcell; BioRad) with exponential pulse settings, utilising 0.4 cm cuvettes. The sample was incubated at a temperature of 37°C for 30 minutes.

The EVs were then purified using SEC with 70 nm 500 µl qEV columns (original; IZON et al.). The elution process involved collecting the 4th and 5th millilitres of the eluate. The eluate was subsequently concentrated to a final volume ranging from 200 to 300 µl. This was achieved by utilising 10 kDa spin filters (Amicon Ultra; Millipore) that were spun at a speed of 4000 RCF. The fluorometer used to analyse doxorubicin was the SpectraMax® i3x, manufactured by Molecular Devices LLC. The concentrations of doxorubicin were determined by comparing them to a standard curve. The standard curve was created by starting with a concentration of 100 µM and halving it 12 times until reaching a concentration of 40 mM. Ultrapure water and PBS were used as blanks. The software used for data analysis was SoftMax Pro v.7, also developed by Molecular Devices LLC. The samples were divided into portions of 90 µl and subjected to excitation at a wavelength of 488 nm, followed by measurement at 530 nm. Effect loading was calculated by determining the amount of millimolar (mM) doxorubicin per billion EVs.

3.16 Stability of encapsulated Doxorubicin in plasma

Dox was loaded into Fc-EVs by electroporation, as described above. The electroporated Fc-EVs were purified by SEC to remove unloaded Dox. After SEC, the sample was concentrated by a 2 ml 10 Kd spin filter. The concentrated samples were mixed with 1 ml of mouse plasma and incubated at three time points (1, 15 and 30 minutes) at 37 ºC. The samples were subsequently purified by SEC and concentrated using a 2 ml 10 Kd spin filter. Encapsulated Doxorubicin was analysed by fluorometer (SpectraMax® i3x; Molecular Devices LLC), and the concentrations were determined in relation to a standard curve starting at 100 µM halving 12 times to 40 mM and blanks of ultrapure water and PBS, using the dedicated software (SoftMax Pro v.7; Molecular Devices LLC). The samples were portioned at 90 µl and excited at 488 nm and read at 530 nm.

3.17 Viability Assay

The viability of the cells after treatment was assessed by 80 µl/well Cell Titre Glo (CellTiterGlo; Promega Biotech) following the provided protocol. 1 x 10^4 B16F10 cells were seeded in a 96 well plate 24 hours prior to treatment, and the plate was read 48 hours post-

treatment, with a luminometer (GloMax 96 Microplate Luminometer: Promega Biotech) using the predesigned protocol provided by the manufacturer. The plate was read each 3rd minutes until the signal stabilized.

3.18 Cell proliferation assay

For the cell proliferation assay, WST-1 was employed. Bone marrow cells were isolated from healthy mice and seeded in a 24-well format at a concentration of 75 x 10^5 cells in 500 µl per well and treated with or without pazopanib and tEVs. After 72 h, 10 µl of WST-1 were added to each well for 4 h at 37 °C and 5% CO2 according to the manufacturing protocol. Then 100 µl of the media were transferred to a 96-well plate. Then the plate was read at 450–650 nm using a fluorometer (SpectraMax® i3x; Molecular Devices LLC, San Jose, CA, USA).

3.19 Animal experiments

All of the animal experiments were performed in accordance with ethical permissions approved by The Swedish Local Board for Laboratory Animals and designed to minimise the suffering and pain of the animals.

3.19.1 Malignant Melanoma Model

Female C57BL/6 (20 ± 2 g) mice were subcutaneously implanted with 5x10^5 B16F10 cells at day 0. They were monitored daily and developed palpable tumours within 7 days. The mice were sacrificed after pre decided time points, if the tumour size exceeded 1500 mm^3, or if the mice exceeded the scoring of pre-set humane endpoints. For distribution experiments, the mice (n=7-10) were injected intravenously (if not otherwise indicated) at day 14 with 2x10^{11} Fc-EVs which had been incubated for 2 hours at 37 °C in 0.22-µm filtered PBS with 5 µg anti-PD-L1 (Atezolizumab) or 5 µg REA(S)-APC human IgG isotype control antibody (Miltenyi Biotec). 30 minutes after the injection the mice were sacrificed for tissue and blood harvest. For luminescent reading nLuc positive Fc-EVs were used, whereas mNG-positive Fc-EV were used for flow cytometry applications. The tissues were processed, with lysed tissue and nLuc-positive EV input being analysed for nanoluc luminescence or for single cell suspension for flow cytometry. For tumour treatment experiments with repetitive injections, mice were treated by intraperitoneal injections every third day starting from eight days after inoculation of mice with palpable tumours. In the short-term experiment all mice were sacrificed no later than day 20.

In the long-term experiment the mice were sacrificed no later than day 35 and were treated with treatment, n=10. The mice were observed daily, and tumour size was measured every third day using a calliper. Blood was collected when possible before sacrificing the animals. The group of animals mentioned in **Paper III**.

3.19.2 Human Breast cancer HER2 positive model

Biodistribution studies were performed in SKBR3-bearing Swiss Nude mice as previously described 35. Briefly, 35 6-week-old female swiss nude mice (Charles River, Germany) were orthotopically grafted (mammary fat pad) with 5×10^6 SKBR3 cells in 60% matrigel (CLS354234-1EA, Sigma-Aldreich). They were monitored daily and developed palpable tumours within two months. The mice were sacrificed after pre decided time points if the

tumour size exceeded 1500 mm^3, or if the mice exceeded the scoring of pre-set humane endpoints. The mice (n = 5–9) were injected intravenously at day 60 with $1x10^{11}$ Fc-EVs, which had been incubated for 2 hours at 37 °C in 0.22-µm filtered PBS with 25 µg anti-HER2 (Trastuzumab) or 25 µg human IgG isotype control antibody (Catalogue #12000C, Thermo Fisher). Thirty minutes after the injection, the mice were sacrificed for tissue and blood harvest. The tissues were processed as described in35, with lysed tissue and nLuc-positive EV input being analysed for nanoluc luminescence or for single cell suspension for flow cytometry, as described above, but with the HER2 Ab (R&D Systems, FAB9896V-100UG) used for flow cytometry applications.

3.20 *In vivo* treatment with tEVs derived from B16F10 melanoma cells

To relatively mimic the condition for the production of tEVs at the immune escape phase, a group of female C57BL/6 mice (3 mice/group) were injected intraperitoneally (i.p.) with tEVs (with or without heat inactivation) at a concentration of $1x10^{11}$ particles/mouse for 5 subsequent days. An untreated group of the same strain was injected with PBS and used as the control group. On day 8, the injected animals were weighed, bled by cardiac puncture under isoflurane anaesthesia, and thereafter euthanized by cervical dislocation. The spleen and the femur and tibia bones were dissected out, and thereafter, haematological, histological, biochemical, and flow cytometric analyses of the blood and organs were performed.

3.20.1 Preparation of single cell suspensions from tissue

Mice were sacrificed and organs (liver, spleen, lymph nodes) were surgically resected and kept on ice submerged in appropriate amounts of PBS supplemented with 1% FBS until further processing. Next, tissues were homogenised by mashing the cells through a 70 µm Falcon cell strainer (Thermo Fisher Scientific) with a syringe plunger. The cell strainer was washed several times with ice-cold PBS/1% FBS buffer to elute all remaining cells into a 50 ml conical tube. Cell suspensions were filled up to 25 ml with ice-cold PBS/1% FBS. Here, 10% of liver suspensions were transferred into a new tube with sufficient amounts of PBS/1% FBS for further processing. Next, suspensions were centrifuged at 500xg for 5 min to collect the cells, and the supernatants were carefully decanted. Liver cells and spleen cells were resuspended in 500 µl 1X BD Pharm Lyse™ lysing solution (BD Biosciences) and incubated for 10 min at room temperature in the dark to lyse remaining red blood cells (RBCs). To stop the lysis, suspensions were filled up to 30 ml with ice-cold PBS/1% FBS and centrifuged at 500xg for 5 min. The supernatants were removed carefully by pipetting. Pellets from lymph node cell suspensions were not subjected to RBC lysis but processed in parallel in all subsequent steps. Next, cell pellets were washed by resuspension in 10 ml PBS/1% FBS, transferred to fresh 15 ml conical tubes and centrifuged at 500xg for 5 min. Supernatants were carefully removed and pellets were resuspended in 500 µl PBS/1% FBS. The final cell suspensions were kept at 4°C until further processing for flow cytometry.

3.20.2 Preparation of peripheral blood mononuclear cells (PBMCs) from blood

To obtain suspensions of erythrocyte depleted PBMCs, mice were sacrificed and 200 µl blood was collected into BD Microtainer™ tubes (BD Biosciences) containing EDTA by heart puncture. 180 µl EDTA-blood were transferred to a 1.5 ml tube and centrifuged at 500xg for 7 min at 4°C. The supernatant was removed, cells were gently resuspended in 200 µl FBS/1% PBS, transferred to 15 ml conical tubes containing 500 µl 1X BD Pharm Lyse™ lysing solution

(BD Biosciences) and incubated for 10 min at room temperature in the dark to lyse red blood cells (RBCs). To stop the lysis, suspensions were filled up to 10 ml with ice-cold PBS/1% FBS and centrifuged at 500xg for 5 min. After supernatants were removed carefully, the RBC lysis step was repeated for 8 min, followed by lysis stop and centrifugation as before. The final cell pellet was resuspended in 500 µl PBS/1% FBS and kept at 4°C until further processing for flow cytometry.

3.20.3 Preparation of single cell suspension from B16F10 cell-engrafted tumours

After mice were sacrificed, tumours were surgically resected, placed into a 60-mm dish, and submerged in RT PBS. The tissue was minced with a scalpel to obtain small pieces (1-3 mm3) and pieces were transferred into a 50 ml conical tube containing 5 ml pre-warmed B16F10 cell culture medium. The tissue was centrifuged at 100xg for 5 min at RT and the supernatant was removed carefully. Next, tissue pieces were submerged in 4.7 ml pre-warmed B16F10 cell culture medium and 250 µl 20X Collagenase II (2500 CDU/mL (20 mg/ml, Sigma Aldrich) and 50 µl 100X DNase I (10,000 Kunitz/ml, Sigma Aldrich) were added to final concentrations of collagenase II and DNase I at 1 mg/ml and 100 Kunitz/ml, respectively. The tubes were fixed on a rocking platform and incubated at 37°C for 60 min. After digestion, the cell suspensions were carefully pipetted for at least 25 times with a 10-ml serological pipette until the suspensions appeared homogenous without apparent tissue pieces. Next, the suspensions were filtered through a 70 µm Falcon cell strainer (Thermo Fisher Scientific) into a fresh 50 ml conical tube, followed by a subsequent filtration through a 40 µm Falcon cell strainer (Thermo Fisher Scientific) into another fresh 50 ml conical tube. The cell strainer was washed slowly with 10 ml of pre-warmed B16F10 cell culture medium to collect remaining cells. Cell suspensions were centrifuged at 500xg for 10 min to pellet the cells and the supernatant was removed carefully. The cell pellets were resuspended in 500 µl cold PBS/1% FBS and kept at 4°C until further processing for flow cytometry.

3.20.4 Analysis of tissue, blood, and tumour single cell suspensions

To remove cell aggregates, appropriate dilutions of tissue and tumour cell suspensions (1:10 in PBS/1% FBS for tumour, liver, spleen cell suspensions; no dilution for peripheral blood mononuclear cell (PBMC) suspensions and lymph node cell suspensions) were prepared and filtered through a 40 µm cell strainer cap directly into a 5 ml round bottom tube (Corning) for flow cytometry to remove aggregates. All samples were subjected to four different antibody staining protocols to detect PD-L1 simultaneously with T cells (CD3, CD8), B cells (CD45R/B220), monocytes (CD11b), or macrophages (F4/80), respectively. For all stainings, 25 µl of cell suspension were added to a well of a 96-well V-bottom microplate (Sarstedt) and 25 µl of PBS/1% FBS were added containing a mix of the respective antibody combinations. Cells were stained for 30 min at 4°C in the dark. To wash off unbound antibody, wells were filled up with PBS/1% FBS and the plate was centrifuged at 900xg for 5 min. Cell pellets were resuspended in 90 µl PBS/1% FBS and kept dark at 4°C until flow cytometric measurement on a MACSQuant Analyzer 10 instrument equipped with 3 lasers (405 nm, 488 nm, 635 nm, Miltenyi Biotec) using the 96-well plate experiment layout. For live/dead cell discrimination 10 µl of a 10X DAPI (4′,6-diamidino-2-phenylindole, Sigma Aldrich) stock solution was added to each well. The data was analysed using the FlowJo Analysis Software (FlowJo LLC, BD Biosciences). Antibodies (fluorophore, final dilution, clone, and manufacturer): rabbit anti-mouse PD-L1 (APC, 1:100, 485, Sino Biological), rat anti-mouse CD3 (PerCP/Cy5.5, 1:100, 17A2, BioLegend), rat anti-mouse CD8a (BV510, 1:100, 53-6.7, BioLegend), rat anti-mouse CD45R/B220 (BV510, 1:100, RA3.6B2, BioLegend), rat anti-mouse CD11b (BV510, 1:100,

M1/70, BD Biosciences, APC, clone M1/70)), rat anti-mouse F4/80 (BV510, 1:100, T45-2342, BD Biosciences), rat anti-mouse CD71 labelled PE (clone C2), and rat anti-mouse TER 119 labelled APC (clone TER 119) rat-anti-mouse Gr1 (Pharmingen, BD Biosciences).

3.21 Collection of blood and body organs

Mice with advanced tumours (14-21) days after tumour cell inoculation), were weighed and thereafter, bled by cardiac puncture under isoflurane anesthesia and thereafter euthanized by cervical dislocation. The spleens, livers, femur, and tibia bones were dissected out. The livers were used for histological analysis, and the spleens were cut into two pieces; one was used for histological analysis, and the second for flow cytometry.

Blood samples were collected in blood collection tubes (Microtainer, BD Bioscience, NJ, USA) containing either EDTA dipotassium (for the analysis of haematological parameters), haemoglobin concentration was performed using the alkaline hematin method based on the manufacturer's instructions (51280-1G, Sigma-Aldrich) or no additive (for the analysis of enzymes and cytokines).

3.22 Histological analysis

Spleens and livers were fixed in 4% (v/v) formaldehyde in PBS for 24 h, placed in 70% (v/v) ethanol for 24 h, and then embedded in paraffin. Sections (5–6 μm) were stained with haematoxylin and eosin (H&E) for examination by light microscopy (ZEISS, Carl Ziess, AG, Germany). The images obtained were converted to an EGB colour format with the Adobe Photoshop CS4 program (Adobe systems, San Jose, CA, USA).

3.23 Ex-vivo

To investigate the potential direct effect of tEVs on hematopoietic cells, bone marrow cells were isolated from healthy mice and seeded in a 24-well format at a concentration of 75 x 10^5 cells in 500 µl per well, using RPMI supplemented with 20% FBS, 1% penicillin-streptomycin (5,000 U/mL, Gibco™ Life Technology), and 50 µM 2-mercaptoethanol (Sigma Aldrich). While cells were seeded, the tEVs were added to the wells as follow: 5 x 10^9 non-heated tEVs, 5 x 10^9 56 ºC heated tEVs, and 5 x 10^9 100 ºC heated tEVs. Three days after incubation in a humidified incubator at 37 °C and 5% CO2, cells were stained with Gr1/CD11b and CD71/TER119 and analysed by flow cytometry with a MACSQuant Analyzer 10 flow cytometer (Miltenyi Biotec). FlowJo (v. 10.8.1, FlowJo) was used to analyse flow cytometry data.

3.24 Blocking assay

The inhibitory effect of pazopanib, a VEGFR inhibitor (SML3076, Sigma-Aldrich, Germany), was evaluated to assess its ability to prevent the possible impact of tEVs on hematopoietic cells. Bone marrow cells were extracted from healthy mice and afterward placed in a 24-well format at a concentration of 75 x 10^5 cells in 500 µl per well, following the method outlined earlier. Pazopanib was introduced into the wells after the seeding of cells, in the following manner: cells were exposed to concentrations of 10 µM and 20 µM for a duration of 2 hours after which the cells were treated with 5 x 10^9 tEVs. Following a three-day incubation period in a controlled

environment with a humidified incubator set at a temperature of 37 °C and a CO2 concentration of 5%, the cells were assessed using the WST-1 method.

3.25 Kidney and liver function tests

Tests for creatinine (Abcam: ab65340) and urea (Abcam: a234052) for kidney function were performed based on the manufacturer's instructions. Briefly, serum samples were separated by 10 kDa and spin-filtered at 10,000 x g for 10 min at 4 °C. After collecting the filtrate, 2-10 µL of samples were added to a 96-well plate, the final volume was adjusted to 50 µL with dH2O, and absorbance was measured by fluorometer (SpectraMax® i3x; Molecular Devices LLC) at 570 nm and 505 nm, respectively. Aspartate aminotransferase (AST) (Abcam: ab105135) and alanine transaminase (ALT) (Abcam: ab105134) for liver function tests were performed based on the manufacturer's instructions. In brief, serum samples were directly diluted in the assay buffer. Samples were prepared at up to 50 µl/well with assay buffer in a 96-well plate. absorbance was measured by fluorometer (SpectraMax® i3x; Molecular Devices LLC) at 450 nm and 570 nm, respectively.

4. RESULT AND DISCUSSION

4.1 Paper I

Extracellular vesicles (EVs) are a type of cellular communication that can be autocrine or paracrine in nature. Owing to their pivotal role in intercellular communication, EVs are thought to play an important role in physiological and pathophysiological processes. However, current imaging techniques to spatiotemporally track EVs *in vitro* and *in vivo* are associated with several limitations[273]. The EV-tracking technologies used today are not specific or sensitive enough to accurately identify EVs[273]. In addition, commonly used lipophilic dyes have the potential to modify the characteristics of EVs, they can diffuse to other lipid membranes, and there is a risk of following the dye rather than the EVs because they are non-covalently bound to the EV surface[274]. Bioluminescent labelling of EVs could be an alternative way to tag and monitor EVs both *in vitro* and *in vivo*. However, previous bioluminescent labelling methods have limited efficiency and poor quantum yield[275].

In this study, we developed a highly specific and sensitive method for bioluminescent labelling of distinct EV subtypes. We selected five promising luciferase enzymes, including Super-Luc, Firefly, ThermoLuc, NanoLuc, and CRB-Luc, based on their biological half-life, signal stability, compatibility, and high sensitivity detection for *in vivo* experiments. We initially assessed suitable EV sorting proteins to label EVs with tetraspanins like CD9, CD63, and CD81 being primary candidates.

To evaluate the efficacy of bioluminescent labelling, EVs were isolated from the cells transfected with plasmids that produce the luciferase independently or tagged with CD63 at either the N-terminus or C-terminus. We found that the EVs with luciferase fused to CD63 at the C-terminus, exhibited higher bioluminescent labelling per particle. ThermoLuc and NanoLuc showed superior labelling efficiency compared to Super-Luc, Firefly, and CRB-Luc. In addition, ThermoLuc and NanoLuc-tagged EVs demonstrated long-term stability in FBS for up to 2 and 4 days, respectively. The surface proteins on the EVs with CD63-luciferase remained unchanged, as evidenced by multiplex bead-based FCM analysis.

Based on these results, we employed luciferase labelling to monitor EV secretion and uptake *in vitro*. We found no significant variation in the secretion of EV from cells overexpressing CD9, CD81, or CD63 constructs. However, when cells were cultured under serum-free conditions, more EVs were released than those cultured in serum-containing media. In the context of *in vitro* internalisation assay, ThermoLuc EVs indicated a dose-dependent internalisation in Huh7 and B16F10 cells.

NanoLuc labelling was used to conduct *in vivo* biodistribution experiments, assessing the pharmacokinetics of MSCs-EVs. Administering CD63 NanoLuc MSC-EVs into mice resulted in rapid elimination of the labelled EVs from circulation (90% of the dose was eliminated in 5 minutes). NanoLuc labelled EVs rapidly accumulated in different organs (brain, thymus, lung, heart, diaphragm, liver, spleen, pancreas, kidneys, intestine, muscle, and bone marrow) within 5 minutes. Most of the NanoLuc EVs accumulated in the spleen and liver, indicating a swift uptake and immune clearance by macrophages[273] of the NanoLuc EVs. However, *in vivo* biodistribution profile of NanoLuc EVs is influenced by its interaction with plasma components. Administering EVs through other routes (peroral or intracerebral) exhibited minimal systemic dissemination. Altogether, this study underscores the potential of NanoLuc labelling in enhancing the pharmacokinetics of MSCs-EVs.

While NanoLuc EVs are rapidly internalised by most of the tissues within 5 minutes, the rate at which the signal degraded varied across the different tissues. This is likely in relation to variations in the cellular uptake of EVs within these tissues. NanoLuc signal rapidly decreased over time, ultimately resulting in either no signal or a significantly diminished signal 24 hours after injection. NanoLuc labelling offers a precise and highly sensitive measurement of EVs *in vivo* and *in vitro*. But the rapid *in vivo* clearance of the NanoLuc substrate limits its application for non-invasive imaging studies. Hence, ThermoLuc labelling was employed to achieve non-invasive imaging of EV biodistribution. The pharmacokinetics of Thermoluc EVs was found to be comparable to that of NanoLuc, whereby a significant portion of EVs were internalised in spleen, lung, and liver 30 seconds post-administration, subsequently leading to the gradual degradation of the payload over time. In contrast, lipophilic dyes have a half-life of five to more than 100 days, which may result in inaccurate conclusions of EV biodistribution in various tissues [273].

Thus, Nano- and Thermo-luciferase are highly effective for monitoring EVs in *vivo* and *in vitro*. It allows for endogenous labelling as well as the assessment of the protein cargo's integrity. This labelling method enables the accurate visualization of the EVs' half-life. Given its high sensitivity and capacity to accurately capture the spatiotemporal characteristics *in vivo*, this labelling technique has potential applications to track engineered EVs *in vivo*. Particularly, it will be helpful to determine EV half-life and monitor the targeted delivery of EVs.

4.2 Paper II

EVs are naturally occurring nanoparticles with potential applications in drug delivery. Enhancing the encapsulation efficiency of EVs is imperative for the efficient use of EVs as a nano-delivery system. Electroporation is a widely employed technique to load drugs in EVs [243], [276]. However, current electroporation protocols are limited in their drug loading efficiency. Therefore, we optimised the protocol to improve the encapsulation efficiency of EVs.

Doxorubicin (DOX) is a commonly used chemotherapeutic agent belonging to the group of anthracyclines that intercalates with DNA base pairs and inhibits topoisomerase II. In addition to its function as a chemotherapeutic drug, doxorubicin also displays fluorescent characteristics, which were utilised in this study. Here, we optimised parameters to enhance the encapsulation efficiency, and loading capacity of EVs, and to improve EV recovery rates, and the efficacy of the drug.

We isolated EVs as reported in previous studies[277] and initially optimised the procedure for recovering intact EVs from storage. Generally, rapid thawing techniques preserve cellular membrane integrity and minimise the adverse effects of osmotic stress and ice recrystallisation[278]. We found that the process of quick thawing at RT enhanced EV recovery by 50% compared to thawing on ice.

Next, we tested the optimal concentration of EVs and DOX to maximise the encapsulation efficiency. We eliminated free doxorubicin from the sample by SEC to precisely measure DOX enclosed within the EVs. Crucial parameters for effective electroporation are the sample composition and fine-tuning the proportions of EVs and DOX. We found a positive link between the total volume of loaded DOX, the initial concentration of EVs on the recovery of DOX-loaded EVs. This correlation was evident until 1 mM:5×10^{11}, drug: EV ratio. A plateau was reached following this drug: EV ratio, possibly due to the constrained payload capacity of

EVs. The ratio employed for electroporation is considerably variable across the previous studies[279].

We used 5×10^{11}, 1×10^{11}, or 5×10^{10} EVs together with 2.0 mM of DOX for the electroporation procedure. There was a direct correlation between the quantity of EVs that led to the recovery of DOX-loaded EVs. However, the highest number of EVs that could be loaded per EV was 1×10^{11}, with a concentration of 0.42 µM per 1×10^{9} EVs. Our results demonstrate that optimal concentrations of EVs results in better overall loading efficiency. In contrast, a higher concentration of EVs results in a higher proportion of recovery. Notably an inverse relationship between effective loading and recovery indicates that decreased recovery was linked to enhanced effective loading.

Previous studies have demonstrated that using various electroporation buffers to stabilise EVs before and after electroporation resulted in satisfactory EV recovery[280], [281]. However, when compared to our optimised buffers, these buffers resulted in poor loading of DOX in EVs. We found that the electroporation buffer with 400 mM sucrose exhibited better loading efficiency. Additionally, this buffer improved EV recovery after electroporation. The EVs retained their ability to efficiently transport and deliver therapeutic cargo in a controlled environment, indicating that the structural integrity and biological function of EVs remain intact in this buffer. Then, we optimised the electroporation voltage to load DOX into EVs in the optimised buffer.

We subsequently verified the adaptability of the optimised electroporation protocol on EVs isolated from different cell types. We observed comparable recovery and efficient loading levels across EVs isolated from two different cell lines (HEK293, B16F10). Further, DOX-loaded EVs generated from both cell lines exhibited comparable performance in vitro, providing further evidence for the universal adaptability of this technique. Doxorubicin-loaded EVs showed a 190-fold increase in effectiveness compared to doxorubicin alone. Additionally, EVs loaded with DOX using electroporation showed two-fold higher than Lipodox, a commercial DOX loaded liposome.

The optimised electroporation settings improved the encapsulation and loading efficiency, and enhanced the recovery of intact EVs. Nevertheless, we observed that specific electroporation settings resulted in a discernible alteration in the colouration of the samples, transitioning from red to purple. A comparable alteration in colour has already been observed with free DOX and was ascribed to a possible chemical cleavage of amino sugars crucial for the active component. This cleavage is believed to modify the chemical characteristics and, perhaps, the bioactivity of the medication[282]. One possible suggestion is that the observed result was due to the electroporation cuvettes used. Previous studies have demonstrated that the electrodes in these cuvettes release aluminium cations into the sample when subjected to high-intensity electric pulses. Furthermore, it has been proved that DOX changes colour following excessive interaction with aluminium[241]. Nevertheless, it is worth noting that many factors, such as non-physiological pH, light exposure, and alkaline interactions, have been linked to comparable effects observed with DOX. Consequently, it is essential to consider a range of alternative possibilities[283], [284]. Through our evaluation of DOX treated using various loading processes, we established that the loading condition could impact the fluorescence properties and effectiveness of DOX in its unmodified form. We concluded that our method had a minimal effect on the characteristics above. This emphasises the need to consider cargo degradation, even in the case of stable molecules, and further demonstrates the benefits of our proposed streamlined methodology.

EVs have been identified as a practical platform for drug delivery due to their inherent biocompatibility and intrinsic capacity to target specific cells and tissues[285]. Here, we aimed

to comprehensively enhance the existing electroporation procedure to boost loading efficiency, recovery, and drug potency *in vitro*. Our results demonstrated a significant improvement in drug potency, achieving a 190-fold increase compared to the administration of naked DOX. Furthermore, the optimised protocol's potency was twice as effective as that of the liposomal formulation of DOX (lipodox). Our results align with those of previous studies that have shown the enhanced therapeutic efficacy of small chemotherapeutic molecules when encapsulated within EVs, compared to unencapsulated chemotherapy *in vitro*. These findings hold significant promise for future studies in EV-based drug delivery.

4.3 Paper III

Fc-engineered extracellular vesicles (Fc-EV) technology combines EVs' therapeutic capabilities with the efficacy of monoclonal antibodies[239], [286]. It allows for interchangeable antibodies tailored to specific tissues, where the EV surface is modified to bind to the Fc region of antibodies. Cells producing EVs are genetically modified to express EV sorting proteins fused to FC binders. Imaging flow cytometry (IFC) was used to detect antibody binding to EVs at the individual vesicle level[172], with tetraspanins, specifically CD63 C-terminal fusions, demonstrated superior performance to other EV sorting domains in terms of the number of positive events (mNG tagged Fc EVs) per millilitre.

The characterisation of Fc-EVs was evaluated using NTA, EM, and SEC[126], [277]. The medium size was around 100 nm, and most mNG+ Fc- and control-EVs were found in their anticipated SEC fractions. Western blot analysis confirmed classical EV markers, CD63, TSG101[20], and the CD63-fused luminescent reporter Nano-Luc. Immunofluorescence microscopy confirmed the binding of antibodies to Fc-EVs with a dose-dependent binding pattern. The affinity of human IgG1 to Fc-EVs was exceptionally high, indicating successful engineering.

The stability of Fc-EVs was assessed using a stability assay with mouse or human plasma. The mNG+ve Fc-EVs were incubated with APC-labelled IgG and exposed to either PBS or human or mouse plasma. The flow cytometry analysis showed that the double positive EVs (mNG & APC) Fc-EV: IgG complexes remained unaltered.

The Fc-EVs exhibited potent antibody binding, obviating the need for additional functionalisation. The EV-bound APC tagged IgG co-localised with mNG+ve Fc-EVs in HeLa cells, while no antibodies were detected when cells were exposed to naked IgG or a combination of mNG+ve control-EVs. A single-particle profiler (SPP)[287] was used to quantify the number of antibodies bound per Fc-EV. Various characterisation techniques demonstrated effective and consistent binding of antibodies to Fc-EVs, confirming the potential of targeted delivery of antibody-tagged Fc-EVs in *in vitro* and *in vivo* studies.

An in vitro assessment of Fc-EV technology demonstrated its diverse capabilities in treating cancer. The oncogene HER2, a biomarker and therapeutic target in multiple cancer types, was evaluated in HER2-positive breast cancer cells[288]. The HER2 antibody Trastuzumab, commonly used in clinical settings, increased EV uptake in HER2-EVs by 339-fold. However, pre-treatment with free Trastuzumab reduced EV internalisation, indicating the system's specificity and antibody's ability to facilitate increased cellular uptake. Nevertheless, the decline was relatively small, perhaps attributed to the fast recycling of HER2[289]. We then explored the effectiveness of targeting PD-L1, a well-known immune checkpoint, in enhancing Fc-EV uptake against malignant melanoma cells (B16F10) in vitro. Atezolizumab, a PD-L1 antibody, significantly increased EV uptake in B16F10 cells, a common in vivo model for melanoma

tumours[290]. The cells were stimulated with interferon-gamma (IFNγ)[291], resulting in a 509-fold increase in Fc-EV uptake when guided by Atezolizumab.

Next, we tested the potential of Fc-EVs in mice with B16F10 tumours. The administration of NanoLuc+ve Fc-EVs alone or in combination with PD-L1-Ab (Atezolizumab) resulted in a significant increase in Fc-EV+ PD-L1-Ab accumulation within tumours, approximately 46-fold higher than Fc-EVs alone at 30 minutes. The isotype control did not change the accumulation of Fc-EVs in tumours. The spleen exhibited reduced levels of EVs, while a marginal decline was observed in the liver for Fc-EV+PD-L1-Ab compared to Fc-EV+IgG-ctrl. The modified tissue distribution confirms the effective targeting of Fc-EV+PD-L1-Ab, with a higher concentration in tissues that expressed PD-L1 and seemingly lower uptake in the spleen and liver. Consistent with the results in paper I, the plasma half-life of Fc-EVs was found to be 3-4 minutes. There was no notable distinction in half-life between Fc-EVs alone or when presenting PD-L1-Ab or IgG-ctl.

In parallel, regional lymph nodes were enriched with PD-L1-Ab bound Fc-EVs. These findings align with the discovery that immune cells in lymph nodes that tumours have influenced an increase in the expression of PD-L1, which limits the immune response against tumours and is considered a significant target for cancer therapy[292]. The study found that the liver and spleen had fewer EVs when Fc-EV+PD-L1-Ab was present than when Fc-EV+IgG-ctrl was present. This demonstrates the efficacy of targeting by showing increased accumulation in PD-L1-positive tissue and decreased uptake in the spleen and liver. The liver and spleen are components of the mononuclear phagocyte system (MPS), which is responsible for removing non-specific nanoparticles[293]. The continuous and heightened buildup corresponds to the improved ability of nanoparticles to pass through and stay in the body, known as the enhanced permeability and retention (EPR) effect[294]. This emphasises the potential use of PD-L1-Ab, showing Fc-EVs as a targeted therapy for cancer.

It was also shown that the predominant population of immune cells within the tumour consisted of CD3+ T-cells, wherein 99% of these T-cells were identified as CD3+CD8-. It also showed that 95% of these T-cells were PD-L1+. It is worth mentioning that T cells expressing PD-L1 have been demonstrated to have various suppressive effects on the immune response against tumours. Therefore, they represent a potentially significant target for cancer treatments[295]. As predicted, Fc-EVs exhibited a notable increase in abundance within the population of PD-L1+ T-cells when directed by PD-L1-Ab. There was no observed disparity in the uptake of Fc-EVs among B-cells, monocytes, and macrophages. Furthermore, these cell types exhibited a lower PD-L1 expression than the T-cells.

Moreover, to evaluate the broader applicability of Fc-EVs in targeting tumours, a xenograft mouse model was used to evaluate the applicability of Fc-EVs for tumour targeting involving SKBR-3 cells in the mammary gland[296]. The tumour accumulation of Fc-EV+HER2-Ab was lower than that for PD-L1 targeting in B16F10, which was attributed to smaller tumour sizes and lower cell proportions in dissected SKBR3 tumours.

The efficacy of chemotherapeutic drugs in melanoma animal models and patients is often limited due to the substantial, possibly lethal doses required to achieve a therapeutic outcome [297]. To address this issue, the implementation of targeted therapies is imperative. Here, electroporation was exploited to introduce the chemotherapy drug DOX into Fc-EVs based on the findings of paper II. This method exhibited strong efficacy in loading and retrieving EVs, enhancing drug effectiveness and notable cytotoxic effects on B16F10 cells as shown in paper II. Mice bearing B16F10 were then treated with PD-L1 Ab tagged Fc-EVs containing DOX, resulting in notable inhibition of tumour advancement and enhanced survival rates. The

combination therapy results demonstrated a 100% survival rate at the designated endpoint of 20 days, in contrast to the 35% survival rate observed in mice that received a mock treatment.

Thus, our Fc-EV technology presents a practical and specific therapeutic approach by combining EVs with antibody-targeted therapy. Targeting and therapeutic antibodies enable the precise delivery of EVs carrying therapeutic cargo, promoting a synergistic therapeutic effect. Its applications are not restricted solely to classical antibodies but can also encompass Fc-fused proteins, antibody-drug conjugates, and bi-specific antibodies, among others. Future investigations on the Fc-EV concept will explore its therapeutic potential and facilitate translation into clinical applications.

4.4 Paper IV

Cellular communication plays a crucial role in the development of cancer, allowing tumour cells to change the activity of nearby or distantly located stromal and immune cells[298], [299]. Tumour-derived EVs (tEVs) have been linked to various aspects of tumour induced immunosuppression, including the inactivation of NK and T cell anti-tumour activity, the inhibition of dendritic cell maturation, the stimulation of MDSC growth, and macrophage polarization[300]. Furthermore, haematopoiesis dysregulation, as well as the presence of immature myeloid and erythroid immunosuppressive cells, are important hallmarks of the immune escape phase of cancer growth.

Here, we aimed to elucidate the of EVs originating from cancer cells to the progression of the immune escape phase during cancer immunoediting. The primary objective of our study was to examine the role of tEVs in the impairment of haematopoiesis, a well-documented phenomenon associated with diverse immunosuppressive characteristics[300]. The preliminary results of our investigation revealed that EVs isolated from B16F10 cells exhibited a size distribution spanning from 100 to 200 nm. The tEVs presented CD63, CD9, and Alix proteins on their surface and displayed a spherical morphology characterised by a lipid bilayer membrane adorned with proteins. The physical, chemical, and morphological attributes described closely correspond to the typical features observed in small EVs, such as exosomes and microvesicles [301]. Therefore, akin to tEVs and soluble factors derived from tumour cells, can facilitate intercellular communication in tumour progression and the evasion of immune responses. In agreement with this concept, our protein profiling analysis revealed that the cell culture media and extracellular vesicles derived from B16F10 cells exhibited a similar composition of angiogenic factors. It is worth mentioning that Vascular Endothelial Growth Factor (VEGF), Osteopontin, Tissue Factor, ADAMTS1, Endoglin, Platelet-Derived Growth Factor (PDGF), Placental Growth Factor (PIGF), Thrombospondin-2 (TSP-2), and Tissue Inhibitor of Metalloproteinase-1 (TIMP-1), were identified as the predominant factors in both types of samples. Indeed, a majority of these factors, specifically VEGF, Osteopontin, PIGF, and PDGF have also been detected in individuals diagnosed with melanoma[302]–[304]. Therefore, in the phase of immune escape, the tumour cells' abnormal release of angiogenic factors, whether in a soluble state or incorporated into EVs, can have a detrimental impact on the cellular components and functions of remote organs. Consistent with this observation, mice with advanced melanoma displayed an enlarged spleen and a noticeable paleness in the liver, kidney, and lungs.

Furthermore, previous research has provided evidence indicating a correlation between liver pallor, metabolic dysfunction in the liver, and the development of fatty liver disease, specifically in mice with B16F10 melanoma[196]. The results of this study show a correlation between the occurrence of splenomegaly and the onset of tumour-induced extramedullary

haematopoiesis (EMH), which is characterised by the proliferation of granulocytic myeloid-derived suppressor cells (G-MDSCs) and endothelial progenitor cells (EPCs). Moreover, the diminished cell population and compromised erythropoiesis mechanism in the bone marrow could also be ascribed to the anomalous secretion of angiogenic factors originating from B16F10 cells.

Our research showed that administering tEV cells disrupted the process of haematopoiesis. This disruption resulted in characteristics similar to those observed during the immune escape phase of tumour development. It is worth noting that cancer cells can release EVs that can systematically impact the function of nearby and distant organs. As an example, mice that were administered tEVs demonstrated extramedullary haematopoiesis (EMH), decreased bone marrow cell count, expansion of G-MDSCs in the medullary region, and the onset of anaemia. These findings were similar to those in mice afflicted with advanced melanoma. Subsequent *in vivo* experiments revealed that the tEVs harboured factors responsible for the disruption of haematopoiesis, and these factors exhibited sensitivity to heat. For further confirmation, we briefly exposed them to 100℃, which effectively counteracted the proliferation of G-MDSCs induced by tEVs in the bone marrow cell culture. This suggests that one or more components within tEVs may regulate the initiation of haematopoiesis dysregulation. Within this context, our findings indicate that the presence of VEGF, the most prevalent angiogenic factor on tEVs, may be such a component. For example, previous studies have demonstrated that the continuous infusion of VEGF can effectively suppress the maturation of dendritic cells while simultaneously promoting the proliferation of G-MDSCs and B cells[305]. Additional research has revealed that the VEGF triggers the accumulation of G-MDSCs by binding to its receptor VEGFR1 and uses VEGFR2 to support the proliferation of B cells[306].

Moreover, previous studies have shown that VEGF triggers erythropoietin production in the kidney, liver, and spleen, irrespective of hypoxia conditions. This process ultimately contributes to the emergence of extramedullary erythropoiesis[307]. Following these observations, our *ex vivo* investigations have demonstrated that EVs originating from melanoma cells can autonomously stimulate the proliferation of bone marrow G-MDSCs and B cells while concurrently diminishing the prevalence of cells associated with the erythropoietic lineage. Significantly, our *ex vivo* investigation demonstrated a substantial reduction in the effectiveness of tEVs when subjected to 56°C and when the VEGFR on the BM cells was obstructed. These findings suggest the direct involvement of VEGF, a protein component found in tEVs, in the initiation of dysregulated haematopoiesis.

Our study demonstrated the significant involvement of tEVs in facilitating indirect intercellular communication, leading to the dysregulation of haematopoiesis. This phenomenon is observed during the process of immune evasion. Moreover, we found that tEVs with high levels of angiogenic factors, specifically VEGF, could modify the haematopoiesis process in primary and secondary immune organs. Hence, it is imperative that future studies are aimed at promoting tEV production to mitigate the immune escape phase and avert dysregulation of haematopoiesis during cancer progression.

5. FUTURE PERSPECTIVES

In recent decades, the field of EVs has made significant advancements, transitioning from being perceived as insignificant to being recognised as crucial facilitators in cell-to-cell communication. Due to their distinctive ability to transport bioactive molecules across cellular barriers, EVs are considered promising in medication delivery. Significantly, EVs surpass many artificial delivery vectors in effectiveness, delivery to areas outside the liver, and have reduced toxicity compared to other drug delivery vehicles. Multiple clinical trails employing EVs as a therapeutic intervention have shown their compatibility with living organisms. However, these trials have failed to achieve the desired outcome, showing significant gaps in our understanding of EVs.

Despite the growing abundance of knowledge on EVs, research in this field is still nascent, and technological and biological constraints must be resolved. The technical restrictions mostly revolve around the manufacturing, purification, and quantification of EVs. Hence, it is imperative to generate methods that enable the ability to mass manufacture EVs with utmost purity, while preserving their reliability and properties. Moreover, the standardisation of quantification is a crucial feature that needs to be more consistent within the field. Hence, exploring alternate EV bioactive cargo quantification methods, or EV potency experiments, is imperative.

In addition, the loading methods for EVs as drug carriers can be broadly categorised into pre- and post-separation cargo loading. Various loading methods yield varying levels of loading efficiencies and stabilities. Currently, the endogenously loaded methods are the preferred approach for gene therapy. Moreover, modification of EV surfaces enhances their inherent characteristics and targeting capabilities, enhancing their potential in biomedical applications. Nevertheless, this technique may result in gene alteration of producer cells. Although electroporation is widely considered the preferred exogenous technique, it may compromise the integrity of the cellular membrane. Regardless of the chosen loading technique, challenges persist in achieving high loading efficiency, preserving membrane texture, and preventing degradation or inactivation of the loaded cargo. In future research endeavours, mitigating the drawbacks mentioned to the greatest extent possible while simultaneously combining the benefits and formulating an optimal approach for efficient cargo loading is imperative.

From a biological perspective, tEVs can dysregulate haematopoiesis and modulate the immune process. It is worth noting that further studies are needed to investigate other potential roles of tEVs in addition to haematopoiesis dysregulation. For example, they could be potential targets for therapeutics and exploited as biomarkers in liquid biopsies, aiding early detection. Further, our understanding of biological EVs is crucial for their potential therapeutic uses. The choice of cell source for EV synthesis can affect their targeting within living organisms and their ability to modulate the immune system. Despite different technological challenges, progress has been made, and medicines based on EVs may eventually be available. Therefore, a comprehensive understanding of EVs' key components is essential for future therapeutic applications.

6. ACKNOWLEDGEMENTS

I express my most significant appreciation and recognise the invaluable help rendered by individuals who have contributed significantly to the successful completion of my doctoral degree over the past five years. Initially, I would like to express my gratitude and thank the divine entity, the Lord of the universe, God (Allah), for the abundant blessings and boundless mercy I have received during my doctoral studies.

I sincerely appreciate and thank my supervisor, **Dr. Oscar Wiklander**, for your guidance and assistance with my study. I also appreciate the opportunity to enhance and improve my current skill set. Under your guidance, I have learned to push my boundaries rather than restrict my challenges. I learned to see the forest for what it is, not just the trees. I appreciate your knowledge, invaluable advice, support, and brilliant ideas.

My special gratitude is expressed to my former supervisor and co-supervisor, Professor **Samir El Andaloussi**. I would like to express my appreciation for the chance to join your research group and continue my doctoral studies at Karolinska Institutet. I am grateful for your guidance, leadership, and generous support during my research.

I sincerely thank my co-supervisor and his family, **Dr. Dara Mohamad.** Thank you for arranging an interview with Professor El-Andaloussi for this Ph. D position. Thank you for your unwavering scrutiny and intellectual contribution to the research. I always saw our connection as a friendship rather than as a co-supervisor and student.

Thanks to my co-supervisor, **Dr. Andre Görgens**, for your generosity in providing comments, invaluable advice, assistance, and recommendations during my Ph. D studies.

My heartfelt gratitude goes to **Dr. Manucher Abedi**, a unique and devoted friend. You are a wonderful and supportive person. I am pleased to have met you.

Dr. Alamdar Hussain, I am eternally grateful for your advice, aid, and encouragement.

I am deeply thankful to my closest friend and his family, **Safa**. You were always accessible. Thank you for the great time I had with you, and best wishes with your Ph.D.

Special thanks to all current and previous members of the BMM family:

Manuela (Thank you for presenting the lab instructions and assisting with NTA and TFF), **Ming** (Thank you for the scientific conversations and advice), **Joel** (I appreciate your scientific discussion), **Wenyi** (Thank you for your generous assistance and scientific discussion), **Daniel** (Thank you for engaging in scientific conversations), **Svetlana** (Many thanks for the help and being a great company in the lab), **Rim** (Thank you for your assistance with cell culture), **Antje** (Thank you for your assistance with cloning).

Kariem (I appreciate the joy you brought us with your drumming)**, Osama** (Thanks for your kindness and help), **Dhanu** (Thank you for your assistance with cell sorting and scientific discussion), **Angus** (Thank you for working with me to have the first paper published)**, Samantha** (Many thanks for the cookies and help), **Julia**, **Oskar**, **and Jeremy** (Thank you for your help), **Tobz**, **Hema**, **and Gina** (Thank you for your help and being a great company in the

lab), **Risul**, **Giulia**, **Yesid**, **Malgorzata**, **Lisa**, **Tom**, **Annamaria** (Thank you for your help), **Mariana**, **Guannan**, **Carleen**, **Roberta**, **Roger**, **and Mattias.**

I want to thank everyone in Nordin's group for their kindness and the warm environment when I worked in the lab. **Juliette** (Thank you for being such a social person in the lab), **Zankruti**, **Yawen**, **Juan**, **Houze**, **Eric**, **Radek**, **Yong**, **and Yang**.

I want to thank all the people in the MCG, especially **Ted, Rula, Tony, Abdulrahman, Laia, Karin**, **Negin**, **Raul** (Thank you for your help), **Qing**, **Salome**, **Anna**, **and Brisejda**.

A special thanks to **Theresia**, **Carolina**, **Daria**, **Kathrin**, **Kirsti**, **Isa, Saliha**, **Tomas**, **and Moustapha Hassan's group**.

I want to thank my college teachers and colleagues**, Dr. Mazhar**, **Dr. Abbas**, **Dr. Khder**, **and Dr. Ramiar**, for being a pain relief during my PhD.

I am eternally grateful to my father, **Rashid Mamand**, and mother, **Zahida Qader**, for your unending love and care from the first day of elementary school until now. I would also like to thank my sister and brothers for their help.

I thank all my **nieces**, **nephews**, **uncles**, **aunts**, **and cousins.**

I want to convey my deep admiration and gratitude to my extraordinary and adored wife, **Aven**, for your patience, support, and infinite affection. You have a fantastic personality. I am very proud of you. You were tolerating and caring for three children as well as myself. By establishing a pleasant environment at home, you enabled individuals to leave work early and return home. My children, **Astera**, **Brusk**, and **Baran**, provide a source of solace and relief from the demands of my professional tasks, adding a sweet and reassuring atmosphere to my life. All of you have my best wishes for a happy future.

7. REFERENCES

[1] M. Yáñez-Mó *et al.*, "Biological properties of extracellular vesicles and their physiological functions," *J. Extracell. Vesicles*, vol. 4, pp. 1–60, 2015.

[2] E. CHARGAFF and R. WEST, "The biological significance of the thromboplastic protein of blood.," *J. Biol. Chem.*, vol. 166, no. 1, pp. 189–197, 1946.

[3] P. Wolf, "The nature and significance of platelet products in human plasma.," *Br. J. Haematol.*, vol. 13, no. 3, pp. 269–288, 1967.

[4] E. Bonucci, "Fine structure and histochemistry of 'calcifying globules' in epiphyseal cartilage," *Zeitschrift für Zellforsch. und Mikroskopische Anat.*, vol. 103, no. 2, pp. 192–217, 1970.

[5] H. C. Anderson, "Vesicles associated with calcification in the matrix of epiphyseal cartilage.," *J. Cell Biol.*, vol. 41, no. 1, pp. 59–72, 1969.

[6] E. A. Nunez, J. Wallis, and M. D. Gershon, "Secretory processes in follicular cells of the bat thyroid. 3. The occurrence of extracellular vesicles and colloid droplets during arousal from hibernation." *Am J Anat.*, vol. 141, no. 2, pp.179-201,1974.

[7] R.L. Chandler, R.G. Bird, and A.P. Bland, "PARTICLES ASSOCIATED WITH MICROVILLOUS BORDER OF INTESTINAL MUCOSA," *THE LANCET*, Vol. 306, no. 7941, pp. 931–932, 1975.

[8] A. J. Dalton, "Microvesicles and vesicles of multivesicular bodies versus 'virus like' particles," *J. Natl. Cancer Inst.*, vol. 54, no. 5, pp. 1137–1148, 1975.

[9] J. B. Stevens, "Membrane fragments with koinozymic properties released from villous adenoma of the rectum" *THE LANCET*, vol. 306, no. 7946, pp. 1161–1220, 1975.

[10] E. W. Benz and H. L. Moses, "Brief communication: Small, virus-like particles detected in bovine sera by electron microscopy," *J. Natl. Cancer Inst.*, vol. 52, no. 6, pp. 1931–1934, 1974.

[11] R. M. Johnstone, M. Adam, J. R. Hammond, L. Orr, and C. Turbide, "Vesicle formation during reticulocyte maturation. Association of plasma membrane activities with released vesicles (exosomes).," *J. Biol. Chem.*, vol. 262, no. 19, pp. 9412–9420, 1987.

[12] C. Harding, J. Heuser, and P. Stahl, "Receptor-mediated endocytosis of transferrin and recycling of the transferrin receptor in rat reticulocytes.," *J. Cell Biol.*, vol. 97, no. 2, pp. 329–339, 1983.

[13] B. T. Pan and R. M. Johnstone, "Fate of the transferrin receptor during maturation of sheep reticulocytes in vitro: Selective externalization of the receptor," *Cell*, vol. 33, no. 3, pp. 967–978, 1983.

[14] H. F. Dvorak *et al.*, "Tumor shedding and coagulation," *Science*, vol. 212, no. 4497, pp. 923–924, 1981.

[15] B. Stegmayr and G. Ronquist, "Promotive effect on human sperm progressive motility by prostasomes," *Urol. Res.*, vol. 10, no. 5, pp. 253–257, 1982.

[16] G. Raposo *et al.*, "B lymphocytes secrete antigen-presenting vesicles," *J. Exp. Med.*, vol. 183, no. 3, pp. 1161–1172, 1996.

[17] M. Mack *et al.*, "Transfer of the chemokine receptor CCR5 between cells by

membrane- derived microparticles: A mechanism for cellular human immunodeficiency virus 1 infection," *Nat. Med.*, vol. 6, no. 7, pp. 769–775, 2000.

[18] T. Rozmyslowicz *et al.*, "Platelet- and megakaryocyte-derived microparticles transfer CXCR4 receptor to CXCR4-null cells and make them susceptible to infection by X4-HIV," *Aids*, vol. 17, no. 1, pp. 33–42, 2003.

[19] E. van der Pol, A. N. Böing, E. L. Gool, and R. Nieuwland, "Recent developments in the nomenclature, presence, isolation, detection and clinical impact of extracellular vesicles," *J. Thromb. Haemost.*, vol. 14, no. 1, pp. 48–56, 2016.

[20] C. Théry *et al.*, "Minimal information for studies of extracellular vesicles 2018 (MISEV2018): a position statement of the International Society for Extracellular Vesicles and update of the MISEV2014 guidelines," *J. Extracell. Vesicles*, vol. 7, no. 1, 2018.

[21] E Van der Pol, AN Böing, P Harrison, A Sturk, and R Nieuwland, "Classification , Functions , and Clinical Relevance of Extracellular Vesicles," *Pharmacol. Rev.*, vol. 64, no. 3, pp. 676–705, 2012.

[22] Y. Zhang, Y. Liu, H. Liu, and W. H. Tang, "Exosomes : biogenesis , biologic function and clinical potential," *Cell Biosci.*, vol. 9, pp. 1–18, 2019.

[23] E. G. Trams, C. J. Lauter, J. Norman Salem, and U. Heine, "Exfoliation of membrane ecto-enzymes in the form of micro-vesicles," *BBA - Biomembr.*, vol. 645, no. 1, pp. 63–70, 1981.

[24] T. Kajimoto, T. Okada, S. Miya, L. Zhang, and S. I. Nakamura, "Ongoing activation of sphingosine 1-phosphate receptors mediates maturation of exosomal multivesicular endosomes," *Nat. Commun.*, vol. 4, 2013.

[25] M. Babst, D. J. Katzmann, E. J. Estepa-Sabal, T. Meerloo, and S. D. Emr, "ESCRT-III: An endosome-associated heterooligomeric protein complex required for MVB sorting," *Dev. Cell*, vol. 3, no. 2, pp. 271–282, 2002.

[26] K. Tamai *et al.*, "Biochemical and Biophysical Research Communications Exosome secretion of dendritic cells is regulated by Hrs , an ESCRT-0 protein," *Biochem. Biophys. Res. Commun.*, vol. 399, no. 3, pp. 384–390, 2010.

[27] S. Stuffers, C. S. Wegner, H. Stenmark, and A. Brech, "Multivesicular Endosome Biogenesis in the Absence of ESCRTs," *Traffic*, vol. 10, no. 7, pp. 925–937, 2009.

[28] W. M. Henne, N. J. Buchkovich, and S. D. Emr, "Review The ESCRT Pathway," *Dev. Cell*, vol. 21, no. 1, pp. 77–91, 2011.

[29] J. H. Hurley, "ESCRTs are everywhere," *EMBO J.* vol. 34, no. 19, pp. 2398–2407, 2015.

[30] X. Li *et al.*, "Biogenesis and function of multivesicular bodies in plant immunity," *Front. Plant Sci.*, vol. 9, pp. 1–7, 2018.

[31] H. Teo *et al.*, "ESCRT-I Core and ESCRT-II GLUE Domain Structures Reveal Role for GLUE in Linking to ESCRT-I and Membranes," *Cell*, vol. 125, no. 1, pp. 99–111, 2006.

[32] K. Trajkovic *et al.*, "Ceramide triggers budding of exosome vesicles into multivesicular endosomes," *Science*, vol. 319, no. 5867, pp. 1244-1247, 2008.

[33] R. Wubbolts *et al.*, "Proteomic and biochemical analyses of human B cell-derived

exosomes: Potential implications for their function and multivesicular body formation," *J. Biol. Chem.*, vol. 278, no. 13, pp. 10963–10972, 2003.

[34] S. I. Buschow *et al.*, "MHC II In dendritic cells is targeted to lysosomes or t cell-induced exosomes via distinct multivesicular body pathways," *Traffic*, vol. 10, no. 10, pp. 1528–1542, 2009.

[35] A. Chairoungdua, D. L. Smith, P. Pochard, M. Hull, and M. J. Caplan, "Exosome release of β-catenin: a novel mechanism that antagonizes Wnt signaling," *J. Cell Biol.*, vol. 190, no. 6, pp. 1079–1091, 2010.

[36] S. N. Hurwitz, M. M. Conlon, M. A. Rider, N. C. Brownstein, and D. G. Meckes Jr, "Nanoparticle analysis sheds budding insights into genetic drivers of extracellular vesicle biogenesis," *J. Extracell. Vesicles*, vol. 5, no. 1,, 2016.

[37] G. Raposo and W. Stoorvogel, "Extracellular vesicles: Exosomes, microvesicles, and friends," *J. Cell Biol.*, vol. 200, no. 4, pp. 373–383, 2013.

[38] S. L. N. Maas, X. O. Breake, and A. M. Weaver, "Extracellular Vesicles : Unique Intercellular Delivery Vehicles," *Trends Cell Biol.*, vol. 27, no. 3, pp. 172-188, 2017.

[39] N. P. Hessvik and A. Llorente, "Current knowledge on exosome biogenesis and release," *Cell. Mol. Life Sci.*, vol. 75, no. 2, pp. 193–208, 2018.

[40] S. Xie, Q. Zhang, and L. Jiang, "Current Knowledge on Exosome Biogenesis, Cargo-Sorting Mechanism and Therapeutic Implications," *Membranes (Basel).*, vol. 12, no. 5, 2022.

[41] M. P. Zaborowski, L. Balaj, X. O. Breakefield, and C. P. Lai, "Extracellular Vesicles: Composition, Biological Relevance, and Methods of Study," *Bioscience*, vol. 65, no. 8, pp. 783–797, 2015.

[42] G. Van Niel, G. D'Angelo, and G. Raposo, "Shedding light on the cell biology of extracellular vesicles," *Nat. Rev. Mol. Cell Biol.*, vol. 19, no. 4, pp. 213–228, 2018.

[43] V. Muralidharan-Chari *et al.*, "ARF6-Regulated Shedding of Tumor Cell-Derived Plasma Membrane Microvesicles," *Curr. Biol.*, vol. 19, no. 22, pp. 1875–1885, 2009.

[44] C. D'Souza-Schorey and P. Chavrier, "ARF proteins: Roles in membrane traffic and beyond," *Nat. Rev. Mol. Cell Biol.*, vol. 7, no. 5, pp. 347–358, 2006.

[45] J. C. Akers, D. Gonda, R. Kim, B. S. Carter, and C. C. Chen, "Biogenesis of extracellular vesicles (EV): Exosomes, microvesicles, retrovirus-like vesicles, and apoptotic bodies," *J. Neurooncol.*, vol. 113, no. 1, pp. 1–11, 2013.

[46] J. F. Nabhan, R. Hu, R. S. Oh, S. N. Cohen, and Q. Lu, "Formation and release of arrestin domain-containing protein 1-mediated microvesicles (ARMMs) at plasma membrane by recruitment of TSG101 protein," *Proc. Natl. Acad. Sci. U. S. A.*, vol. 109, no. 11, pp. 4146–4151, 2012.

[47] J. M. Pasquet, J. Dachary-Prigent, and A. T. Nurden, "Calcium influx is a determining factor of calpain activation and microparticle formation in platelets," *Eur. J. Biochem.*, vol. 239, no. 3, pp. 647–654, 1996.

[48] T. Wang *et al.*, "Hypoxia-inducible factors and RAB22A mediate formation of microvesicles that stimulate breast cancer invasion and metastasis," *Proc. Natl. Acad. Sci. U. S. A.*, vol. 111, no. 31, 2014.

[49] E. Morita and W. I. Sundquist, "Retrovirus budding," *Annu. Rev. Cell Dev. Biol.*, vol.

20, pp. 395–425, 2004.

[50] S. Toné *et al.*, “Three distinct stages of apoptotic nuclear condensation revealed by time-lapse imaging, biochemical and electron microscopy analysis of cell-free apoptosis,” *Exp. Cell Res.*, vol. 313, no. 16, pp. 3635–3644, 2007.

[51] N. Gebara, A. Rossi, R. Skovronova, J. M. Aziz, A. Asthana, and B. Bussolati, “Extracellular Vesicles, Apoptotic Bodies and Mitochondria: Stem Cell Bioproducts for Organ Regeneration,” *Curr. Transplant. Reports*, vol. 7, no. 2, pp. 105–113, 2020.

[52] J. C. Mills, N. L. Stone, J. Erhardt, and R. N. Pittman, “Apoptotic membrane blebbing is regulated by myosin light chain phosphorylation,” *J. Cell Biol.*, vol. 140, no. 3, pp. 627–636, 1998.

[53] S. N. Hurwitz, M. A. Rider, J. L. Bundy, X. Liu, R. K. Singh, and D. G. Meckes, “Proteomic profiling of NCI-60 extracellular vesicles uncovers common protein cargo and cancer type-specific biomarkers,” *Oncotarget*, vol. 7, no. 52, pp. 86999–87015, 2016.

[54] F. G. Kugeratski *et al.*, “Quantitative proteomics identifies the core proteome of exosomes with syntenin-1 as the highest abundant protein and a putative universal biomarker, ” *Nature Cell Biology volume*, vol. 23, pp. 631–641, 2021.

[55] J. M. Escola, M. J. Kleijmeer, W. Stoorvogel, J. M. Griffith, O. Yoshie, and H. J. Geuze, “Selective enrichment of tetraspan proteins on the internal vesicles of multivesicular endosomes and on exosomes secreted by human B-lymphocytes,” *J. Biol. Chem.*, vol. 273, no. 32, pp. 20121–20127, 1998.

[56] Z. Andreu and M. Yáñez-Mó, “Tetraspanins in extracellular vesicle formation and function,” *Front. Immunol.*, vol. 5, pp. 1–12, 2014.

[57] C. V. Harding, J. E. Heuser, and P. D. Stahl, “Exosomes: Looking back three decades and into the future,” *J. Cell Biol.*, vol. 200, no. 4, pp. 367–371, 2013.

[58] E. Segura *et al.*, “ICAM-1 on exosomes from mature dendritic cells is critical for efficient naive T-cell priming,” *Blood*, vol. 106, no. 1, pp. 216–223, 2005.

[59] S. Bassani and L. A. Cingolani, “Tetraspanins: Interactions and interplay with integrins,” *Int. J. Biochem. Cell Biol.*, vol. 44, no. 5, pp. 703–708, 2012.

[60] N. Latysheva *et al.*, “Syntenin-1 Is a New Component of Tetraspanin-Enriched Microdomains: Mechanisms and Consequences of the Interaction of Syntenin-1 with CD63,” *Mol. Cell. Biol.*, vol. 26, no. 20, pp. 7707–7718, 2006.

[61] Y. Liang, W. S. Eng, D. R. Colquhoun, R. R. Dinglasan, D. R. Graham, and L. K. Mahal, “Complex N-linked glycans serve as a determinant for exosome/microvesicle cargo recruitment,” *J. Biol. Chem.*, vol. 289, no. 47, pp. 32526–32537, 2014.

[62] F. K. Fordjour, C. Guo, Y. Ai, G. G. Daaboul, and S. J. Gould, “A shared, stochastic pathway mediates exosome protein budding along plasma and endosome membranes,” *J. Biol. Chem.*, vol. 298, no. 10, p. 102394, 2022.

[63] D. K. Jeppesen *et al.*, “Reassessment of Exosome Composition,” *Cell*, vol. 177, no. 2, pp. 428-445.e18, 2019.

[64] S. Phuyal, N. P. Hessvik, T. Skotland, K. Sandvig, and A. Llorente, “Regulation of exosome release by glycosphingolipids and flotillins,” *FEBS J.*, vol. 281, no. 9, pp. 2214–2227, 2014.

[65] W. Fu *et al.*, “CAR exosomes derived from effector CAR-T cells have potent antitumour effects and low toxicity,” *Nat. Commun.*, vol. 10, no. 1, 2019.

[66] P. Arnold *et al.*, “Joint Reconstituted Signaling of the IL-6 Receptor via Extracellular Vesicles,” *Cells*, vol. 9, no. 5, 2020.

[67] N. Blanchard *et al.*, “TCR Activation of Human T Cells Induces the Production of Exosomes Bearing the TCR/CD3/ζ Complex,” *J. Immunol.*, vol. 168, no. 7, pp. 3235–3241, 2002.

[68] K. A. Adamczyk *et al.*, “Characterization of soluble and exosomal forms of the EGFR released from pancreatic cancer cells,” *Life Sci.*, vol. 89, no. 9–10, pp. 304–312, 2011.

[69] Q. Wang and Q. Lu, “Plasma membrane-derived extracellular microvesicles mediate non-canonical intercellular NOTCH signaling,” *Nat. Commun.*, vol. 8, no. 1, pp. 1–8, 2017.

[70] M. D. Keller *et al.*, “Decoy exosomes provide protection against bacterial toxins,” *Nature*, vol. 579, no. 7798, pp. 260–264, 2020.

[71] G. V. Shelke *et al.*, “Endosomal signalling via exosome surface TGFβ-1,” *J. Extracell. Vesicles*, vol. 8, no. 1, pp. 1–20, 2019.

[72] J. Liu *et al.*, “Extracellular vesicle PD-L1 in reshaping tumor immune microenvironment: biological function and potential therapy strategies,” *Cell Commun. Signal.*, vol. 20, no. 1, pp. 1–18, 2022.

[73] H. Rabesandratana, J. P. Toutant, H. Reggio, and M. Vidal, “Decay-accelerating factor (CD55) and membrane inhibitor of reactive lysis (CD59) are released within exosomes during in vitro maturation of reticulocytes,” *Blood*, vol. 91, no. 7, pp. 2573–2580, 1998.

[74] F. Lucien, V. Lac, D. D. Billadeau, A. Borgida, S. Gallinger, and H. S. Leong, “Glypican-1 and glycoprotein 2 bearing extracellular vesicles do not discern pancreatic cancer from benign pancreatic diseases,” *Oncotarget*, vol. 10, no. 10, pp. 1045–1055, 2019.

[75] C. Hsu *et al.*, “Regulation of exosome secretion by Rab35 and its GTPase-activating proteins TBC1D10A-C,” *J. Cell Biol.*, vol. 189, no. 2, pp. 223–232, 2010.

[76] M. D. Beckler *et al.*, “Proteomic analysis of exosomes from mutant KRAS colon cancer cells identifies intercellular transfer of mutant KRAS,” *Mol. Cell. Proteomics*, vol. 12, no. 2, pp. 343–355, 2013.

[77] K. Dooley *et al.*, “A versatile platform for generating engineered extracellular vesicles with defined therapeutic properties,” *Mol. Ther.*, vol. 29, no. 5, pp. 1729–1743, 2021.

[78] Y. Fang, N. Wu, X. Gan, W. Yan, J. C. Morrell, and S. J. Gould, “Higher-order oligomerization targets plasma membrane proteins and HIV Gag to exosomes,” *PLoS Biol.*, vol. 5, no. 6, pp. 1267–1283, 2007.

[79] S. M. Migliano, E. M. Wenzel, and H. Stenmark, “Biophysical and molecular mechanisms of ESCRT functions, and their implications for disease,” *Curr. Opin. Cell Biol.*, vol. 75, p. 102062, 2022.

[80] F. Ghafarian *et al.*, “The clinical impact of exosomes in cardiovascular disorders: From basic science to clinical application,” *J. Cell. Physiol.*, vol. 234, no. 8, pp. 12226–12236, 2019.

[81] C. Caruso Bavisotto *et al.*, "Exosomal HSP60: a potentially useful biomarker for diagnosis, assessing prognosis, and monitoring response to treatment," *Expert Rev. Mol. Diagn.*, vol. 17, no. 9, pp. 815–822, 2017.

[82] E. Y. Komarova *et al.*, "Hsp70-containing extracellular vesicles are capable of activating of adaptive immunity in models of mouse melanoma and colon carcinoma," *Sci. Rep.*, vol. 11, no. 1, pp. 1–16, 2021.

[83] R. A. Sager *et al.*, "Targeting extracellular Hsp90: A unique frontier against cancer," *Front. Mol. Biosci.*, vol. 9, pp. 1–13, 2022.

[84] S. Gill, R. Catchpole, and P. Forterre, "Extracellular membrane vesicles in the three domains of life and beyond," *FEMS Microbiol. Rev.*, vol. 43, no. 3, pp. 273–303, 2019.

[85] J. Skog *et al.*, "Glioblastoma microvesicles transport RNA and proteins that promote tumour growth and provide diagnostic biomarkers," *Nat. Cell Biol.*, vol. 10, no. 12, pp. 1470–1476, 2008.

[86] H. Valadi, K. Ekström, A. Bossios, M. Sjöstrand, J. J. Lee, and J. O. Lötvall, "Exosome-mediated transfer of mRNAs and microRNAs is a novel mechanism of genetic exchange between cells," *Nat. Cell Biol.*, vol. 9, no. 6, pp. 654–659, 2007.

[87] J. Ratajczak *et al.*, "Embryonic stem cell-derived microvesicles reprogram hematopoietic progenitors: Evidence for horizontal transfer of mRNA and protein delivery," *Leukemia*, vol. 20, no. 5, pp. 847–856, 2006.

[88] P. Sansone *et al.*, "Packaging and transfer of mitochondrial DNA via exosomes regulate escape from dormancy in hormonal therapy-resistant breast cancer," *Proc. Natl. Acad. Sci. U. S. A.*, vol. 114, no. 43, pp. E9066–E9075, 2017.

[89] E. R. Abels and X. O. Breakefield, "Introduction to Extracellular Vesicles: Biogenesis, RNA Cargo Selection, Content, Release, and Uptake," *Cell. Mol. Neurobiol.*, vol. 36, no. 3, pp. 301–312, 2016.

[90] B. K. Thakur *et al.*, "Double-stranded DNA in exosomes: A novel biomarker in cancer detection," *Cell Res.*, vol. 24, no. 6, pp. 766–769, 2014.

[91] J. Ghanam, V. K. Chetty, L. Barthel, D. Reinhardt, P. F. Hoyer, and B. K. Thakur, "DNA in extracellular vesicles: from evolution to its current application in health and disease," *Cell Biosci.*, vol. 12, no. 1, pp. 1–13, 2022.

[92] H. Konaka *et al.*, "Secretion of mitochondrial DNA via exosomes promotes inflammation in Behçet's syndrome," *EMBO J.*, pp. 1–27, 2023.

[93] D. W. Hagey *et al.*, "Extracellular vesicles are the primary source of blood-borne tumour-derived mutant KRAS DNA early in pancreatic cancer," *J. Extracell. Vesicles*, vol. 10, no. 12, 2021.

[94] J. P. Tosar, K. Witwer, and A. Cayota, "Revisiting Extracellular RNA Release, Processing, and Function," *Trends Biochem. Sci.*, vol. 46, no. 6, pp. 438–445, 2021.

[95] S. Srinivasan *et al.*, "Small RNA Sequencing across Diverse Biofluids Identifies Optimal Methods for exRNA Isolation," *Cell*, vol. 177, no. 2, pp. 446-462.e16, 2019.

[96] B. Fromm, J. P. Tosar, Y. Lu, M. K. Halushka, and K. W. Witwer, "Human and Cow Have Identical miR-21-5p and miR-30a-5p Sequences, Which Are Likely Unsuited to Study Dietary Uptake from Cow Milk," *J. Nutr.*, vol. 148, no. 9, pp. 1506–1507, 2018.

[97] Z. Wei, A. O. Batagov, D. R. F. Carter, and A. M. Krichevsky, "Fetal Bovine Serum

RNA Interferes with the Cell Culture derived Extracellular RNA," *Sci. Rep.*, vol. 6, 2016.

[98] J. P. Tosar, A. Cayota, E. Eitan, M. K. Halushka, and K. W. Witwer, "Ribonucleic artefacts: are some extracellular RNA discoveries driven by cell culture medium components?," *J. Extracell. Vesicles*, vol. 6, no. 1, pp. 1–10, 2017.

[99] M. Auber, D. Fröhlich, O. Drechsel, E. Karaulanov, and E. M. Krämer-Albers, "Serum-free media supplements carry miRNAs that co-purify with extracellular vesicles," *J. Extracell. Vesicles*, vol. 8, no. 1, 2019.

[100] F. Fabbiano, J. Corsi, E. Gurrieri, C. Trevisan, M. Notarangelo, and V. G. D'Agostino, "RNA packaging into extracellular vesicles: An orchestra of RNA-binding proteins?," *J. Extracell. Vesicles*, vol. 10, no. 2, 2020.

[101] H. Sork *et al.*, "Heterogeneity and interplay of the extracellular vesicle small RNA transcriptome and proteome," *Sci. Rep.*, vol. 8, no. 1, pp. 1–12, 2018.

[102] K. Brinkman *et al.*, "Extracellular vesicles from plasma have higher tumour RNA fraction than platelets," *J. Extracell. Vesicles*, vol. 9, no. 1, 2020.

[103] S. R. Baglio *et al.*, "Sensing of latent EBV infection through exosomal transfer of 5'pppRNA," *Proc. Natl. Acad. Sci. U. S. A.*, vol. 113, no. 5, pp. E587–E596, 2016.

[104] A. O. Batagov and I. V. Kurochkin, "Exosomes secreted by human cells transport largely mRNA fragments that are enriched in the 3′-untranslated regions," *Biol. Direct*, vol. 8, no. 1, pp. 1–8, 2013.

[105] A. Zietzer *et al.*, "The RNA-binding protein hnRNPU regulates the sorting of microRNA-30c-5p into large extracellular vesicles," *J. Extracell. Vesicles*, vol. 9, no. 1, pp. 1–21, 2020.

[106] C. Villarroya-Beltri *et al.*, "Sumoylated hnRNPA2B1 controls the sorting of miRNAs into exosomes through binding to specific motifs," *Nat. Commun.*, vol. 4, pp. 1–10, 2013.

[107] L. Santangelo *et al.*, "The RNA-Binding Protein SYNCRIP Is a Component of the Hepatocyte Exosomal Machinery Controlling MicroRNA Sorting," *Cell Rep.*, vol. 17, no. 3, pp. 799–808, 2016.

[108] F. Hobor *et al.*, "A cryptic RNA-binding domain mediates Syncrip recognition and exosomal partitioning of miRNA targets," *Nat. Commun.*, vol. 9, no. 1, 2018.

[109] S. Ghadami and K. Dellinger, "The lipid composition of extracellular vesicles: applications in diagnostics and therapeutic delivery," *Front. Mol. Biosci.*, vol. 10, pp. 1–19, 2023.

[110] O. Peterka *et al.*, "Lipidomic characterization of exosomes isolated from human plasma using various mass spectrometry techniques," *Biochim. Biophys. Acta - Mol. Cell Biol. Lipids*, vol. 1865, no. 5, p. 158634, 2020.

[111] M. Machala *et al.*, "Changes in sphingolipid profile of benzo[a]pyrene-transformed human bronchial epithelial cells are reflected in the altered composition of sphingolipids in their exosomes," *Int. J. Mol. Sci.*, vol. 22, no. 17, 2021.

[112] A. Llorente *et al.*, "Molecular lipidomics of exosomes released by PC-3 prostate cancer cells," *Biochim. Biophys. Acta - Mol. Cell Biol. Lipids*, vol. 1831, no. 7, pp. 1302–1309, 2013.

[113] S. M. Lam *et al.*, “A multi-omics investigation of the composition and function of extracellular vesicles along the temporal trajectory of COVID-19,” *Nat. Metab.*, vol. 3, no. 7, pp. 909–922, 2021.

[114] J. S. Brzozowski *et al.*, “Lipidomic profiling of extracellular vesicles derived from prostate and prostate cancer cell lines,” *Lipids Health Dis.*, vol. 17, no. 1, pp. 1–12, 2018.

[115] J. Donoso-Quezada, S. Ayala-Mar, and J. González-Valdez, “The role of lipids in exosome biology and intercellular communication: Function, analytics and applications,” *Traffic*, vol. 22, no. 7, pp. 204–220, 2021.

[116] F. W. Pfrieger and N. Vitale, “Thematic review series: Exosomes and microvesicles: Lipids as Key Components of their Biogenesis and Functions Cholesterol and the journey of extracellular vesicles,” *J. Lipid Res.*, vol. 59, no. 12, pp. 2255–2261, 2018.

[117] T. Skotland, N. P. Hessvik, K. Sandvig, and A. Llorente, “Exosomal lipid composition and the role of ether lipids and phosphoinositides in exosome biology,” *J. Lipid Res.*, vol. 60, no. 1, pp. 9–18, 2019.

[118] S. Gandham *et al.*, “Technologies and Standardization in Research on Extracellular Vesicles,” *Trends Biotechnol.*, vol. 38, no. 10, pp. 1066–1098, 2020.

[119] M. Zhang *et al.*, “Methods and Technologies for Exosome Isolation and Characterization,” *Small Methods*, vol. 2, no. 9, pp. 1–10, 2018.

[120] K. Laulagnier, H. Vincent-Schneider, S. Hamdi, C. Subra, D. Lankar, and M. Record, “Characterization of exosome subpopulations from RBL-2H3 cells using fluorescent lipids,” *Blood Cells, Mol. Dis.*, vol. 35, no. 2, pp. 116–121, 2005.

[121] Z. J. Smith *et al.*, “Single exosome study reveals subpopulations distributed among cell lines with variability related to membrane content,” *J. Extracell. Vesicles*, vol. 4, no. 1, pp. 1–15, 2015.

[122] P. Li, M. Kaslan, S. H. Lee, J. Yao, and Z. Gao, “Progress in exosome isolation techniques,” *Theranostics*, vol. 7, no. 3, pp. 789–804, 2017.

[123] N. Salmond and K. C. Williams, “Isolation and characterization of extracellular vesicles for clinical applications in cancer - time for standardization?,” *Nanoscale Adv.*, vol. 3, no. 7, pp. 1830–1852, 2021.

[124] R. Crescitelli, C. Lässer, and J. Lötvall, “Isolation and characterization of extracellular vesicle subpopulations from tissues,” *Nat. Protoc.*, vol. 16, no. 3, pp. 1548–1580, 2021.

[125] J. Moll and S. Carotta, *Target Identification and Validation in Drug Discovery Methods and Protocols Second Edition Methods in Molecular Biology*. 2019.

[126] J. Z. Nordin *et al.*, “Ultrafiltration with size-exclusion liquid chromatography for high yield isolation of extracellular vesicles preserving intact biophysical and functional properties,” *Nanomedicine Nanotechnology, Biol. Med.*, vol. 11, no. 4, pp. 879–883, 2015.

[127] Z. Zhang, C. Wang, T. Li, Z. Liu, and L. Li, “Comparison of ultracentrifugation and density gradient separation methods for isolating Tca8113 human tongue cancer cell line-derived exosomes,” *Oncol. Lett.*, vol. 8, no. 4, pp. 1701–1706, 2014.

[128] Z. Onódi *et al.*, “Isolation of high-purity extracellular vesicles by the combination of iodixanol density gradient ultracentrifugation and bind-elute chromatography from blood plasma,” *Front. Physiol.*, vol. 9, pp. 1–11, 2018.

[129] M. L. Merchant *et al.*, “Microfiltration isolation of human urinary exosomes for characterization by MS,” *Proteomics - Clin. Appl.*, vol. 4, no. 1, pp. 84–96, 2010.

[130] S. Busatto *et al.*, “Tangential flow filtration for highly efficient concentration of extracellular vesicles from large volumes of fluid,” *Cells*, vol. 7, no. 12, 2018.

[131] J. E. Rollings, A. Bose, J. M. Caruthers, G. T. Tsao, and M. R. Okos, “Aqueous Size Exclusion Chromatography.,” *Adv. Chem. Ser.*, pp. 345–360, 1983.

[132] M. L. Alvarez, M. Khosroheidari, R. Kanchi Ravi, and J. K. Distefano, “Comparison of protein, microRNA, and mRNA yields using different methods of urinary exosome isolation for the discovery of kidney disease biomarkers,” *Kidney Int.*, vol. 82, no. 9, pp. 1024–1032, 2012.

[133] H. Zheng, S. Guan, X. Wang, J. Zhao, M. Gao, and X. Zhang, “Deconstruction of Heterogeneity of Size-Dependent Exosome Subpopulations from Human Urine by Profiling N-Glycoproteomics and Phosphoproteomics Simultaneously,” *Anal. Chem.*, vol. 92, no. 13, pp. 9239–9246, 2020.

[134] Y. Yuana, J. Levels, A. Grootemaat, A. Sturk, and R. Nieuwland, “Co-isolation of extracellular vesicles and high-density lipoproteins using density gradient ultracentrifugation,” *J. Extracell. Vesicles*, vol. 3, no. 1, 2014.

[135] K. Brennan *et al.*, “A comparison of methods for the isolation and separation of extracellular vesicles from protein and lipid particles in human serum,” *Sci. Rep.*, vol. 10, no. 1, pp. 1–13, 2020.

[136] T. Liangsupree, E. Multia, and M. L. Riekkola, “Modern isolation and separation techniques for extracellular vesicles,” *J. Chromatogr. A*, vol. 1636, p. 461773, 2021.

[137] C. Théry, L. Zitvogel, and S. Amigorena, “Exosomes: Composition, biogenesis and function,” *Nat. Rev. Immunol.*, vol. 2, no. 8, pp. 569–579, 2002.

[138] K. P. De Sousa, I. Rossi, M. Abdullahi, M. I. Ramirez, D. Stratton, and J. M. Inal, “Isolation and characterization of extracellular vesicles and future directions in diagnosis and therapy,” *Wiley Interdiscip. Rev. Nanomedicine Nanobiotechnology*, vol. 15, no. 1, pp. 1–29, 2023.

[139] R. Samsonov *et al.*, “Lectin-induced agglutination method of urinary exosomes isolation followed by mi-RNA analysis: Application for prostate cancer diagnostic,” *Prostate*, vol. 76, no. 1, pp. 68–79, 2016.

[140] X. Gallart-Palau *et al.*, “Extracellular vesicles are rapidly purified from human plasma by PRotein Organic Solvent PRecipitation (PROSPR),” *Sci. Rep.*, vol. 5, pp. 1–12, 2015.

[141] N. García-Romero *et al.*, “Polyethylene glycol improves current methods for circulating extracellular vesicle-derived DNA isolation,” *J. Transl. Med.*, vol. 17, no. 1, pp. 1–11, 2019.

[142] M. I. Ramirez *et al.*, “Technical challenges of working with extracellular vesicles,” *Nanoscale*, vol. 10, no. 3, pp. 881–906, 2018.

[143] Z. Brownlee, K. D. Lynn, P. E. Thorpe, and A. J. Schroit, “A novel ‘salting-out’ procedure for the isolation of tumor-derived exosomes,” *J. Immunol. Methods*, vol. 407, pp. 120–126, 2014.

[144] M. C. Deregibus *et al.*, “Charge-based precipitation of extracellular vesicles,” *Int. J. Mol. Med.*, vol. 38, no. 5, pp. 1359–1366, 2016.

[145] M. Morani *et al.*, “Electrokinetic characterization of extracellular vesicles with capillary electrophoresis: A new tool for their identification and quantification,” *Anal. Chim. Acta*, vol. 1128, pp. 42–51, 2020.

[146] R. Luna *et al.*, “Enhancement of dielectrophoresis-based particle collection from high conducting fluids due to partial electrode insulation,” *Electrophoresis*, vol. 44, no. 15–16, pp. 1234–1246, 2023.

[147] C. Fernandez-becerra *et al.*, “Guidelines for the purification and characterization of extracellular,” *J. Extracell. Vesicles*, vol. 2, no. 10, 2023.

[148] C. Pelyhe and J. Sturve, “Isolation and characterization of the morphology, size and particle number of rainbow trout (Oncorhynchus mykiss) and zebrafish (Danio rerio) cell line derived large and small extracellular vesicles,” *Fish Physiol. Biochem.*, no. 0123456789, 2023.

[149] R. A. Dragovic *et al.*, “Sizing and phenotyping of cellular vesicles using Nanoparticle Tracking Analysis,” *Nanomedicine Nanotechnology, Biol. Med.*, vol. 7, no. 6, pp. 780–788, 2011.

[150] V. Filipe, A. Hawe, and W. Jiskoot, “Critical evaluation of nanoparticle tracking analysis (NTA) by NanoSight for the measurement of nanoparticles and protein aggregates,” *Pharm. Res.*, vol. 27, no. 5, pp. 796–810, 2010.

[151] V. Palmieri *et al.*, “Dynamic light scattering for the characterization and counting of extracellular vesicles: a powerful noninvasive tool,” *J. Nanoparticle Res.*, vol. 16, no. 9, 2014.

[152] F. A. W. Coumans *et al.*, “Reproducible extracellular vesicle size and concentration determination with tunable resistive pulse sensing,” *J. Extracell. Vesicles*, vol. 3, no. 1, 2014.

[153] J. C. Akers *et al.*, “Comparative analysis of technologies for quantifying extracellular vesicles (EVs) in clinical cerebrospinal fluids (CSF),” *PLoS One*, vol. 11, no. 2, pp. 1–11, 2016.

[154] E. van der Pol *et al.*, “Particle size distribution of exosomes and microvesicles determined by transmission electron microscopy, flow cytometry, nanoparticle tracking analysis, and resistive pulse sensing,” *J. Thromb. Haemost.*, vol. 12, no. 7, pp. 1182–1192, 2014.

[155] J. Lötvall *et al.*, “Minimal experimental requirements for definition of extracellular vesicles and their functions: A position statement from the International Society for Extracellular Vesicles,” *J. Extracell. Vesicles*, vol. 3, no. 1, 2014.

[156] R. Crescitelli *et al.*, “Distinct RNA profiles in subpopulations of extracellular vesicles: Apoptotic bodies, microvesicles and exosomes,” *J. Extracell. Vesicles*, vol. 2, no. 1, 2013.

[157] Y. Yuana *et al.*, “Cryo-electron microscopy of extracellular vesicles in fresh plasma,” *J. Extracell. Vesicles*, vol. 2, no. 1, p. 21494, 2013.

[158] I. Tatischeff, E. Larquet, J. M. Falcón-Pérez, P. Y. Turpin, and S. G. Kruglik, “Fast characterisation of cell-derived extracellular vesicles by nanoparticles tracking analysis, cryo-electron microscopy, and Raman tweezers microspectroscopy,” *J. Extracell. Vesicles*, vol. 1, no. 1, 2012.

[159] Y. Yuana *et al.*, “Atomic force microscopy: A novel approach to the detection of

nanosized blood microparticles," *J. Thromb. Haemost.*, vol. 8, no. 2, pp. 315–323, 2010.

[160] S. El Andaloussi, I. Mäger, X. O. Breakefield, and M. J. A. Wood, "Extracellular vesicles: Biology and emerging therapeutic opportunities," *Nat. Rev. Drug Discov.*, vol. 12, no. 5, pp. 347–357, 2013.

[161] Q. Zhang *et al.*, "Transfer of Functional Cargo in Exomeres," *Cell Rep.*, vol. 27, no. 3, pp. 940-954.e6, 2019.

[162] S. Cavallaro *et al.*, "Multiparametric Profiling of Single Nanoscale Extracellular Vesicles by Combined Atomic Force and Fluorescence Microscopy: Correlation and Heterogeneity in Their Molecular and Biophysical Features," *Small*, vol. 17, no. 14, 2021.

[163] Z. Nizamudeen *et al.*, "Rapid and accurate analysis of stem cell-derived extracellular vesicles with super resolution microscopy and live imaging," *Biochim. Biophys. Acta - Mol. Cell Res.*, vol. 1865, no. 12, pp. 1891–1900, 2018.

[164] R. K. Singh *et al.*, "Detection by super-resolution microscopy of viral proteins inside bloodborne extracellular vesicles," *Extracell. Vesicles Circ. Nucleic Acids*, vol. 4, no. 4, pp. 557–67, 2023.

[165] S. Dechantsreiter *et al.*, "Heterogeneity in extracellular vesicle secretion by single human macrophages revealed by super-resolution microscopy," *J. Extracell. Vesicles*, vol. 11, no. 4, 2022.

[166] H. Shao, H. Im, C. M. Castro, X. Breakefield, R. Weissleder, and H. Lee, "New Technologies for Analysis of Extracellular Vesicles," *Chem. Rev.*, vol. 118, no. 4, pp. 1917–1950, 2018.

[167] R. J. Lobb *et al.*, "Optimized exosome isolation protocol for cell culture supernatant and human plasma," *J. Extracell. Vesicles*, vol. 4, no. 1, 2015.

[168] A. Askeland *et al.*, "Mass-spectrometry based proteome comparison of extracellular vesicle isolation methods: Comparison of ME-kit, size-exclusion chromatography, and high-speed centrifugation," *Biomedicines*, vol. 8, no. 8, pp. 1–15, 2020.

[169] A. F. Orozco and D. E. Lewis, "Flow cytometric analysis of circulating microparticles in plasma," *Cytom. Part A*, vol. 77, no. 6, pp. 502–514, 2010.

[170] O. P. B. Wiklander *et al.*, "Systematic methodological evaluation of a multiplex bead-based flow cytometry assay for detection of extracellular vesicle surface signatures," *Front. Immunol.*, vol. 9, 2018.

[171] S. A. Stoner *et al.*, "High sensitivity flow cytometry of membrane vesicles," *Cytom. Part A*, vol. 89, no. 2, pp. 196–206, 2016.

[172] A. Görgens *et al.*, "Optimisation of imaging flow cytometry for the analysis of single extracellular vesicles by using fluorescence-tagged vesicles as biological reference material," *J. Extracell. Vesicles*, vol. 8, no. 1, 2019.

[173] H Shin, D. Seo, and Y. Choi, "Extracellular Vesicle Identification Using Label-Free Surface-Enhanced Raman Spectroscopy: Detection and Signal Analysis Strategies," *molecules*, vol. 25, no. 21, 2020.

[174] C. Carlomagno, C. Giannasi, S. Niada, M. Bedoni, A. Gualerzi, and A. T. Brini, "Raman Fingerprint of Extracellular Vesicles and Conditioned Media for the Reproducibility Assessment of Cell-Free Therapeutics," *Front. Bioeng. Biotechnol.*,

vol. 9, pp. 1–9, 2021.

[175] L. A. Mulcahy, R. C. Pink, and D. R. F. Carter, “Routes and mechanisms of extracellular vesicle uptake,” *J. Extracell. Vesicles*, vol. 3, no. 1, pp. 1–14, 2014.

[176] D. Fitzner *et al.*, “Selective transfer of exosomes from oligodendrocytes to microglia by macropinocytosis,” *J. Cell Sci.*, vol. 124, no. 3, pp. 447–458, 2011.

[177] A. E. Morelli *et al.*, “Endocytosis, intracellular sorting, and processing of exosomes by dendritic cells,” *Blood*, vol. 104, no. 10, pp. 3257–3266, 2004.

[178] C. Frühbeis *et al.*, “Neurotransmitter-Triggered Transfer of Exosomes Mediates Oligodendrocyte-Neuron Communication,” *PLoS Biol.*, vol. 11, no. 7, 2013.

[179] A. Nanbo, E. Kawanishi, R. Yoshida, and H. Yoshiyama, “Exosomes Derived from Epstein-Barr Virus-Infected Cells Are Internalized via Caveola-Dependent Endocytosis and Promote Phenotypic Modulation in Target Cells,” *J. Virol.*, vol. 87, no. 18, pp. 10334–10347, 2013.

[180] K. J. Svensson *et al.*, “Exosome uptake depends on ERK1/2-heat shock protein 27 signaling and lipid raft-mediated endocytosis negatively regulated by caveolin-1,” *J. Biol. Chem.*, vol. 288, no. 24, pp. 17713–17724, 2013.

[181] H. C. Christianson, K. J. Svensson, T. H. Van Kuppevelt, J. P. Li, and M. Belting, “Cancer cell exosomes depend on cell-surface heparan sulfate proteoglycans for their internalization and functional activity,” *Proc. Natl. Acad. Sci. U. S. A.*, vol. 110, no. 43, pp. 17380–17385, 2013.

[182] N. A. Atai *et al.*, “Heparin blocks transfer of extracellular vesicles between donor and recipient cells,” *J. Neurooncol.*, vol. 115, no. 3, pp. 343–351, 2013.

[183] M. P. Plebanek, R. K. Mutharasan, O. Volpert, A. Matov, J. C. Gatlin, and C. S. Thaxton, “Nanoparticle targeting and cholesterol flux through scavenger receptor type B-1 inhibits cellular exosome uptake,” *Sci. Rep.*, vol. 5, pp. 1–14, 2015.

[184] I. Parolini *et al.*, “Microenvironmental pH is a key factor for exosome traffic in tumor cells,” *J. Biol. Chem.*, vol. 284, no. 49, pp. 34211–34222, 2009.

[185] I. Nakase and S. Futaki, “Combined treatment with a pH-sensitive fusogenic peptide and cationic lipids achieves enhanced cytosolic delivery of exosomes,” *Sci. Rep.*, vol. 5, pp. 1–13, 2015.

[186] L. Margolis and Y. Sadovsky, “The biology of extracellular vesicles: The known unknowns,” *PLoS Biol.*, vol. 17, no. 7, pp. 1–12, 2019.

[187] C. P. Lai *et al.*, “Dynamic biodistribution of extracellular vesicles in vivo using a multimodal imaging reporter,” *ACS Nano*, vol. 8, no. 1, pp. 483–494, 2014.

[188] O. P. B. Wiklander *et al.*, “Extracellular vesicle in vivo biodistribution is determined by cell source, route of administration and targeting,” *J. Extracell. Vesicles*, vol. 4, pp. 1–13, 2015.

[189] E. Lázaro-Ibánez *et al.*, “Selection of fluorescent, bioluminescent, and radioactive tracers to accurately reflect extracellular vesicle biodistribution in vivo,” *ACS Nano*, vol. 15, no. 2, pp. 3212–3227, 2021.

[190] X. Liang *et al.*, “Extracellular vesicles engineered to bind albumin demonstrate extended circulation time and lymph node accumulation in mouse models,” *J. Extracell. Vesicles*, vol. 11, no. 7, 2022.

[191] T. Saleem, A. Sumrin, M. Bilal, H. Bashir, and M. Babar, “Saudi Journal of Biological Sciences Tumor-derived extracellular vesicles : Potential tool for cancer diagnosis , prognosis , and therapy,” *Saudi J. Biol. Sci.*, vol. 29, no. 4, pp. 2063–2071, 2022.

[192] Y. Wei, X. Lai, S. Yu, and S. Chen, “Exosomal miR-221 / 222 enhances tamoxifen resistance in recipient ER-positive breast cancer cells,” *Breast Cancer Res. Treat*, vol.147, no. 2, pp. 423–431, 2014.

[193] H. Saari, E. Lázaro-ibáñez, T. Viitala, E. Vuorimaa-laukkanen, P. Siljander, and M. Yliperttula, “Microvesicle- and exosome-mediated drug delivery enhances the cytotoxicity of Paclitaxel in autologous prostate cancer cells,” *J. Control. Release*, vol. 220, pp. 727–737, 2015.

[194] K. B. Challagundla *et al.*, “Exosome-Mediated Transfer of microRNAs Within the Tumor Microenvironment and Neuroblastoma Resistance to Chemotherapy,” vol. 107, pp. 1–13, 2015.

[195] S. Maacha *et al.*, “Extracellular vesicles-mediated intercellular communication: Roles in the tumor microenvironment and anti-cancer drug resistance,” *Mol. Cancer*, vol. 18, no. 1, pp. 1–16, 2019.

[196] G. Wang *et al.*, “Tumour extracellular vesicles and particles induce liver metabolic dysfunction,” vol. 618, 2023.

[197] B. Guarino *et al.*, “Tumor-Derived Extracellular Vesicles Induce Abnormal Angiogenesis via TRPV4 Downregulation and Subsequent Activation of YAP and,” vol. 9, pp. 1–9, 2021.

[198] T. Yang *et al.*, “Exosome delivered anticancer drugs across the blood-brain barrier for brain cancer therapy in Danio Rerio,” *Pharm. Res.*, vol. 32, no. 6, pp. 2003–2014, 2015.

[199] G. Toffoli *et al.*, “Exosomal doxorubicin reduces the cardiac toxicity of doxorubicin,” *Nanomedicine*, vol. 10, no. 19, pp. 2963–2971, 2015.

[200] M. Hadla *et al.*, “Exosomes increase the therapeutic index of doxorubicin in breast and ovarian cancer mouse models,” *Nanomedicine*, vol. 11, no. 18, pp. 2431–2441, 2016.

[201] G. Li *et al.*, “Current challenges and future directions for engineering extracellular vesicles for heart, lung, blood and sleep diseases,” *J. Extracell. Vesicles*, vol. 12, no. 2, 2023.

[202] R. Rohban and T. R. Pieber, “Mesenchymal stem and progenitor cells in regeneration: Tissue specificity and regenerative potential,” *Stem Cells Int.*, vol. 2017, 2017.

[203] L. Von Bahr *et al.*, “Analysis of tissues following mesenchymal stromal cell therapy in humans indicates limited long-term engraftment and no ectopic tissue formation,” *Stem Cells*, vol. 30, no. 7, pp. 1575–1578, 2012.

[204] M. A. Brennan *et al.*, “Pre-clinical studies of bone regeneration with human bone marrow stromal cells and biphasic calcium phosphate,” *Stem Cell Res. Ther.*, vol. 5, no. 6, pp. 1–15, 2014.

[205] R. C. Lai *et al.*, “Exosome secreted by MSC reduces myocardial ischemia/reperfusion injury,” *Stem Cell Res.*, vol. 4, no. 3, pp. 214–222, 2010.

[206] L. Timmers *et al.*, “Reduction of myocardial infarct size by human mesenchymal stem cell conditioned medium,” *Stem Cell Res.*, vol. 1, no. 2, pp. 129–137, 2008.

[207] A. van Koppen *et al.*, “Human embryonic mesenchymal stem cell-derived conditioned medium rescues kidney function in rats with established chronic kidney disease,” *PLoS One*, vol. 7, no. 6, pp. 1–12, 2012.

[208] T. A. Davis, K. Anam, Y. Lazdun, J. M. Gimble, and A. Eric, “T ISSUE -S PECIFIC P ROGENITOR AND S TEM C ELLS Adipose-Derived Stromal Cells Promote Allograft Tolerance Induction,” vol. 5, pp. 764–774, 2014.

[209] S. Cosenza *et al.*, “Mesenchymal stem cells-derived exosomes are more immunosuppressive than microparticles in inflammatory arthritis,” *Theranostics*, vol. 8, no. 5, pp. 1399–1410, 2018.

[210] A. Eirin *et al.*, “Mesenchymal stem cell–derived extracellular vesicles attenuate kidney inflammation,” *Kidney Int.*, vol. 92, no. 1, pp. 114–124, 2017.

[211] S. Bruno *et al.*, “Mesenchymal stem cell-derived microvesicles protect against acute tubular injury,” *J. Am. Soc. Nephrol.*, vol. 20, no. 5, pp. 1053–1067, 2009.

[212] C. Lee *et al.*, “Exosomes mediate the cytoprotective action of mesenchymal stromal cells on hypoxia-induced pulmonary hypertension,” *Circulation*, vol. 126, no. 22, pp. 2601–2611, 2012.

[213] M. Khatri, L. A. Richardson, and T. Meulia, “Mesenchymal stem cell-derived extracellular vesicles attenuate influenza virus-induced acute lung injury in a pig model,” *Stem Cell Res. Ther.*, vol. 9, no. 1, pp. 1–13, 2018.

[214] S. Y. Ahn *et al.*, “Vascular endothelial growth factor mediates the therapeutic efficacy of mesenchymal stem cell-derived extracellular vesicles against neonatal hyperoxic lung injury,” *Exp. Mol. Med.*, vol. 50, no. 4, 2018.

[215] S. Zhang, W. C. Chu, R. C. Lai, S. K. Lim, J. H. P. Hui, and W. S. Toh, “Exosomes derived from human embryonic mesenchymal stem cells promote osteochondral regeneration,” *Osteoarthr. Cartil.*, vol. 24, no. 12, pp. 2135–2140, 2016.

[216] T. Li *et al.*, “Exosomes derived from human umbilical cord mesenchymal stem cells alleviate liver fibrosis,” *Stem Cells Dev.*, vol. 22, no. 6, pp. 845–854, 2013.

[217] L. Liu, X. Jin, C. F. Hu, R. Li, Z. Zhou, and C. X. Shen, “Exosomes Derived from Mesenchymal Stem Cells Rescue Myocardial Ischaemia/Reperfusion Injury by Inducing Cardiomyocyte Autophagy Via AMPK and Akt Pathways,” *Cell. Physiol. Biochem.*, vol. 43, no. 1, pp. 52–68, 2017.

[218] G. Lou *et al.*, “Exosomes derived from MIR-122-modified adipose tissue-derived MSCs increase chemosensitivity of hepatocellular carcinoma,” *J. Hematol. Oncol.*, vol. 8, no. 1, pp. 1–11, 2015.

[219] C. Biology and M. Clinic, “T ISSUE E NGINEERING AND R EGENERATIVE M EDICINE Extracellular Vesicles from Bone Marrow-Derived Mesenchymal Stem Cells Improve Survival from Lethal Hepatic Failure in Mice,” pp. 1262–1272, 2017.

[220] X. Zou *et al.*, “NK cell regulatory property is involved in the protective role of MSC-derived extracellular vesicles in renal ischemic reperfusion injury,” *Hum. Gene Ther.*, vol. 27, no. 11, pp. 926–935, 2016.

[221] M. Kou *et al.*, “Mesenchymal stem cell-derived extracellular vesicles for immunomodulation and regeneration: a next generation therapeutic tool?,” *Cell Death Dis.*, vol. 13, no. 7, 2022.

[222] M. Khan *et al.*, “Embryonic Stem Cell-Derived Exosomes Promote Endogenous Repair

Mechanisms and Enhance Cardiac Function Following Myocardial Infarction," *Circ. Res.*, vol. 117, no. 1, pp. 52–64, 2015.

[223] B. Zhao *et al.*, "Exosomes derived from human amniotic epithelial cells accelerate wound healing and inhibit scar formation," *J. Mol. Histol.*, vol. 48, no. 2, pp. 121–132, 2017.

[224] J. Zhang *et al.*, "Exosomes released from human induced pluripotent stem cells-derived MSCs facilitate cutaneous wound healing by promoting collagen synthesis and angiogenesis," *J. Transl. Med.*, vol. 13, no. 1, pp. 1–14, 2015.

[225] X. Li *et al.*, "Exosomes derived from endothelial progenitor cells attenuate vascular repair and accelerate reendothelialization by enhancing endothelial function," *Cytotherapy*, vol. 18, no. 2, pp. 253–262, 2016.

[226] X. Qi *et al.*, "Exosomes secreted by human-induced pluripotent stem cell-derived mesenchymal stem cells repair critical-sized bone defects through enhanced angiogenesis and osteogenesis in osteoporotic rats," *Int. J. Biol. Sci.*, vol. 12, no. 7, pp. 836–849, 2016.

[227] P. Gangadaran *et al.*, "Extracellular vesicles from mesenchymal stem cells activates VEGF receptors and accelerates recovery of hindlimb ischemia," *J. Control. Release*, vol. 264, pp. 112–126, 2017.

[228] Y. Wang *et al.*, "Exosomes/microvesicles from induced pluripotent stem cells deliver cardioprotective miRNAs and prevent cardiomyocyte apoptosis in the ischemic myocardium," *Int. J. Cardiol.*, vol. 192, pp. 61–69, 2015.

[229] J. L. Tan *et al.*, "Amnion Epithelial Cell-Derived Exosomes Restrict Lung Injury and Enhance Endogenous Lung Repair," *Stem Cells Transl. Med.*, vol. 7, no. 2, pp. 180–196, 2018.

[230] A. S. Zitvogel L, Regnault A, Lozier A, Wolfers J, Flament C, Tenza D, Ricciardi-Castagnoli P, Raposo G *et al.*, "Eradication of established murine tumors using a novel cell-free vaccine: dendritic cell-derived exosomes.," *Nat. Med.*, vol. 4, no. 5, pp. 594–600, 1998.

[231] N. Chaput *et al.*, "Exosomes as Potent Cell-Free Peptide-Based Vaccine. II. Exosomes in CpG Adjuvants Efficiently Prime Naive Tc1 Lymphocytes Leading to Tumor Rejection," *J. Immunol.*, vol. 172, no. 4, pp. 2137–2146, 2004.

[232] S. Shi, Q. Rao, C. Zhang, X. Zhang, Y. Qin, and Z. Niu, "Dendritic Cells Pulsed with Exosomes in Combination with PD-1 Antibody Increase the Efficacy of Sorafenib in Hepatocellular Carcinoma Model," *Transl. Oncol.*, vol. 11, no. 2, pp. 250–258, 2018.

[233] M. A. Ruffner, H. K. Seon, N. R. Bianco, L. M. Francisco, A. H. Sharpe, and P. D. Robbins, "B7-1/2, but not PD-L1/2 molecules, are required on IL-10-treated tolerogenic DC and DC-derived exosomes for in vivo function," *Eur. J. Immunol.*, vol. 39, no. 11, pp. 3084–3090, 2009.

[234] K. Roy, D. J. Hamilton, G. P. Munson, and J. M. Fleckenstein, "Outer membrane vesicles induce immune responses to virulence proteins and protect against colonization by enterotoxigenic Escherichia coli," *Clin. Vaccine Immunol.*, vol. 18, no. 11, pp. 1803–1808, 2011.

[235] F. Aline, D. Bout, S. Amigorena, P. Roingeard, and I. Dimier-Poisson, "Toxoplasma gondii antigen-pulsed-dendritic cell-derived exosomes induce a protective immune response against T. gondii infection," *Infect. Immun.*, vol. 72, no. 7, pp. 4127–4137,

2004.

[236] S. Bhatnagar, K. Shinagawa, F. J. Castellino, and J. S. Schorey, “Exosomes released from macrophages infected with intracellular pathogens stimulate a proinflammatory response in vitro and in vivo,” *Blood*, vol. 110, no. 9, pp. 3234–3244, 2007.

[237] P. M. Nogueira *et al.*, “Vesicles from different Trypanosoma cruzi strains trigger differential innate and chronic immune responses,” *J. Extracell. Vesicles*, vol. 4, no. 1, 2015.

[238] B. Haneberg *et al.*, “Intranasal Administration of a Meningococcal Outer Membrane Vesicle Vaccine Induces Persistent Local Mucosal Antibodies and Serum Antibodies with Strong Bactericidal Activity in Humans,” *Infect. Immun.*, vol. 66, no. 4, pp. 1334–1341, 1998.

[239] O. P. B. Wiklander, M. Brennan, J. Lötvall, X. O. Breakefield, and S. E. L. Andaloussi, “Advances in therapeutic applications of extracellular vesicles,” *Sci. Transl. Med.*, vol. 11, no. 492, pp. 1–16, 2019.

[240] O. M. Elsharkasy *et al.*, “Extracellular vesicles as drug delivery systems: Why and how?,” *Adv. Drug Deliv. Rev.*, vol. 159, pp. 332–343, 2020.

[241] J. Gehl, “Electroporation: Theory and methods, perspectives for drug delivery, gene therapy and research,” *Acta Physiol. Scand.*, vol. 177, no. 4, pp. 437–447, 2003.

[242] E. Neumann, M. Schaefer-Ridder, Y. Wang, and P. H. Hofschneider, “Gene transfer into mouse lyoma cells by electroporation in high electric fields.,” *EMBO J.*, vol. 1, no. 7, pp. 841–845, 1982.

[243] S. Rankin-Turner, P. Vader, L. O’Driscoll, B. Giebel, L. M. Heaney, and O. G. Davies, “A call for the standardised reporting of factors affecting the exogenous loading of extracellular vesicles with therapeutic cargos,” *Adv. Drug Deliv. Rev.*, vol. 173, pp. 479–491, 2021.

[244] L. Alvarez-Erviti, Y. Seow, H. Yin, C. Betts, S. Lakhal, and M. J. A. Wood, “Delivery of siRNA to the mouse brain by systemic injection of targeted exosomes,” *Nat. Biotechnol.*, vol. 29, no. 4, pp. 341–345, 2011.

[245] N. L. Syn, L. Wang, E. K. H. Chow, C. T. Lim, and B. C. Goh, “Exosomes in Cancer Nanomedicine and Immunotherapy: Prospects and Challenges,” *Trends Biotechnol.*, vol. 35, no. 7, pp. 665–676, 2017.

[246] Y. Tian *et al.*, “A doxorubicin delivery platform using engineered natural membrane vesicle exosomes for targeted tumor therapy,” *Biomaterials*, vol. 35, no. 7, pp. 2383–2390, 2014.

[247] A. Butreddy, N. Kommineni, and N. Dudhipala, “Exosomes as naturally occurring vehicles for delivery of biopharmaceuticals: Insights from drug delivery to clinical perspectives,” *Nanomaterials*, vol. 11, no. 6, 2021.

[248] M. S. Kim *et al.*, “Development of exosome-encapsulated paclitaxel to overcome MDR in cancer cells,” *Nanomedicine Nanotechnology, Biol. Med.*, vol. 12, no. 3, pp. 655–664, 2016.

[249] X. Luan, K. Sansanaphongpricha, I. Myers, H. Chen, H. Yuan, and D. Sun, “Engineering exosomes as refined biological nanoplatforms for drug delivery,” *Acta Pharmacol. Sin.*, vol. 38, no. 6, pp. 754–763, 2017.

[250] D. Sun *et al.*, “A novel nanoparticle drug delivery system: The anti-inflammatory

activity of curcumin is enhanced when encapsulated in exosomes," *Mol. Ther.*, vol. 18, no. 9, pp. 1606–1614, 2010.

[251] E. Narayanan, "Exosomes as Drug Delivery Vehicles for Cancer Treatment," *Curr. Nanosci.*, vol. 16, no. 1, pp. 15–26, 2019.

[252] S. C. Jang *et al.*, "Bioinspired exosome-mimetic nanovesicles for targeted delivery of chemotherapeutics to malignant tumors," *ACS Nano*, vol. 7, no. 9, pp. 7698–7710, 2013.

[253] G. Fuhrmann, A. Serio, M. Mazo, R. Nair, and M. M. Stevens, "Active loading into extracellular vesicles significantly improves the cellular uptake and photodynamic effect of porphyrins," *J. Control. Release*, vol. 205, pp. 35–44, 2015.

[254] M. J. Haney *et al.*, "Exosomes as drug delivery vehicles for Parkinson's disease therapy," *J. Control. Release*, vol. 207, pp. 18–30, 2015.

[255] S. Fu, Y. Wang, X. Xia, and J. C. Zheng, "Exosome engineering: Current progress in cargo loading and targeted delivery," *NanoImpact*, vol. 20, p. 100261, 2020.

[256] Y. T. Sato *et al.*, "Engineering hybrid exosomes by membrane fusion with liposomes," *Sci. Rep.*, vol. 6, no. February, pp. 1–11, 2016.

[257] I. Podolak, A. Galanty, and D. Sobolewska, "Saponins as cytotoxic agents: A review," *Phytochem. Rev.*, vol. 9, no. 3, pp. 425–474, 2010.

[258] P. Wu, B. Zhang, D. K. W. Ocansey, W. Xu, and H. Qian, "Extracellular vesicles: A bright star of nanomedicine," *Biomaterials*, vol. 269, p. 120467, 2021.

[259] R. C. de Abreu *et al.*, "Exogenous loading of miRNAs into small extracellular vesicles," *J. Extracell. Vesicles*, vol. 10, no. 10, 2021.

[260] Z. X. Chong, S. K. Yeap, and W. Y. Ho, "Transfection types, methods and strategies: A technical review," *PeerJ*, vol. 9, pp. 1–37, 2021.

[261] R. E. McConnell, M. Youniss, B. Gnanasambandam, P. Shah, W. Zhang, and J. D. Finn, "Transfection reagent artefact likely accounts for some reports of extracellular vesicle function," *J. Extracell. Vesicles*, vol. 11, no. 10, 2022.

[262] J. McCann *et al.*, "Contaminating transfection complexes can masquerade as small extracellular vesicles and impair their delivery of RNA," *J. Extracell. Vesicles*, vol. 11, no. 10, 2022.

[263] A. Raghav and G. B. Jeong, "A systematic review on the modifications of extracellular vesicles: a revolutionized tool of nano-biotechnology," *J. Nanobiotechnology*, vol. 19, no. 1, pp. 1–19, 2021.

[264] L. Pascucci *et al.*, "Paclitaxel is incorporated by mesenchymal stromal cells and released in exosomes that inhibit in vitro tumor growth: A new approach for drug delivery," *J. Control. Release*, vol. 192, pp. 262–270, 2014.

[265] U. Sterzenbach, U. Putz, L. H. Low, J. Silke, S. S. Tan, and J. Howitt, "Engineered Exosomes as Vehicles for Biologically Active Proteins," *Mol. Ther.*, vol. 25, no. 6, pp. 1269–1278, 2017.

[266] K. Tang *et al.*, "Delivery of chemotherapeutic drugs in tumour cell-derived microparticles," *Nat. Commun.*, vol. 3, 2012.

[267] L. H. Lv *et al.*, "Anticancer drugs cause release of exosomes with heat shock proteins from human hepatocellular carcinoma cells that elicit effective natural killer cell

antitumor responses in vitro," *J. Biol. Chem.*, vol. 287, no. 19, pp. 15874–15885, 2012.

[268] D. Bellavia *et al.*, "Interleukin 3- receptor targeted exosomes inhibit in vitro and in vivo chronic myelogenous Leukemia cell growth," *Theranostics*, vol. 7, no. 5, pp. 1333–1345, 2017.

[269] Z. Li *et al.*, "In Vitro and in Vivo RNA Inhibition by CD9-HuR Functionalized Exosomes Encapsulated with miRNA or CRISPR/dCas9," *Nano Lett.*, vol. 19, no. 1, pp. 19–28, 2019.

[270] D. Gupta *et al.*, "Amelioration of systemic inflammation via the display of two different decoy protein receptors on extracellular vesicles," *Nat. Biomed. Eng.*, vol. 5, no. 9, pp. 1084–1098, 2021.

[271] J. P. K. Armstrong, M. N. Holme, and M. M. Stevens, "Re-Engineering Extracellular Vesicles as Smart Nanoscale Therapeutics," *ACS Nano*, vol. 11, no. 1, pp. 69–83, 2017.

[272] J. P. K. Armstrong and M. M. Stevens, "Strategic design of extracellular vesicle drug delivery systems," *Adv. Drug Deliv. Rev.*, vol. 130, pp. 12–16, 2018.

[273] M. Kang, V. Jordan, C. Blenkiron, and L. W. Chamley, "Biodistribution of extracellular vesicles following administration into animals: A systematic review," *J. Extracell. Vesicles*, vol. 10, no. 8, 2021.

[274] J. B. Simonsen, "Pitfalls associated with lipophilic fluorophore staining of extracellular vesicles for uptake studies," *J. Extracell. Vesicles*, vol. 8, no. 1, 2019.

[275] Y. Takahashi *et al.*, "Visualization and in vivo tracking of the exosomes of murine melanoma B16-BL6 cells in mice after intravenous injection," *J. Biotechnol.*, vol. 165, no. 2, pp. 77–84, 2013.

[276] A. Nasiri Kenari, L. Cheng, and A. F. Hill, "Methods for loading therapeutics into extracellular vesicles and generating extracellular vesicles mimetic-nanovesicles," *Methods*, vol. 177, pp. 103–113, 2020.

[277] G. Corso *et al.*, "Reproducible and scalable purification of extracellular vesicles using combined bind-elute and size exclusion chromatography," *Sci. Rep.*, vol. 7, no. 1, pp. 1–10, 2017.

[278] M. L. Thompson, E. J. Kunkel, and R. O. Ehrhardt, "Cryopreservation and Thawing of Mammalian Cells," *eLS*, 2014.

[279] C. Schindler *et al.*, "Exosomal delivery of doxorubicin enables rapid cell entry and enhanced in vitro potency," *PLoS One*, vol. 14, no. 3, pp. 1–19, 2019.

[280] K. B. Johnsen *et al.*, "Evaluation of electroporation-induced adverse effects on adipose-derived stem cell exosomes," *Cytotechnology*, vol. 68, no. 5, pp. 2125–2138, 2016.

[281] J. L. Hood, M. J. Scott, and S. A. Wickline, "Maximizing exosome colloidal stability following electroporation," *Anal. Biochem.*, vol. 448, no. 1, pp. 41–49, 2014.

[282] S. Alam Khan and M. Jawaid Akhtar, "Structural modification and strategies for the enhanced doxorubicin drug delivery," *Bioorg. Chem.*, vol. 120, p. 105599, 2022.

[283] J. H. Beijnen, O. A. G. J. van der Houwen, and W. J. M. Underberg, "Aspects of the degradation kinetics of doxorubicin in aqueous solution," *Int. J. Pharm.*, vol. 32, no. 2–3, pp. 123–131, 1986.

[284] M. J. Wood and W. J. Irwin, "Photodegradation of doxorubicin, daunorubicin and epirubicin measured by high-performance liquid chromatography," *J. Clin. Pharm.*

Ther. vol. 15, no. 4, pp. 291–300, 1990.

[285] Z. Wang, H. Mo, Z. He, A. Chen, and P. Cheng, "Extracellular vesicles as an emerging drug delivery system for cancer treatment: Current strategies and recent advances," *Biomed. Pharmacother.*, vol. 153, p. 113480, 2022.

[286] B. Claridge, J. Lozano, Q. H. Poh, and D. W. Greening, "Development of Extracellular Vesicle Therapeutics: Challenges, Considerations, and Opportunities," *Front. Cell Dev.* vol. 9, 2021.

[287] T. Sych *et al.*, "High-throughput measurement of the content and properties of nano-sized bioparticles with single-particle profiler," *Nat. Biotechnol.*, 2023.

[288] S. Loibl and L. Gianni, "HER2-positive breast cancer," *THE LANCET*, vol. 389, no. 10087, pp. 2415–2429, 2017.

[289] J. Cheng *et al.*, "Molecular mechanism of HER2 rapid internalization and redirected trafficking induced by anti-HER2 biparatopic antibody," *Antibodies*, vol. 9, no. 3, pp. 1–21, 2020.

[290] M. Hettich, F. Braun, M. D. Bartholomä, R. Schirmbeck, and G. Niedermann, "High-resolution PET imaging with therapeutic antibody-based PD-1/PD-L1 checkpoint tracers," *Theranostics*, vol. 6, no. 10, pp. 1629–1640, 2016.

[291] V. R. Juneja *et al.*, "PD-L1 on tumor cells is sufficient for immune evasion in immunogenic tumors and inhibits CD8 T cell cytotoxicity," *J. Exp. Med.*, vol. 214, no. 4, pp. 895–904, 2017.

[292] N. Cousin, S. Cap, M. Dihr, C. Tacconi, M. Detmar, and L. C. Dieterich, "Lymphatic PD-L1 expression restricts tumor-specific CD8þ T-cell responses," *Cancer Res.*, vol. 81, no. 15, pp. 4133–4144, 2021.

[293] S. Nie, "Editorial: Understanding and overcoming major barriers in cancer nanomedicine," *Nanomedicine*, vol. 5, no. 4, pp. 523–528, 2010.

[294] H. Maeda, H. Nakamura, and J. Fang, "The EPR effect for macromolecular drug delivery to solid tumors: Improvement of tumor uptake, lowering of systemic toxicity, and distinct tumor imaging in vivo," *Adv. Drug Deliv. Rev.*, vol. 65, no. 1, pp. 71–79, 2013.

[295] B. Diskin *et al.*, "PD-L1 engagement on T cells promotes self-tolerance and suppression of neighboring macrophages and effector T cells in cancer," *Nat. Immunol.*, vol. 21, no. 4, pp. 442–454, 2020.

[296] A. Rodallec *et al.*, "Tumor uptake and associated greater efficacy of anti-Her2 immunoliposome does not rely on Her2 expression status: Study of a docetaxel-trastuzumab immunoliposome on Her2+ breast cancer model (SKBR3)," *Anticancer. Drugs*, vol. 31, no. 5, pp. 463–472, 2020.

[297] W. Fink *et al.*, "Clinical phase II study of pegylated liposomal doxorubicin as second-line treatment in disseminated melanoma," *Onkologie*, vol. 27, no. 6, pp. 540–544, 2004.

[298] A. Dominiak, B. Chełstowska, W. Olejarz, and G. Nowicka, "Communication in the cancer microenvironment as a target for therapeutic interventions," *Cancers (Basel).*, vol. 12, no. 5, pp. 1–24, 2020.

[299] C. Chiodoni *et al.*, "Correction to: Cell communication and signaling: How to turn bad language into positive one," *J. Exp. Clin. Cancer Res.*, vol. 38, no. 1, pp. 1–11, 2019.

[300] W. Chiangjong and S. Chutipongtanate, “EV-out or EV-in: Tackling cell-to-cell communication within the tumor microenvironment to enhance anti-tumor efficacy using extracellular vesicle-based therapeutic strategies,” *OpenNano*, vol. 8, p. 100085, 2022.

[301] M. Z. Ratajczak and J. Ratajczak, “Extracellular microvesicles/exosomes: discovery, disbelief, acceptance, and the future?,” *Leukemia*, vol. 34, no. 12, pp. 3126–3135, 2020.

[302] Y. Zhao and C. Huang, “The role of osteopontin in the development and metastasis of melanoma,” *Melanoma Res.*, vol. 31, no. 4, pp. 283–289, 2021.

[303] Z. Wu *et al.*, “The role of angiogenesis in melanoma: Clinical treatments and future expectations,” *Front. Pharmacol.*, vol. 13, pp. 1–16, 2022.

[304] C. Peris-Torres *et al.*, “Extracellular protease adamts1 is required at early stages of human uveal melanoma development by inducing stemness and endothelial-like features on tumor cells,” *Cancers (Basel).*, vol. 12, no. 4, pp. 1–20, 2020.

[305] D. Gabrilovich *et al.*, “Vascular endothelial growth factor inhibits the development of dendritic cells and dramatically affects the differentiation of multiple hematopoietic lineages in vivo,” *Blood*, vol. 92, no. 11, pp. 4150–4166, 1998.

[306] Y. Huang *et al.*, “Distinct roles of VEGFR-1 and VEGFR-2 in the aberrant hematopoiesis associated with elevated levels of VEGF,” *Blood*, vol. 110, no. 2, pp. 624–631, 2007.

[307] A. C. Greenwald *et al.*, “VEGF expands erythropoiesis via hypoxia-independent induction of erythropoietin in noncanonical perivascular stromal cells,” *J. Exp. Med.*, vol. 216, no. 1, pp. 215–230, 2019.